Washington University in St. Louis
Washington University Open Scholarship

Arts & Sciences Electronic Theses and Dissertations | Arts & Sciences

Summer 8-15-2016

The p38MAPK-MK2-HSP27 axis regulates the mRNA stability of the pro-tumorigenic senescence-associated secretory phenotype

Hayley Reynolds Moore
Washington University in St. Louis

Follow this and additional works at: https://openscholarship.wustl.edu/art_sci_etds

Recommended Citation
Moore, Hayley Reynolds, "The p38MAPK-MK2-HSP27 axis regulates the mRNA stability of the pro-tumorigenic senescence-associated secretory phenotype" (2016). *Arts & Sciences Electronic Theses and Dissertations*. 873.
https://openscholarship.wustl.edu/art_sci_etds/873

This Dissertation is brought to you for free and open access by the Arts & Sciences at Washington University Open Scholarship. It has been accepted for inclusion in Arts & Sciences Electronic Theses and Dissertations by an authorized administrator of Washington University Open Scholarship. For more information, please contact digital@wumail.wustl.edu.

WASHINGTON UNIVERSITY IN ST. LOUIS

Division of Biology and Biomedical Sciences
Molecular Cell Biology

Dissertation Examination Committee:
Sheila A. Stewart, Chairperson
Peter Burgers
Nicholas Davidson
Sergej Djuranovic
Joshua Rubin
Zhongsheng You

The p38MAPK-MK2-HSP27 axis regulates the mRNA stability of the pro-tumorigenic senescence-associated secretory phenotype

by
Hayley R. Moore

A dissertation presented to the
Graduate School of Arts & Sciences
of Washington University in
partial fulfillment of the
requirements for the degree
of Doctor of Philosophy

August 2016
St. Louis, Missouri

Table of Contents

List of Figures

Chapter 1: Background and Significance, Senescence

Chapter 2: The p38MAPK-MK2-HSP27 axis regulates the mRNA stability of the senescence-associated secretory phenotype

Chapter 4: Background and Significance, DNA metabolism

Chapter 5: An Okazaki fragment processing-independent role for human Dna2 during DNA replication

Chapter 6: Conclusions and Future Directions, DNA metabolism

Acknowledgements

When I first talked to Sheila about a rotation, she asked me whether I was more interested in the telomere/DNA damage side or the senescence side of her lab's research. I was somewhat unprepared for that question, as I hadn't really weighed the pros and cons of the two areas of research. We discussed telomeres and DNA damage, and I did a rotation studying Dna2 with Julien. Sheila then lured me into joining her lab by brining up Star Trek and saying she wanted to develop a tricorder, and my interest in studying basic DNA processes combined with the not-so-secret geek in me led me to join the lab. When things got tough, she helped me to see the importance of asking "where will this experiment lead", and knowing when work is not necessarily the same as progress. My initial indecision of stroma vs. DNA was apparently somewhat prophetic, and I got to experience both sides of the lab in the end. I would like to thank her for the balance of guidance and freedom and her great mentorship all around, which has taught me to be an independent and hopefully thoughtful scientist.

I would like to thank my committee for thoughtful discussions during my updates, and for the guidance they provided therein. My project evolved quite a bit from the start, and their advice was a valuable part of the process. I appreciate their availability for discussion both inside and outside of official meetings.

I thank the Stewart lab for all of their support, both scientifically and emotionally. The lab has changed quite a bit since I started, and each new lab member has brought something great

to the table. I'd like to thank Mira and Julien for the great discussions at lab meeting, as well as during lunch. Julien played an invaluable role in the initial part of my research, and I know he will have a successful and impactful career in the DNA field, or if not, on the golf course. I thank bendao for the humor and delicious food he brought to lab. I would like to thank Daniel for being my DNA sounding board, as well as for getting at least some of the obscure nerdy references I'd make, whether he was happy about understanding them or not. I'd like to than Elise and Megan for being great friends during our time at the Stewart lab. Being in the same year and the same program, Megan and I shared many experiences, and I appreciate her constant source of humor and sympathetic ear. Elise was a similar source of friendship and support, and I am additionally grateful that she allowed me to continue her work on HSP27 even though it means constant texts asking about reagents and protocols, and her advice on the project as a whole. I thank Xianmin for looking out for me, for her life advice, and for her birthday cakes. I'd like to thank Shankar, Kevin, and Bhavna for doing their best to carry on the torch of Whiskey Friday, and their constant entertainment during lunch.

I would like to thank my friends from St. Louis. Your friendship and support has meant the world. From SITCDs and TV nights and trips and weddings to griping about the realities and annoyances (both major and minor) of graduate school and science, I couldn't have wished for a better group of people to experience it with. I thank my family for the endless supply of support and encouragement they have provided. I thank Dan for ten years of companionship, love, and support, and I can't wait to see what the next phase of our life together has in store.

I thank the Siteman Cancer Center's Cancer Biology Pathway for financial support.

ABSTRACT OF THE DISSERTATION

The p38MAPK-MK2-HSP27 axis regulates the mRNA stability of the pro-tumorigenic senescence-associated secretory phenotype

by

Hayley R. Moore

Doctor of Philosophy in Biology and Biomedical Sciences

Molecular Cell Biology

Washington University in St. Louis, 2016

Dr. Sheila A. Stewart, Chairperson

Protecting the genome is a vital aspect of safeguarding organismal health. Inability to efficiently and effectively replicate the genome or repair damage the genome may encounter can lead to mutational accumulation or senescence, both of which are drivers of multiple diseases including cancer. Understanding the mechanisms by which the genome is maintained, as well as the consequences of repeated rounds of replication or exposure to DNA damaging agents, will allow for greater understanding of the diseases they promote as well as development of targeted therapies aimed at mitigating the detrimental effects of genomic insult. The first section of my work focuses on cellular senescence, a consequence of both aging and DNA damage. Aging is a significant risk factor for the development of cancer. The increase in disease in aged individuals is due in part to the time required for epithelial cells to accumulate mutations necessary to become tumorigenic, and by the increase in senescent cells within their tissues. Senescent cells express a coordinately upregulated family of pro-tumorigenic factors termed the senescence-

associated secretory phenotype, or SASP. The SASP is rich in growth factors, immune modulators, and matrix remodelers that together create an environment primed for tumor development. Here, I study the mechanisms that regulate expression of the SASP in response to DNA damage. In cells exposed to a senescence-inducing stimulus but that do not yet display classical senescence markers, SASP expression is reliant upon active transcription for upregulation. However, senescent cells maintain SASP factor upregulation through post-transcriptional stabilization. Previous work demonstrated that this transition is dependent on the stress kinas p38MAPK, and p38MAPK inhibition prevents upregulation and stabilization of SASP factor mRNAs by modulating the binding of AUF1, a protein that binds regulatory sequences in target mRNAs and largely targets them for degradation. AUF1 is not a direct target of p38MAPK activity, however. In this work, I demonstrate that AUF1 regulation and therefore mRNA stabilization of SASP factors occurs through the p38MAPK-MK2-HSP27 pathway. Furthermore, inhibition of MK2 activity abrogates the ability of senescent cells to promote preneoplastic cell growth, suggesting MK2 inhibition is an attractive therapeutic target that warrants further investigation. In the second section of this work, the role of the essential helicase/nuclease Dna2 in DNA replication is investigated. Maintaining genomic stability is essential to preventing mutational accumulation and cancer development, and both elevated Dna2 expression levels in human cancers and heterozygous deletion in mice have been linked to cancer incidence and poor disease outcome. Dna2's role in DNA replication was initially described in yeast, where it was hypothesized to function in lagging strand DNA replication, namely in Okazaki fragment maturation. However, work described here demonstrates that while shRNA-mediated depletion of Dna2 results in activation of the replication stress checkpoint and phenotypes indicative of replication defects, Okazaki fragment maturation is not measurably

affected in human cells. Therefore, Dna2 plays an additional role in DNA replication that is required to ensure high fidelity duplication of the genome during cell division. Together, my work highlights the essential nature of genomic preservation, and consequences that arise when genome stability is threatened.

Chapter 1

Background and Significance

Senescence

1.1 Overview and significance

Cellular senescence was first described *in vitro* over half a century ago, as Hayflick and colleague observed that cultured primary fibroblasts have a limited replicative lifespan (1, 2). Due to the mechanics of DNA replication and the end replication problem, telomeres, the protective nucleoprotein structures at chromosome ends, shorten with each round of cell division. As cells reach this "Hayflick limit," telomeres become critically short and induce senescence, wherein metabolically active cells are prevented from reentering the cell cycle (3-6). Cellular senescence also occurs *in vivo*, as evidenced by age-dependent increases in senescent cells in skin samples from both lower primate and human tissue (7, 8). Indeed, senescent cells have been observed in many additional human tissues including kidney, prostate, and liver (7, 9-13). Cellular senescence is largely induced by the DNA damage signaling pathway, either through exogenous insults such as DNA breaks caused by DNA damaging agents or oxidative stress, or endogenous processes such as replication associated telomere attrition and telomere dysfunction due to loss of function in telomere binding proteins, among others (14-17). Upon exposure to a senescence-inducing stimulus, activation of the p53 and Rb tumor suppressor pathways lead to a permanent growth arrest, accompanied by changes in overall morphology, epigenetic structure, and gene expression patterns.

Senescence is thought to have evolved largely as a tumor protective mechanism. In order for a cell to become tumorigenic, it needs to accumulate key mutations in multiple pathways, and since it takes many years for the mutations to accumulate, older cells are more likely to have one or more of these mutations. Exposure to DNA damage is one mechanism by which cells can acquire these mutations, and both telomere attrition due to aging and activation of the DNA

damage response pathway are potent senescence inducers. By preventing further expansion of cells with potentially harmful mutations, cellular senescence functions as a potent tumor suppressor mechanism, acting as a hurdle that incipient tumor cells must overcome before becoming fully neoplastic. Indeed, inactivation of senescence-inducing pathways like p53 or the DNA damage response results in larger, more invasive tumors and an increased rate of progression from premalignancy to malignancy (18, 19). In addition to limiting transformation, more recent work has shown that senescence is associated with the secretion of a variety of factors, and these factors are capable of promoting immune-mediated clearance of tumor cells (20).

Conversely, cellular senescence can have a pro-tumorigenic function in the context of the tissues and regions surrounding tumors. In addition to epithelial cells requiring time to acquire the mutations needed to become neoplastic, accumulation of senescent cells in the stroma and the changes they elicit therein may provide a mechanistic explanation for the significant age-related increase in cancer incidence. Rather than being simply a homogenous collection of tumor cells, tumors are more akin to dysfunctional organs with their own specialized microenvironment and a dedicated blood supply. Changes to the stromal compartment such as a permissive, altered extracellular matrix; tumor-promoting immune milieu including reduced tumor-clearing cell types and an increase in immune-suppressive cells; and increased levels of growth-promoting factors in the tumor microenvironment are all critical components tumor formation, expansion, invasion, and metastasis, driven by the tumor microenvironment rather than the tumor itself (21-23). Indeed, changes in the expression profile of senescent cells, both in the epithelium and the stroma, include increased expression of factors that drive these alterations to the tumor

microenvironment and thus promote many aspects of tumorigenesis and tumor evolution. Therefore, targeting these senescent cells and the pro-tumorigenic modifications to the tumor microenvironment is an attractive therapeutic avenue.

1.2 Mechanisms governing senescence

Senescence can be induced for a variety of reasons, and a major age-related senescence inducer is replication-driven telomere attrition. The addition of telomeric repeats to the ends of chromosomes by telomerase can counteract replication-associated telomere erosion, but the majority of human cells do not express telomerase at high enough levels to combat this telomere loss (24). Once telomeres reach a critical length, the DNA damage response (DDR) pathway and p53 are persistently activated, resulting in senescence induction (**Fig. 1.1**).

Other cellular stresses can activate this pathway as well, including DNA damaging agents, hypoxia, reactive oxygen species (ROS), and epigenetic alterations, resulting in p53 activation and SIPS (stress-induced premature senescence) (14, 25). Once activated, if p53 does not direct the cell towards apoptosis, it activates p21 to induce a transient growth arrest, which can progress to permanent growth arrest and senescence via activation of $p16^{INK4a}$ if the stress is not resolved. By inhibiting the cyclin-dependent kinases CDK4 and CDK6, $p16^{INK4a}$ inhibits phosphorylation of the retinoblastoma protein (Rb), and unphosphorylated Rb arrests the cell in G1 by binding and inhibiting the E2F transcriptional factors (26).

When cells enter senescence, several characteristic changes occur. Increased expression of the cell-cycle inhibitors p53, p21, and $p16^{INK4a}$ are accompanied by accumulation of several different protein foci in the nucleus. Large, unresolved DNA damage foci persist in the nucleus, particularly at the telomeres, underscoring the importance of DDR signaling in senescence induction (27-29). Furthermore, epigenetic alterations associated with senescence result in the accumulation of senescence-associated heterochromatin foci (SAHF), characterized by increased histone modifications associated with heterochromatin, such as methylation of histone 3 on lysine 9 (H3K9me). SAHFs form at E2F target genes that play an important role in cell cycle progression, reinforcing the senescence-associated cell cycle arrest (29). Senescent cells also undergo characteristic morphological changes, taking on a large, flattened appearance and developing stress fibers. Furthermore, senescent cells express senescence-associated β-galactosidase (SA-β-gal), which is active at a lower pH than most cellular β-galactosidases, making it a useful senescence marker. Importantly, senescent cells display an altered gene expression profile termed the senescence-associated secretory phenotype (SASP, or senescence messaging secretome, SMS), which is enriched in a wide variety of factors that impact every step of tumorigenesis, tumor growth, and metastasis, by affecting both the tumor itself as well as the tumor microenvironment.

1.3 The senescence-associated secretory phenotype

The senescence-associated secretory phenotype, or SASP, is a group of factors coordinately upregulated in senescent cells. Different cell or tissue types and cells induced to senesce using different methodologies express different subsets of SASP factors, but they generally include factors that fall into the following categories: immune modulators (including

interleukins, cytokines, and chemokines that alter the inflammatory state and immune profile of the tissue), cell cycle regulators (such as mitogens, pro-proliferative factors, and proangiogenic factors), and matrix remodelers (such as matrix metalloproteases and serine proteases). Therefore, as an individual ages, accumulation of the necessary tumor-promoting mutations in the epithelial compartment over time is accompanied by increased senescent cells in the stromal compartment, where SASP expression primes the microenvironment by creating a favorable immune microenvironment which suppress anti-tumor immunity, promotes tumor growth through promotion of angiogenesis and expression of growth factors, and remodels the matrix to make it more amenable to tumor expansion and migration (**Fig. 1.2**) (21, 30, 31). In addition to the increased angiogenesis and vascularization, SASP factors promote epithelial-to-mesenchymal transition (EMT), and SASP expression at distal sites can create a favorable pre-metastatic niche, therefore further promoting disease progression by establishing an environment primed for metastasis (21, 32, 33).

Given the ability of SASP factors to promote a wide variety of tumorigenic processes, it is unsurprising that senescent stroma and the SASP have been shown to be protumorigenic both *in vitro* and *in vivo*. In cell culture models, senescent fibroblasts promote prostate epithelial cell proliferation through secretion of amphiregulin, and the SASP factors interleukins 6 and 8 (IL6 and IL8) and osteopontin (OPN) expressed by senescent stromal cells have been shown to be necessary and sufficient to drive breast cancer cell growth (21, 34, 35). Matrix metalloproteases expressed by senescent fibroblasts, such as MMP3, promote the tumorigenicity of breast epithelial cells in a xenograft setting, by altering the matrix to allow for increased diffusion to the cancer cells of mitogenic and other protumorigenic signals (36, 37). The SASP also affects the

differentiation and motility of epithelial cells. *In vitro*, IL6 and IL8 can promote invasion of several breast cancer cell lines, and MMP3 secreted by senescent cells inhibits the expression of differentiation markers and promotes cell invasion (21, 23, 37). Recently, it was demonstrated that IL6 expressed from senescent stroma in the skin was sufficient to create an immunosuppressive microenvironment by recruiting myeloid-derived suppressor cells in the absence of a tumor. This immunosuppression was sufficient to drive significantly greater tumor growth, demonstrating that the SASP can prime the microenvironment for tumor growth even before a tumor develops (31). Furthermore, IL6 secretion by senescent osteoblasts in the bone creates a favorable environment for metastatic breast cancer lesions to form, leading to increased metastasis to the bone (33).

1.4 Transcriptional regulation of the SASP

SASP upregulation relies on a variety of transcriptional programs, largely dependent upon signaling through persistent activation of the DDR and ataxia telangiectasia mutated (ATM). Although not all SASP factors rely on ATM signaling for upregulation, it is a common characteristic of inflammatory SASP factors (38). Regulation of the inflammatory components of the SASP is the best understood; several signaling pathways converge on activation of NF-κB, a well-established regulator of a wide variety not only inflammatory genes but the SASP as a whole, and inhibition or depletion of both ATM and NF-κB prevent SASP upregulation in senescent cells (39-41). One mechanism by which NF-κB is activated in senescence relies on DDR signaling. ATM is activated and phosphorylates NEMO, a regulatory component of the

IKK signaling complex. ATM and NEMO are then shuttled into the cytoplasm where they bind to the IKK complex and activate IKKα/β, which phosphorylates and inhibits the inhibitory IκB proteins, leading to NF-κB activation (41). Expression of the NF-κB-dependent SASP factor IL6 in cells induced to senesce *via* oncogene-induced senescence (OIS) drives a positive feedback loop with the transcription factor C/EBPβ (40). Depletion of IL6 or C/EBPβ results in senescence bypass and loss of cytokine upregulation, demonstrating that this feedback loop is required for entry into OIS and amplification of SASP-driven cytokine and chemokine expression.

NF-κB activity is decreased in senescent cells in response to ATM inhibition suggesting they act in the same pathway, however, DDR signaling is not required for senescence-mediated NF-κB activation. Indeed, p38 mitogen-activated protein kinase (MAPK) signaling, which is not dependent upon DDR signaling during senescence, is sufficient to activate NK-κB and drive SASP expression (39). Furthermore, abrogation of p38MAPK activity either through RNAi or small molecule inhibitors of p38MAPK resulted in decreased NF-κB activity and subsequently decreased expression of SASP factors. Highlighting the importance of p38MAPK-dependent SASP factor expression, p38MAPK inhibitor treatment abrogated the ability of senescent stroma to promote preneoplastic cell growth in a xenograft model (42). p38MAPK is a downstream target of ATM, but p38MAPK activation in response to senescence occurs with slow kinetics that to not match the rapid activation of ATM in response to genotoxic stress. Furthermore, DDR signaling is not required to activate p38MAPK in senescent cells, leaving the mechanism by which p38MAPK is activated in senescence yet to be identified (39).

1.5 Post-transcriptional regulation of SASP mRNAs

Recent work by our lab demonstrated that maintaining upregulation of SASP factors shifts from a transcriptionally-driven process to a mechanism dependent on post-transcriptional stabilization of SASP mRNAs (42). In cells that have been exposed to a senescence-inducing stimulus such as DNA damaging agents, but that do not yet display the canonical characteristics of senescence including a flattened morphology or SA-β-Gal expression (pre-senescent cells), active transcription is required to maintain upregulation of a subset of SASP factors and transcriptional inhibition leads to degradation of these messages. Conversely, once cells display the characteristic changes associated with senescence, transcriptional inhibition no longer results in degradation of many SASP factor mRNAs, demonstrating a shift to post-transcriptional mechanisms of maintaining upregulation. AU-rich element (ARE) binding protein 1 (AUF1, discussed below) drives the degradation of SASP factor mRNAs in pre-senescent cells by binding regulatory sequences in the 3' untranslated regions (3'UTRs) of certain SASP factor mRNAs and targets them for ARE-mediated decay. This process is p38MAPK dependent, since treatment with a small molecule p38MAPK inhibitor blocks the post-transcriptional stabilization of SASP mRNAs in senescent cells by preventing removal of AUF1 from SASP factor mRNAs.

p38MAPK may be regulating the turnover of SASP mRNAs through multiple mechanisms. Herranz and colleagues described a mechanism by which mammalian target of rapamycin (mTOR) regulated the translation of the downstream p38MAPK target MAP kinase-associated protein kinase 2 (MAPKAPK2, or MK2), leading to inactivation of the RNA binding protein ZFP36L1 and protection of target mRNAs from degradation (43). Indeed, they demonstrated that inhibiting mTOR prevented SASP induction by decreasing MK2 synthesis,

which in turn prevented sufficient phospho-MK2 from phosphorylating and inactivating ZFP36L1, an ARE binding protein that targets mRNAs for degradation. Together, inactivation or removal of AUF1 and/or ZFP36L1 appears to be a crucial step in promoting SASP expression.

1.5.1 AUF1 and AU-rich-element-mediated mRNA degradation

AU-rich elements (AREs) are *cis*-acting regulatory regions within the 3' untranslated regions (UTRs) of many transcripts (particularly those of cytokines and proto-oncogenes) that act through recruitment of *trans*-acting factors to modulate the rate of RNA turnover (44). ARE binding protein 1 (AUF1, also called heterogeneous nuclear ribroprotein D0, or hnRNPD) modulates the stability of these factors by regulating their entry into ARE-mediated decay, or AMD. AUF1 binds to AREs as a dimer, and this can promote the sequential binding of additional AUF1 dimers and eventual oligomerization on target transcripts (45). AUF1 then recruits additional *trans*-acting factors (termed the AUF1-and signal transduction-regulated complex or ASTRC), which may include the eukaryotic translation initiation factor 4G (eIF4G), poly(A)-binding protein (PABP), the heat shock response proteins HSP70, HSC70, and HSP27, and additional as-of-yet-unidentified factors (44, 46). Although the precise mechanism of AMD is not yet delineated, it is thought to occur through decapping of the message followed by accelerated deadenylation and nucleolytic decay. The mechanism by which AUF1 regulates this process is complex, and varies depending on cell type and physiological condition.

The AUF1 family is comprised of four splice isoforms: p37, p40, p42, and p45. All isoforms are found in both the nucleus and the cytoplasm, although $p42^{AUF1}$ and $p45^{AUF1}$ may preferentially localize to the nucleus (47, 48). All isoforms are capable of forming dimers and

binding ARE substrates, and although AUF1 is generally considered to promote mRNA degradation (with destabilization activity proportional to the binding affinity of the isoform (45, 49)), all four isoforms have been shown to protect RNAs from decay in certain circumstances (50-53). Further illustrating the complexity of the regulatory mechanisms governing AUF1-mediated decay, AUF1 can be phosphorylated at two serines, and this phosphorylation has seemingly contradictory outcomes. $p40^{AUF1}$ and $p45^{AUF1}$ contain exon 2, which include two phosphorylation sites, although only phosphorylation of $p40^{AUF1}$ has been demonstrated. Protein kinase A phosphorylates $p40^{AUF1}$ at Ser87, and glycogen synthase kinase 3-beta (GSK3β) phosphorylates $p40^{AUF1}$ at Ser83 (54). In THP monocytes, these phosphorylations are associated with degradation of TNFα mRNA. However, treatment with 12-*O*-tetradecanoylphorbol-13-acetate (TPA) to simulate monocyte adherence results in rapid stabilization of the target mRNAs and concurrent loss of $p40^{AUF1}$ phosphorylation (54, 55). In contrast, as discussed in section 1.5b, phosphorylation of $p40^{AUF1}$ is required for ubiquitin-mediated AUF1 degradation in HeLa cells and is therefore associated with increased mRNA stability (56).

1.5.2 The p38MAPK-MK2 mRNA degradation pathway

In addition to regulating gene expression at the transcriptional level, p38MAPK regulates expression levels of target factors (cytokines in particular) through regulation of mRNA stability. In conjunction with its downstream target MK2, p38MAPK signaling stabilizes mRNAs such as IL6, IL8, and GM-CSF through their AU-rich 3'UTRs (57). Furthermore, p38MAPK signaling in response to lipopolysaccharide treatment has been shown to result in MK2-dependent phosphorylation of the RNA binding protein hnRNP A0. This phosphorylation is necessary to

enhance the interaction of hnRNP A0 with cytokine AREs therefore stabilizing them, potentially through outcompeting other RNA binding proteins such as AUF1 (58).

Although we have previously demonstrated that AUF1 regulation of SASP factor mRNA stability is p38MAPK-dependent, AUF1 is not a direct downstream target of p38MAPK. However, the ASTRC component and AUF1 interacting partner HSP27 is phosphorylated by MK2 in a p38MAPK-dependent manner (59). Indeed, phosphomimetic mutation of the three MK2 target sites on HSP27 (HSP27-TriD) increases the half-life of mRNAs targeted for degradation by AUF1 (60). The authors observed decreased interaction between HSP27 and AUF1 as well as increased proteolytic degradation of AUF1 in response to HSP27-TriD expression, and suggested that proteasomal degradation of AUF1 protein was responsible for the increased mRNA half-lives.

Utilizing HeLa cells expressing phospho-mimetic and phospho-dead constructs of HSP27, AUF1, and the β-transducin repeat-containing protein (β-TrCP) subunit of the SCF (Skp1-cullin-F-box protein) ubiquitin ligase complex, Li and colleagues suggest HSP27-dependent ubiquitination of AUF1 mediates AUF1 proteolysis in response to p38MAPK-dependent HSP27 phosphorylation (56). Phosphorylation of $p40^{AUF1}$ at serines 83 and 87 creates a non-canonical β-TrCP binding site leading to ubiquitination and degradation of $p40^{AUF1}$, and subsequent stabilization of target mRNAs. Expression of HSP27-TriD to mimic HSP27 phosphorylation was required to facilitate the interaction between phospho-$p40^{AUF1}$ and β-TrCP in this context. The mechanisms by which other isoforms of AUF1 are degraded and regulate

mRNA stability in response to HSP27 phosphorylation remain to be elucidated, since only $p40^{AUF1}$ has the ability to be both phosphorylated and ubiquitinated (54, 55, 61).

Interestingly, both HSP27 and AUF1 are associated with aging and disease. AUF1 has been shown to suppress cellular senescence by activating transcription of the telomerase subunit *Tert*, as well as promoting degradation of mRNAs for the cell cycle inhibitors $p16^{INK4a}$, $p19^{Arf}$, and p21 (62). Indeed, $Auf1^{-/-}$ mice display telomere shortening and loss, increased cytokine expression, and premature aging phenotypes. High levels of HSP27 expression is correlated with resistance to chemotherapy as well as with markers of aggressive tumors and decreased survival in melanoma and breast cancer (63-65). Inhibition or suppression of HSP27 has been shown to sensitize different types of cancers to chemotherapy, and phase II clinical trials of the small molecule HSP27 inhibitor apatorsen (OGX-427) are currently underway (64-66).

1.6 Summary

Elucidating the mechanisms by which aging tissues contribute to tumorigenesis and cancer as a whole is essential for our understanding of the disease, as well as for designing the next generation of targeted cancer therapies. By understanding the pathways underlying the senescence-associated secretory phenotype and how the microenvironment promotes tumor growth and development, we will be able to treat not only the tumor itself, but also the support network that provides the tumor with the factors it needs to thrive. This work focuses on characterizing post-transcriptional regulation of the senescence-associated secretory phenotype in senescent cells. In chapter 2, I demonstrate that the p38MAPK-MK2-HSP27 pathway

regulates AUF1 activity in senescent cells, and that disruption of this pathway inhibits growth promotion by senescent fibroblasts. In chapter 3, I discuss the significance of this work and the intriguing avenues of investigation it opens.

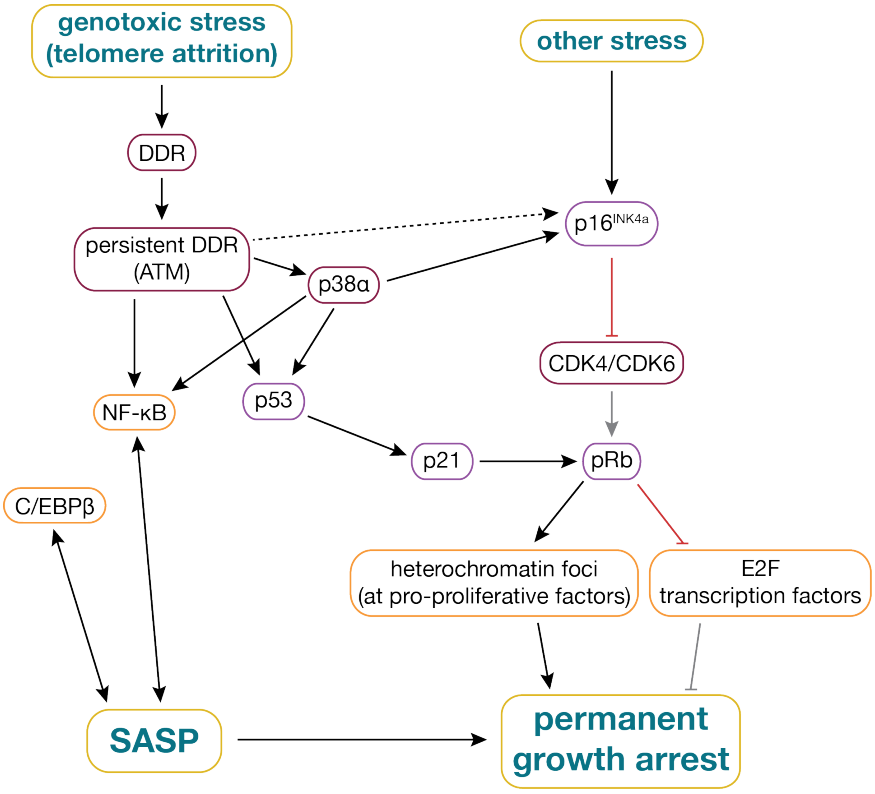

Figure 1.1: Regulation of senescence and the senescence-associated secretory phenotype.

Senescence is induced upon exposure to many stresses including telomere dysfunction, exposure to DNA damage, and others. Stresses that activate the DNA damage response lead to senescence and SASP expression through activation of p53, which activates p21 and enforces growth arrest through non-phosphorylated Rb (38, 67, 68). Persistent DDR signaling and other stressors can also indirectly activate the cell cycle regulator $p16^{INK4a}$ (dashed line), which also prevents phosphorylation of Rb by inhibiting the cyclin dependent kinases CDK4 and CDK6. Nonphosphorylated Rb prevents cell cycle progression by binding and inhibiting the E2F transcription factors, as well as by promoting heterochromatin at E2F targets and other pro-proliferative genes (29). p38MAPK can be activated by DDR signaling, but DDR-dependent activation is not required for p38MAPK signaling during senescence. p38MAPK can reinforce senescence through activation of $p16^{INK4a}$ and p53, and promote SASP expression through activation of NF-κB as well as through stabilization of SASP factor transcripts (39, 42, 69). SASP expression also reinforces senescence through IL6 expression, as well as through feedback loops via C/EBPβ and NF-κB (40). Adapted from (16).

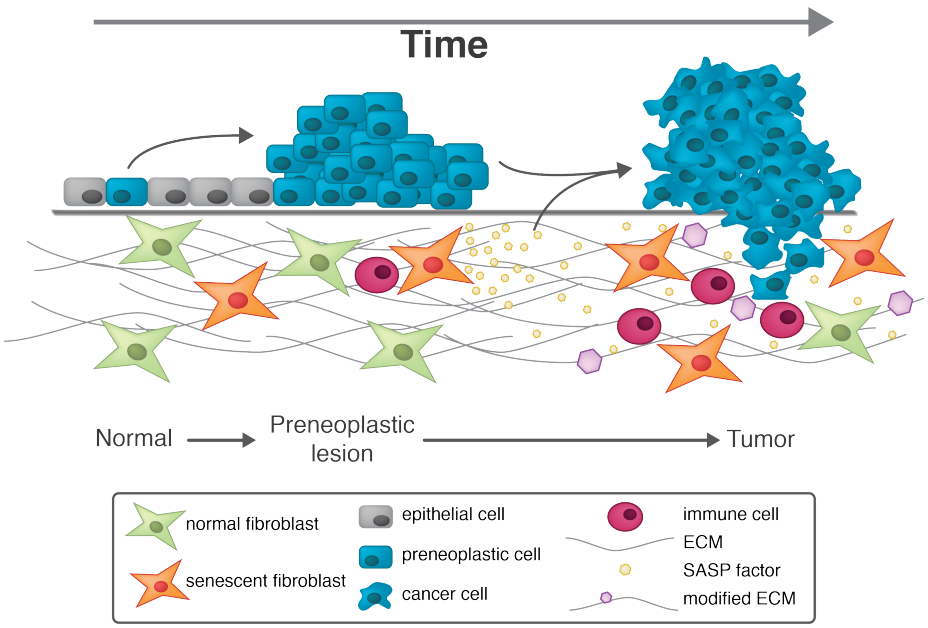

Figure 1.2: Accumulation of senescent cells alters the stromal compartment over time, priming the environment and driving tumorigenesis.

Multiple aspects of tumor development come together to drive tumorigenesis over time in human tissues. As mutations accumulating in epithelial cells drive neoplasia, changes in the stromal compartment contribute to transformation to malignancy. Accumulation of senescent cells and SASP expression can promote this transformation through microenvironmental changes such as promotion of chronic inflammation and a tumor-permissive immune milieu, increased expression of growth factors and proangiogenic factors, and modifications to the extracellular matrix that promote both tumor growth as well as motility and invasion through the basement membrane. Adapted from (17).

References

1. **Hayflick L.** 1965. The Limited in Vitro Lifetime of Human Diploid Cell Strains. Exp Cell Res **37:**614-636.

2. **Hayflick L, Moorhead PS.** 1961. The serial cultivation of human diploid cell strains. Exp Cell Res **25:**585-621.

3. **Allsopp RC, Chang E, Kashefi-Aazam M, Rogaev EI, Piatyszek MA, Shay JW, Harley CB.** 1995. Telomere shortening is associated with cell division in vitro and in vivo. Exp Cell Res **220:**194-200.

4. **Allsopp RC, Harley CB.** 1995. Evidence for a critical telomere length in senescent human fibroblasts. Exp Cell Res **219:**130-136.

5. **Figueroa R, Lindenmaier H, Hergenhahn M, Nielsen KV, Boukamp P.** 2000. Telomere erosion varies during in vitro aging of normal human fibroblasts from young and adult donors. Cancer Res **60:**2770-2774.

6. **Olovnikov AM.** 1973. A theory of marginotomy. The incomplete copying of template margin in enzymic synthesis of polynucleotides and biological significance of the phenomenon. J Theor Biol **41:**181-190.

7. **Dimri GP, Lee X, Basile G, Acosta M, Scott G, Roskelley C, Medrano EE, Linskens M, Rubelj I, Pereira-Smith O, Peacocke M, Campisi J.** 1995. A biomarker that identifies senescent human cells in culture and in aging skin in vivo. Proc Natl Acad Sci U S A **92:**9363-9367.

8. **Herbig U, Ferreira M, Condel L, Carey D, Sedivy JM.** 2006. Cellular senescence in aging primates. Science **311:**1257.

9. **Chkhotua AB, Gabusi E, Altimari A, D'Errico A, Yakubovich M, Vienken J, Stefoni S, Chieco P, Yussim A, Grigioni WF.** 2003. Increased expression of p16(INK4a) and p27(Kip1) cyclin-dependent kinase inhibitor genes in aging human kidney and chronic allograft nephropathy. Am J Kidney Dis **41:**1303-1313.

10. **Choi J, Shendrik I, Peacocke M, Peehl D, Buttyan R, Ikeguchi EF, Katz AE, Benson MC.** 2000. Expression of senescence-associated beta-galactosidase in enlarged prostates from men with benign prostatic hyperplasia. Urology **56:**160-166.

11. **Lee AC, Fenster BE, Ito H, Takeda K, Bae NS, Hirai T, Yu ZX, Ferrans VJ, Howard BH, Finkel T.** 1999. Ras proteins induce senescence by altering the intracellular levels of reactive oxygen species. J Biol Chem **274:**7936-7940.

12. **Melk A, Schmidt BM, Takeuchi O, Sawitzki B, Rayner DC, Halloran PF.** 2004. Expression of p16INK4a and other cell cycle regulator and senescence associated genes in aging human kidney. Kidney Int **65:**510-520.

13. **Wiemann SU, Satyanarayana A, Tsahuridu M, Tillmann HL, Zender L, Klempnauer J, Flemming P, Franco S, Blasco MA, Manns MP, Rudolph KL.** 2002. Hepatocyte telomere shortening and senescence are general markers of human liver cirrhosis. FASEB J **16:**935-942.

14. **Alspach E, Fu Y, Stewart SA.** 2013. Senescence and the pro-tumorigenic stroma. Crit Rev Oncog **18:**549-558.

15. **Blackburn EH, Epel ES, Lin J.** 2015. Human telomere biology: A contributory and interactive factor in aging, disease risks, and protection. Science **350:**1193-1198.

16. **Campisi J.** 2013. Aging, cellular senescence, and cancer. Annu Rev Physiol **75:**685-705.

17. **Pazolli E, Stewart SA.** 2008. Senescence: the good the bad and the dysfunctional. Curr Opin Genet Dev **18:**42-47.

18. **Bartkova J, Rezaei N, Liontos M, Karakaidos P, Kletsas D, Issaeva N, Vassiliou LV, Kolettas E, Niforou K, Zoumpourlis VC, Takaoka M, Nakagawa H, Tort F, Fugger K, Johansson F, Sehested M, Andersen CL, Dyrskjot L, Orntoft T, Lukas J, Kittas C, Helleday T, Halazonetis TD, Bartek J, Gorgoulis VG.** 2006. Oncogene-induced senescence is part of the tumorigenesis barrier imposed by DNA damage checkpoints. Nature **444:**633-637.

19. **Chen Z, Trotman LC, Shaffer D, Lin HK, Dotan ZA, Niki M, Koutcher JA, Scher HI, Ludwig T, Gerald W, Cordon-Cardo C, Pandolfi PP.** 2005. Crucial role of p53-dependent cellular senescence in suppression of Pten-deficient tumorigenesis. Nature **436:**725-730.

20. **Xue W, Zender L, Miething C, Dickins RA, Hernando E, Krizhanovsky V, Cordon-Cardo C, Lowe SW.** 2007. Senescence and tumour clearance is triggered by p53 restoration in murine liver carcinomas. Nature **445:**656-660.

21. **Coppe JP, Patil CK, Rodier F, Sun Y, Munoz DP, Goldstein J, Nelson PS, Desprez PY, Campisi J.** 2008. Senescence-associated secretory phenotypes reveal cell-nonautonomous functions of oncogenic RAS and the p53 tumor suppressor. PLoS Biol **6:**2853-2868.

22. **Krtolica A, Parrinello S, Lockett S, Desprez PY, Campisi J.** 2001. Senescent fibroblasts promote epithelial cell growth and tumorigenesis: a link between cancer and aging. Proc Natl Acad Sci U S A **98:**12072-12077.

23. **Parrinello S, Coppe JP, Krtolica A, Campisi J.** 2005. Stromal-epithelial interactions in aging and cancer: senescent fibroblasts alter epithelial cell differentiation. J Cell Sci **118:**485-496.

24. **Harley CB, Futcher AB, Greider CW.** 1990. Telomeres shorten during ageing of human fibroblasts. Nature **345:**458-460.

25. **Pazolli E, Alspach E, Milczarek A, Prior J, Piwnica-Worms D, Stewart SA.** 2012. Chromatin remodeling underlies the senescence-associated secretory phenotype of tumor stromal fibroblasts that supports cancer progression. Cancer Res **72:**2251-2261.

26. **Lasry A, Ben-Neriah Y.** 2015. Senescence-associated inflammatory responses: aging and cancer perspectives. Trends Immunol **36:**217-228.

27. **Fumagalli M, Rossiello F, Clerici M, Barozzi S, Cittaro D, Kaplunov JM, Bucci G, Dobreva M, Matti V, Beausejour CM, Herbig U, Longhese MP, d'Adda di Fagagna F.** 2012. Telomeric DNA damage is irreparable and causes persistent DNA-damage-response activation. Nat Cell Biol **14:**355-365.

28. **Hewitt G, Jurk D, Marques FD, Correia-Melo C, Hardy T, Gackowska A, Anderson R, Taschuk M, Mann J, Passos JF.** 2012. Telomeres are favoured targets of a persistent DNA damage response in ageing and stress-induced senescence. Nat Commun **3:**708.

29. **Narita M, Nunez S, Heard E, Narita M, Lin AW, Hearn SA, Spector DL, Hannon GJ, Lowe SW.** 2003. Rb-mediated heterochromatin formation and silencing of E2F target genes during cellular senescence. Cell **113:**703-716.

30. **Coppe JP, Kauser K, Campisi J, Beausejour CM.** 2006. Secretion of vascular endothelial growth factor by primary human fibroblasts at senescence. J Biol Chem **281:**29568-29574.

31. **Ruhland MK, Loza AJ, Capietto AH, Luo X, Knolhoff BL, Flanagan KC, Belt BA, Alspach E, Leahy K, Luo J, Schaffer A, Edwards JR, Longmore G, Faccio R, DeNardo DG, Stewart SA.** 2016. Stromal senescence establishes an immunosuppressive microenvironment that drives tumorigenesis. Nat Commun (in press).

32. **Coppe JP, Desprez PY, Krtolica A, Campisi J.** 2010. The senescence-associated secretory phenotype: the dark side of tumor suppression. Annu Rev Pathol **5:**99-118.

33. **Luo X, Fu Y, Loza AJ, Murali B, Leahy KM, Ruhland MK, Gang M, Su X, Zamani A, Shi Y, Lavine KJ, Ornitz DM, Weilbaecher KN, Long F, Novack DV, Faccio R, Longmore GD, Stewart SA.** 2016. Stromal-Initiated Changes in the Bone Promote Metastatic Niche Development. Cell Rep **14:**82-92.

34. **Bavik C, Coleman I, Dean JP, Knudsen B, Plymate S, Nelson PS.** 2006. The gene expression program of prostate fibroblast senescence modulates neoplastic epithelial cell proliferation through paracrine mechanisms. Cancer Res **66:**794-802.

35. **Pazolli E, Luo X, Brehm S, Carbery K, Chung JJ, Prior JL, Doherty J, Demehri S, Salavaggione L, Piwnica-Worms D, Stewart SA.** 2009. Senescent stromal-derived osteopontin promotes preneoplastic cell growth. Cancer Res **69:**1230-1239.

36. **Liu D, Hornsby PJ.** 2007. Senescent human fibroblasts increase the early growth of xenograft tumors via matrix metalloproteinase secretion. Cancer Res **67:**3117-3126.

37. **Tsai KK, Chuang EY, Little JB, Yuan ZM.** 2005. Cellular mechanisms for low-dose ionizing radiation-induced perturbation of the breast tissue microenvironment. Cancer Res **65:**6734-6744.

38. **Rodier F, Coppe JP, Patil CK, Hoeijmakers WA, Munoz DP, Raza SR, Freund A, Campeau E, Davalos AR, Campisi J.** 2009. Persistent DNA damage signalling triggers senescence-associated inflammatory cytokine secretion. Nat Cell Biol **11:**973-979.

39. **Freund A, Patil CK, Campisi J.** 2011. p38MAPK is a novel DNA damage response-independent regulator of the senescence-associated secretory phenotype. EMBO J **30:**1536-1548.

40. **Kuilman T, Michaloglou C, Vredeveld LC, Douma S, van Doorn R, Desmet CJ, Aarden LA, Mooi WJ, Peeper DS.** 2008. Oncogene-induced senescence relayed by an interleukin-dependent inflammatory network. Cell **133:**1019-1031.

41. **Salminen A, Kauppinen A, Kaarniranta K.** 2012. Emerging role of NF-kappaB signaling in the induction of senescence-associated secretory phenotype (SASP). Cell Signal **24:**835-845.

42. **Alspach E, Flanagan KC, Luo X, Ruhland MK, Huang H, Pazolli E, Donlin MJ, Marsh T, Piwnica-Worms D, Monahan J, Novack DV, McAllister SS, Stewart SA.** 2014. p38MAPK plays a crucial role in stromal-mediated tumorigenesis. Cancer Discov **4:**716-729.

43. **Herranz N, Gallage S, Mellone M, Wuestefeld T, Klotz S, Hanley CJ, Raguz S, Acosta JC, Innes AJ, Banito A, Georgilis A, Montoya A, Wolter K, Dharmalingam G, Faull P, Carroll T, Martinez-Barbera JP, Cutillas P, Reisinger F, Heikenwalder M, Miller RA, Withers D, Zender L, Thomas GJ, Gil J.** 2015. mTOR regulates MAPKAPK2 translation to control the senescence-associated secretory phenotype. Nat Cell Biol **17:**1205-1217.

44. **Gratacós FM, Brewer G.** 2010. The role of AUF1 in regulated mRNA decay. Wiley Interdiscip Rev RNA **1:**457-473.

45. **Wilson GM, Sun Y, Lu H, Brewer G.** 1999. Assembly of AUF1 oligomers on U-rich RNA targets by sequential dimer association. J Biol Chem **274:**33374-33381.

46. **White EJ, Brewer G, Wilson GM.** 2013. Post-transcriptional control of gene expression by AUF1: mechanisms, physiological targets, and regulation. Biochim Biophys Acta **1829:**680-688.

47. **Arao Y, Kuriyama R, Kayama F, Kato S.** 2000. A nuclear matrix-associated factor, SAF-B, interacts with specific isoforms of AUF1/hnRNP D. Arch Biochem Biophys **380:**228-236.

48. **Zhang W, Wagner BJ, Ehrenman K, Schaefer AW, DeMaria CT, Crater D, DeHaven K, Long L, Brewer G.** 1993. Purification, characterization, and cDNA cloning of an AU-rich element RNA-binding protein, AUF1. Mol Cell Biol **13:**7652-7665.

49. **DeMaria CT, Brewer G.** 1996. AUF1 binding affinity to A+U-rich elements correlates with rapid mRNA degradation. J Biol Chem **271:**12179-12184.

50. **Loflin P, Chen CY, Shyu AB.** 1999. Unraveling a cytoplasmic role for hnRNP D in the in vivo mRNA destabilization directed by the AU-rich element. Genes Dev **13:**1884-1897.

51. **Lu JY, Bergman N, Sadri N, Schneider RJ.** 2006. Assembly of AUF1 with eIF4G-poly(A) binding protein complex suggests a translation function in AU-rich mRNA decay. RNA **12:**883-893.

52. **Palanisamy V, Park NJ, Wang J, Wong DT.** 2008. AUF1 and HuR proteins stabilize interleukin-8 mRNA in human saliva. J Dent Res **87:**772-776.

53. **Raineri I, Wegmueller D, Gross B, Certa U, Moroni C.** 2004. Roles of AUF1 isoforms, HuR and BRF1 in ARE-dependent mRNA turnover studied by RNA interference. Nucleic Acids Res **32:**1279-1288.

54. **Wilson GM, Lu J, Sutphen K, Sun Y, Huynh Y, Brewer G.** 2003. Regulation of A + U-rich element-directed mRNA turnover involving reversible phosphorylation of AUF1. J Biol Chem **278:**33029-33038.

55. **Wilson GM, Lu J, Sutphen K, Suarez Y, Sinha S, Brewer B, Villanueva-Feliciano EC, Ysla RM, Charles S, Brewer G.** 2003. Phosphorylation of p40AUF1 regulates binding to A + U-rich mRNA-destabilizing elements and protein-induced changes in ribonucleoprotein structure. J Biol Chem **278:**33039-33048.

56. **Li ML, Defren J, Brewer G.** 2013. Hsp27 and F-box protein beta-TrCP promote degradation of mRNA decay factor AUF1. Mol Cell Biol **33:**2315-2326.

57. **Winzen R, Kracht M, Ritter B, Wilhelm A, Chen CY, Shyu AB, Muller M, Gaestel M, Resch K, Holtmann H.** 1999. The p38 MAP kinase pathway signals for cytokine-induced mRNA stabilization via MAP kinase-activated protein kinase 2 and an AU-rich region-targeted mechanism. EMBO J **18:**4969-4980.

58. **Rousseau S, Morrice N, Peggie M, Campbell DG, Gaestel M, Cohen P.** 2002. Inhibition of SAPK2a/p38 prevents hnRNP A0 phosphorylation by MAPKAP-K2 and its interaction with cytokine mRNAs. EMBO J **21:**6505-6514.

59. **Zheng C, Lin Z, Zhao ZJ, Yang Y, Niu H, Shen X.** 2006. MAPK-activated protein kinase-2 (MK2)-mediated formation and phosphorylation-regulated dissociation of the signal complex consisting of p38, MK2, Akt, and Hsp27. J Biol Chem **281:**37215-37226.

60. **Knapinska AM, Gratacos FM, Krause CD, Hernandez K, Jensen AG, Bradley JJ, Wu X, Pestka S, Brewer G.** 2011. Chaperone Hsp27 modulates AUF1 proteolysis and AU-rich element-mediated mRNA degradation. Mol Cell Biol **31:**1419-1431.

61. **Laroia G, Schneider RJ.** 2002. Alternate exon insertion controls selective ubiquitination and degradation of different AUF1 protein isoforms. Nucleic Acids Res **30:**3052-3058.

62. **Pont AR, Sadri N, Hsiao SJ, Smith S, Schneider RJ.** 2012. mRNA decay factor AUF1 maintains normal aging, telomere maintenance, and suppression of senescence by activation of telomerase transcription. Mol Cell **47:**5-15.

63. **Liu CL, Chen SF, Wu MZ, Jao SW, Lin YS, Yang CY, Lee TY, Wen LW, Lan GL, Nieh S.** 2016. The Molecular and Clinical Verification of Therapeutic Resistance via the p38 MAPK-Hsp27 Axis in Lung Cancer. Oncotarget doi:10.18632/oncotarget.7306.

64. **Lu H, Sun C, Zhou T, Zhou B, Guo E, Shan W, Xia M, Li K, Weng D, Meng L, Xu X, Hu J, Ma D, Chen G.** 2016. HSP27 Knockdown Increases Cytoplasmic p21 and Cisplatin Sensitivity in Ovarian Carcinoma Cells. Oncol Res **23:**119-128.

65. **Straume O, Shimamura T, Lampa MJ, Carretero J, Oyan AM, Jia D, Borgman CL, Soucheray M, Downing SR, Short SM, Kang SY, Wang S, Chen L, Collett K, Bachmann I, Wong KK, Shapiro GI, Kalland KH, Folkman J, Watnick RS, Akslen LA, Naumov GN.** 2012. Suppression of heat shock protein 27 induces long-term dormancy in human breast cancer. Proc Natl Acad Sci U S A **109:**8699-8704.

66. **Chi KN, Yu EY, Jacobs C, Bazov J, Kollmannsberger C, Higano CS, Mukherjee SD, Gleave ME, Stewart PS, Hotte SJ.** 2016. A phase I dose-escalation study of apatorsen (OGX-427), an antisense inhibitor targeting heat shock protein 27 (Hsp27), in patients with castration-resistant prostate cancer and other advanced cancers. Ann Oncol doi:10.1093/annonc/mdw068.

67. **Adams PD.** 2009. Healing and hurting: molecular mechanisms, functions, and pathologies of cellular senescence. Mol Cell **36:**2-14.

68. **Collins CJ, Sedivy JM.** 2003. Involvement of the INK4a/Arf gene locus in senescence. Aging Cell **2:**145-150.

69. **Xu Y, Li N, Xiang R, Sun P.** 2014. Emerging roles of the p38 MAPK and PI3K/AKT/mTOR pathways in oncogene-induced senescence. Trends Biochem Sci **39:**268-276.

Chapter 2

The p38MAPK-MK2-HSP27 axis regulates the mRNA stability of the senescence-associated secretory phenotype

Hayley R. Moore, Elise Alspach, Joseph Monahan, Sheila A. Stewart

Abstract

Age is a significant risk factor for the development of cancer. Both accumulation of cell autonomous mutations within neoplastic cells and increases in senescent stromal cells within the tumor microenvironment are thought to collaborate to drive tumorigenesis. Senescent cells express a number of pro-tumorigenic factors termed the senescence-associated secretory phenotype (SASP) that are subject to a variety of regulatory mechanisms that remain to be fully elucidated. Previous work demonstrated that p38 mitogen-activated protein kinase (p38MAPK)-dependent regulation of AUF1 occupancy on SASP factor mRNAs post-transcriptionally stabilizes many SASP mRNAs and contributes to their increased expression. Here, we address the mechanism by which p38MAPK regulates AUF1's occupancy and activity on SASP factor mRNAs. We found that the p38MAPK-MK2-HSP27 pathway regulates both mRNA stability and AUF1 occupancy in cells induced to senesce. Furthermore, inhibiting this pathway blunted the tumor-promoting abilities of senescent stromal cells, suggesting that this pathway may represent a viable therapeutic target within the tumor microenvironment.

Introduction

Cellular senescence arises in response to a wide array of cytotoxic stresses including replication-driven telomere attrition, DNA damage, oncogene activation and increases in ROS, and other cellular stresses. Senescence is characterized by an irreversible cell cycle arrest that is mediated by activation of p21, and subsequently $p16^{INK4a}$ and Rb. As such, senescence functions as a potent tumor suppressor mechanism when it occurs within incipient tumor cells (1). In

addition to permanent growth arrest, senescence is characterized by an altered cell morphology that includes a flattened appearance and development of stress fibers, increased expression of senescence-associated β-galactosidase (SA-β-gal), and expression of the senescence-associated secretory phenotype or SASP (also known as the senescence messaging secretome or SMS) (2-4). This secretory phenotype can lead to an immune-mediated clearance of tumor cells, but when it occurs in stromal cells it has been shown to function as a potent tumor promoter (2, 5-7). The SASP consists of a group of proteins including a large number of pro-inflammatory cytokines and other immune modulators, matrix remodeling proteins, and pro-proliferative factors, among others, that are coordinately upregulated in senescent cells. Senescent fibroblast-derived SASP can promote epithelial cell proliferation while simultaneously remodeling the stromal compartment to create an environment conducive to tumor proliferation, as well as promoting epithelial-to-mesenchymal transition (EMT) to allow for tumor extravasation and metastasis (2, 7, 8).

Upon induction of senescence, the immediate DNA damage response (DDR) and delayed activation of the p38 mitogen-activated protein kinase (p38MAPK) pathway function together to induce numerous SASP factors, primarily through activation of NFκB (9). This initial rapid transcriptional activation is accompanied by establishment of other characteristics of senescence such as SA-β-gal expression and morphological changes which occur more slowly, on the scale of days after genotoxic stress, with similar kinetics to p38MAPK phosphorylation.

Immediately following a senescence-inducing stimulus such as treatment with the DNA damaging agent bleomycin, cells referred to here as pre-senescent begin to upregulate numerous

SASP factors through the activity of transcription factors like NFκB but do not yet display classic signs of senescence, including a flattened morphology or SA-β-Gal activity (9-11). We recently demonstrated that maintaining SASP factor upregulation results from a transition from a transcriptionally-driven process in pre-senescent cells to a post-transcriptional stabilization mechanism in cells displaying the morphological changes and SA-β-Gal activity characteristic of senescent cells (10). In spite of their increased transcriptional levels, several SASP factor mRNAs in pre-senescent cells, including IL-6, IL-8, and GM-CSF, are targeted for post-transcriptional degradation by AU-rich elements (AREs) in their 3' untranslated regions (UTRs), through a process termed ARE-mediated decay (AMD), which is mediated by the ARE binding protein 1 (AUF1, also called heterogeneous nuclear ribonucleoprotein D0 or hnRNPD). However, once senescence is established as evidenced by SA-β-Gal expression, AUF1 binding is decreased and SASP mRNAs are stabilized. Elevated SASP mRNA levels are sustained predominantly by a p38MAPK-dependent mRNA stabilization mechanism. Indeed, p38MAPK inhibition with the small molecule inhibitor SB203580 prevented the removal of AUF1 from these 3'UTRs and the mRNA stabilization phenotype (10).

During AMD, AUF1 binds to target AREs and recruits other *trans*-acting factors (termed the AUF1- and signal transduction-regulated complex or ASTRC), which results in mRNA degradation. The precise mechanisms and order of events that leads to mRNA degradation remain to be determined, but it is thought to occur through acceleration of deadenylation and subsequent nucleolytic degradation of the target mRNA (12, 13). While AUF1 is known to be important in this process, its precise role in mRNA decay is incompletely understood. AUF1 is expressed in four splice isoforms generated from a common pre-mRNA: p37, p40, p42, and p45.

Although all isoforms can promote mRNA degradation, there are circumstances wherein certain isoforms of AUF1 bind and act to protect mRNAs from decay, underscoring the complexity of the system and demonstrating that AUF1-mediated decay is not regulated simply at the level of AUF1 binding (14-17). Post-translational modification of AUF1 also appears to differentially affect mRNA stability. It has been shown that $p40^{AUF1}$ can be phosphorylated on Ser^{83} by protein kinase A (PKA) and Ser^{87} by glycogen synthase kinase 3β (GSK3β), and this phosphorylation has contradictory consequences on mRNA stability (18, 19). In THP-1 monocytic leukemia cells, phosphorylated $p40^{AUF1}$ is actively involved in mRNA degradation. Treatment with 12-*O*-tetradecanoylphorbol-13-acetate (TPA) to simulate monocyte adherence results in rapid stabilization of the target mRNAs and concurrent loss of $p40^{AUF1}$ phosphorylation, suggesting that $p40^{AUF1}$ promotes mRNA degradation when phosphorylated, and mRNA stabilization in its non-phosphorylated state (19). In contradiction, phosphorylation of AUF1 leads to its ubiquitin-mediated degradation (and subsequent AUF1 target mRNA stabilization) in response to p38MAPK signaling through HSP27 in HeLa cells (20). The varied consequences of AUF1 phosphorylation and differential outcomes of AUF1 binding to target AREs demonstrate that complex regulatory mechanisms including the phosphorylation state of AUF1 and/or other ASTRC members are involved in AMD.

We previously demonstrated that p38MAPK inhibition led to destabilization of SASP mRNAs through alteration of AUF1 binding in senescent fibroblasts. However, p38MAPK does not directly target AUF1 and thus the mechanism by which p38MAPK influences AUF1 activity remained to be elucidated. Interestingly, recent work by Herranz *et al.* demonstrated that MAPKAPK2 (MK2) in senescent IMR90 lung fibroblasts participated in SASP factor regulation.

MK2 is a p38MAPK target which when activated is known to regulate mRNA stability and phosphorylate the small heat shock protein HSP27, an ASTRC member that has been shown to regulate AUF1 levels and mRNA stability in lymphocytes (21-24).

Given our previous findings, we investigated whether p38MAPK regulates mRNA stabilization in senescent cells through MK2 and HSP27. Our results indicate that p38MAPK and MK2 govern mRNA stabilization through phosphorylation of HSP27, but that HSP27 does not act solely through regulation of AUF1 protein levels or binding to SASP mRNAs. Furthermore, we find that MK2 pathway inhibition not only prevents the upregulation and stabilization of SASP factor mRNAs, it also prevents senescent fibroblasts from promoting preneoplastic cell growth in a co-culture model, suggesting that targeting MK2 in the tumor microenvironment may be a promising therapeutic avenue in cancer treatment.

Materials and Methods

Cell lines and treatments

BJ human foreskin fibroblasts were cultured in DMEM supplemented with 15% M-199, 15% heat-inactivated FBS, and 1% penicillin/streptomycin (all from Sigma). Fibroblasts were treated with bleomycin sulfate (0.1 units/mL, Sigma) for 24 hours, followed by incubation in normal culture medium (unless otherwise stated) for the time points indicated. Fibroblasts were treated with actinomycin D (10 μg/mL, Sigma) for 24 hours, and SB203580 (10 μM, Millipore), CDD111 (also referred to as SD0006, 1 μM), or CDD450 (1μM, both from Confluence Life Sciences, St. Louis, MO) every 24h unless indicated otherwise. HaCaT preneoplastic

keratinocyte cells obtained from Dr. Norbert E. Fusenig (German Cancer Research Center, Heidelberg, Germany) stably expressing click beetle red (CBR) luciferase (HaCaT-CBR) and HEK293T embryonic kidney cells (6) were grown in DMEM supplemented with 10% heat-inactivated FBS and 1% penicillin/streptomycin (Sigma). All cells were cultured at 37°C in 5% CO_2 and 5% O_2. No cell lines used were authenticated.

Virus production and plasmids

Virus production was carried out as described previously (25). Briefly, HEK239T cells were transfected with Trans-IT LT1 (Mirus) and virus was collected 48h later. Infections were carried out in the presence of 1μg/mL protamine sulfate. 48h post-infection, cells were selected with 1μg/mL puromycin or 50 μg/mL hygromycin.

Short hairpin RNA sequences targeting HSP27 (5'-CCCGGACGAGCTGACGGTCAA-3') and control SCR (5'-TCCTAAGGTTAAGTCGCCCTC-3') were obtained from the Children's Discovery Institute's viral vector-based RNAi core at Washington University in St. Louis, and were supplied in the pLKO.1-puro backbone. When not combined with knockdown, FLAG-tagged HSP27-TriD was expressed from the pBABE-hyrgo backbone. Knockdown rescue experiments utilized the pRESQ-puro backbone with the indicated hairpins. Hairpin-resistant Flag-HSP27 WT and TriD were manufactured by IDT and cloned into pRESQ from pUC57. The sequence was based on constructs provided by Dr. Gary Brewer with the following silent mutations to the shHSP27 hairpin recognition sequence: 5'-CCG GAC GAG CTG ACG GTC-3' to 5'-CCC GAT GAA CTC ACC GTG-3'. Hairpin-resistant HSP27-TriA was generated utilizing QuikChange Lightning site directed mutagenesis (Agilent Technologies) of pUC57-HSP27-WT

and published primers (22) to generate the Ser-to-Ala mutations at serines 15, 78 and 82, and similarly cloned into pRESQ.

Western blot analysis

Cell pellets were lysed in MCLB (50 mM Tris pH 8.0, 5 mM EDTA, 0.5% NP40 and 100 mM sodium chloride, with aprotenin, leupeptin, pepstatin, phenylmethylsulfonyl fluoride, microcystin LR, sodium orthovanidate and sodium fluoride) for 20 minutes at 4°C. Protein concentration was quantified using the Bradford Protein Assay (Bio-Rad). The primary antibodies used were: monoclonal p-HSP27 Ser^{82} (1:1000, clone D1H2, catalog number 9707S), polyclonal p-HSP27 Ser^{15} (1:1000, catalog number 2404S), monoclonal HSP27 (1:1500, catalog number 2402), and polyclonal p38 (1:1000, catalog number 9218S) all from Cell Signaling Technology; monoclonal p-HSP27 Ser^{78} (1:2000, clone Y175, catalog number ab32501, Abcam); polyclonal AUF1 (1:4000, catalog number 07260MI, Millipore); polyclonal p-p38 (1:1000, catalog number p190-1802, PhosphoSolutions)*;* monoclonal α-tubulin (1:5000, catalog number ab6160, Abcam); monoclonal β-actin (1:2000, clone AC-15, catalog number A2228, Sigma); polyclonal γ-actin (1:5000, catalog number NB600-533, Novus Biologicals); and monoclonal GAPDH (1:2500, clone GAPDH-71.1, catalog number G8795, Sigma). All secondary antibodies from the appropriate species were horseradish peroxidase-conjugated (Jackson Laboratories) and diluted 1:10000.

Quantitative PCR

RNA was isolated using TRI Reagent (Life Technologies) or RNeasy kit (Qiagen) at the time points indicated. cDNA synthesis and quantitative PCR was performed using previously published protocols and manufacturers' instructions (10) (SYBR Green, Life Technologies). Primers for GAPDH (F: 5'-GCATGGCCTTCGGTGTCC-3', R: 5'-AATGCCAGCCCCAGCGTCAAA-3'), IL-6 (F: 5'-ACATCCTCGACGGCATCTCA-3', R: 5'-TCACCAGGCAAGTCTCCTCA-3'), IL-8 (F: 5'-GCTCTGTGTGAAGGTGCAGT-3', R: 5'-TGCACCCAGTTTTCCTTGGG-3'), GMCSF cDNA was amplified using a Taqman probe/primer set and normalized to GAPDH (catalog numbers Hs00929873_m1 and Hs02758991_g1, respectively, and Taqman Fast Advanced master mix, Life Technologies).

RNA immunoprecipitation (RIP)

Cell pellets from two 150mm dishes of BJ fibroblasts were lysed in the same buffer used for western blot analysis (MCLB). Protein concentration was analyzed using the Bradford Protein Assay (Bio-Rad). 1 mg of protein was used for each immunoprecipitation. 15 μg of polyclonal AUF1 (catalog number 07260MI, Millipore) was used. An equivalent amount of normal rabbit IgG antibody (catalog number 2729S, Cell Signaling) was used to control for specific immunoprecipitation. Cell lysates were pre-cleared with 20 μL protein A Dynabeads (Life Technologies) for 30 minutes at 4°C prior to incubation with the indicated antibody overnight at 4˚C in total volume of 1mL MCLB supplemented with 1μL RNAseOUT (Invitrogen). 100 μL Protein A Dynabeads were used for each immunoprecipitation. Beads were washed 2 times in 0.1 M monosodium phosphate, 3 times in Buffer A (1x PBS, 0.1% SDS, 0.3% sodium deoxycholate, 0.3% NP40), and 2 times in MCLB, then incubated with samples for 4 hours at

4˚C with rotation. Immunoprecipitated beads were washed 2 times with each of the following buffers: Buffer A, Buffer B (5x PBS, 0.1% SDS, 0.5% sodium deoxycholate, 0.5% NP40) and Buffer C (50 mM Tris pH 7.4, 10 mM magnesium chloride, 0.5% NP40). RNA was isolated from the beads by adding 1 mL of TRI Reagent (Life Technologies). Following cDNA synthesis, mRNA levels of SASP factors were analyzed by qPCR using the primers and procedures described above.

Senescence-associated β-galactosidase

SA-β-gal staining was carried out on subconfluent cells as described previously (6, 26).

Co-culture

Co-culture experiments were performed as previously described (10). Briefly, 1.3×10^4 BJ fibroblasts were plated in black-walled 96-well plates. 24h later, cells were treated with 0.1 units/mL bleomycin for 24h. Cells were then incubated in starve medium (DMEM F-12 + 1% penicillin/streptomycin) for 24h before addition of CDD111 and CDD450. Inhibitors were refreshed daily for 2 days before the addition of HaCaT-CBR cells. HaCaT-CBR cells were cultured in starve medium for 24 hours prior to plating on fibroblasts. 1.0×10^3 HaCaT-CBR cells were plated on fibroblasts and incubated with inhibitors for 72h. After 72h, D-luciferin (Biosynth, Naperville, IL) was added to a final concentration of 150 μg/mL. After ten minutes, plates were imaged using an IVIS 100 camera (PerkinElmer) using the following settings: exposure=5 min, field of view=15, binning=16, f/stop=1, open filter.

Results

HSP27 destabilizes SASP factor mRNA in pre-senescent cells.

SASP factor mRNAs are regulated at the transcriptional and post-transcriptional levels (10). Indeed, our previous work demonstrated that the stress kinase p38MAPK stabilizes SASP factor mRNAs by altering the RNA binding and destabilizing ability of AUF1, which can target these mRNAs for degradation. Importantly, the increased mRNA stability is induced only after the establishment of the senescent phenotype as indicated by expression of senescence-associated β-galactosidase (SA-β-Gal) and morphological changes. In verification of our previous results, when transcription is inhibited with actinomycin D (ActD) immediately following a senescence-inducing dose of bleomycin but before SA-β-Gal is expressed and morphological changes are observed (pre-senescent), abundance of the SASP factor mRNAs IL6, IL8, and GM-CSF is significantly reduced compared to similar treatment of senescent cells (**Fig. 2.1A & 2.1B**). This indicates that transcriptionally-driven mechanisms are responsible for inducing increased SASP expression in pre-senescent cells, and SASP factor mRNA levels are maintained by post-transcriptional mechanisms in senescent but not pre-senescent cells.

Our previous work demonstrated that p38MAPK inhibition decreased SASP factor mRNA stability in senescent cells in part by allowing AUF1 to remain active and bound to the UTRs of these mRNAs, resulting in their degradation (10). Because AUF1 is not a p38MAPK target, we wanted to determine how p38MAPK impacted the ability of AUF1 to regulate SASP factor mRNA degradation following the induction of senescence. For this reason, we turned our attention to HSP27 because it is a downstream target of p38MAPK through MK2, and previous

studies demonstrated that HSP27 could regulate mRNA stability as a member of the AUF1-containing ASTRC complex in other experimental settings (22, 23, 27). To determine whether HSP27 could regulate mRNA stability in pre-senescent cells, we transduced BJ fibroblasts with a control short hairpin (shSCR) or a short hairpin targeting HSP27 (shHSP27), resulting in an 80% reduction of HSP27 protein (**Fig. 2.1C**). Next, we treated control and HSP27-depleted cells with bleomycin to induce senescence and found that HSP27 depletion did not significantly affect the ability of cells to enter senescence as quantified by SA-β-Gal activity (**Fig. 2.1D & 2.1E**). 24h after bleomycin addition, cells were treated with ActD to assess the stability of SASP factor transcripts. Indeed, there was a significant increase in the amount of IL6, IL8, and GM-CSF mRNA remaining in pre-senescent cells depleted of HSP27 relative to shSCR-expressing cells after transcriptional inhibition (**Fig. 2.1F**), demonstrating that HSP27 acts to destabilize target SASP mRNAs in pre-senescent cells. Previous studies have demonstrated that HSP27 can regulate AUF1 levels, suggesting that HSP27 regulates mRNA stability by modulating AUF1 abundance (20, 22). In our system, we failed to find evidence that HSP27 modulated AUF1 levels, suggesting the mRNA stabilization we observed was not a result of a change in AUF1 abundance (**Fig. 2.1C**).

Because depletion of AUF1 stabilizes SASP factor mRNAs in pre-senescent cells suggesting AUF1 functions to destabilize these mRNAs (10), we next wanted to determine whether HSP27 affected the ability of AUF1 to bind to SASP mRNAs and alter their stability. To test this possibility, we utilized RNAi to deplete HSP27 from BJ fibroblasts, and induced senescence via bleomycin treatment. We then performed an RNA-immunoprecipitation (RIP) to capture AUF1-bound mRNAs. GAPDH mRNA, which does not contain an ARE, was not

significantly immunoprecipitated by an anti-AUF1 antibody relative to IgG control, but the anti-AUF1 antibody did immunoprecipitate the ARE-containing IL-6 and IL-8 mRNAs. Surprisingly, depletion of HSP27 resulted in increased AUF1 binding to IL-6 and IL-8 mRNAs, from 0.36% to 0.74% of input for IL-6, and 1.62% to 2.51% of input for IL-8 in shSCR versus shHSP27-expressing cells (**Fig. 2.1G**). This finding demonstrates that although AUF1 is necessary for mRNA degradation in pre-senescent cells (10), its binding alone is insufficient to induce mRNA degradation in pre-senescent fibroblasts depleted of HSP27. Together these data suggest that an additional, HSP27-dependent activity is required to drive AUF1-mediated mRNA degradation in pre-senescent cells.

p38MAPK and MK2 regulate mRNA stability in senescent cells.

We previously demonstrated that p38MAPK regulates the transition from unstable SASP factor mRNAs in pre-senescent cells to stable mRNAs with longer half-lives in senescent cells, in part by regulating the ability of AUF1 to bind and target these mRNAs for degradation (10). In response to p38MAPK activation, the downstream kinase MK2 can induce stabilization of certain ARE-containing mRNAs, and the p38MAPK-MK2-HSP27-AUF1 axis has been implicated in regulation of mRNA stability in THP-1 monocytes (22, 24). Furthermore, MK2 was recently shown to impact SASP expression (21, 28). Thus, to interrogate the role of the p38MAPK-MK2 pathway in the senescence-associated mRNA stabilization phenotype, we utilized two inhibitor compounds. SB203580 (p38i) is a small molecule inhibitor of p38α and p38β, which we used at a concentration that minimizes off-target effects (10μM) (29, 30). CDD450 (MK2i) is a novel p38/MK2 pathway inhibitor that selectively targets the p38MAPK/MK2 complex, inhibiting activation of MK2 by p38MAPK while allowing

p38MAPK to phosphorylate other downstream targets (data not shown), providing us with a tool to investigate the effects of p38MAPK-dependent MK2 phosphorylation on SASP mRNA stabilization. Treatment with p38i or MK2i as indicated resulted in a 90% and 95% reduction in p38MAPK and MK2 activity, respectively, as measured by average inhibition of HSP27 phosphorylation (**Fig. 2.2A-2.2C**).

To confirm the role of p38MAPK activity in the transition from transcriptional regulation to post-transcriptional stabilization of SASP mRNAs as cells become senescent, we assayed mRNA stability in cells treated with p38i. As previously reported (10), we found that treatment with p38i significantly reduced the expression of the SASP factors IL-6, IL-8, and GM-CSF by 62%, 92%, and 67% relative to vehicle-treated senescent cells (**Fig. 2.2D**). p38i also significantly inhibited the stabilization of these mRNAs in senescent cells, by 61%, 46%, and 75% for IL-6, IL-8, and GM-CSF, respectively (**Fig. 2.2E**). Demonstrating that MK2 functioned downstream of p38MAPK in senescent cells, we found that MK2i treatment inhibited expression of IL-6, IL-8, and GM-CSF by 32%, 71%, and 56% relative to vehicle-treated senescent cells (**Fig. 2.2D**). Furthermore, MK2 pathway inhibition prevented mRNA stabilization in senescent cells, with a 62%, 57%, and 60% reduction in mRNA remaining after 24h ActD treatment for IL-6, IL-8, and GM-CSF, respectively (**Fig. 2.2E**). Thus, MK2 activity is required for the stabilization of SASP factor transcript stability in senescent fibroblasts.

The p38MAPK-MK2-AUF1 axis regulates mRNA stability in senescent cells through HSP27 phosphorylation.

Because HSP27 is required for mRNA degradation in pre-senescent cells, and p38MAPK and MK2 are required for SASP factor mRNA stability in senescent cells, we next asked if p38MAPK-MK2-dependent HSP27 phosphorylation impacted mRNA stability in pre-senescent and senescent cells. In pre-senescent cells, AUF1 activity and increased levels of non-phosphorylated HSP27 correlate with mRNA degradation (10). Because MK2-dependent phosphorylation of HSP27 on Ser^{15}, Ser^{78}, and Ser^{82} in THP-1 monocytes and HeLa cells impacts mRNA stability (20, 22, 23), we asked what role HSP27 phosphorylation plays in mRNA stability in senescent cells. Analysis of HSP27 phosphorylation revealed a p38MAPK- and MK2-dependent increase in phosphorylation at all three serines in senescent versus pre-senescent cells (**Fig. 2.2B**). To investigate the role of p38MAPK-MK2-dependent HSP27 phosphorylation, we simultaneously depleted cells of endogenous HSP27 and ectopically expressed either a FLAG-tagged wild type or mutant HSP27 allele. HSP27-TriD has serine-to-asparagine phosphomimetic mutations at each of the three key serine residues. If HSP27 phosphorylation drives SASP mRNA stability, expression of HSP27-TriD in pre-senescent cells should create a senescent-like mRNA stability phenotype in pre-senescent cells. Conversely, HSP27-TriA has serine-to-alanine mutations at the key serine residues that prevent it from being phosphorylated, and should therefore result in a pre-senescent-like, lower mRNA stability state in senescent cells.

To assess in the impact of HSP27 phosphorylation on mRNA stability in senescent cells, we first simultaneously knocked down the endogenous HSP27 with an HSP27 short hairpin

(shHSP27) and ectopically expressed shRNA-resistant FLAG-tagged HSP27 alleles in BJ fibroblasts. As previously reported in monocytes, HSP27-TriD expression is very low compared to HSP27-WT or HSP27-TriA (22), however in contrast to that report, AUF1 protein levels were not affected by the expression of these mutants (**Fig. 2.3A**). Importantly, the expression of neither wild type nor the HSP27 mutants affected the ability of cells to enter senescence as quantified by SA-β-Gal staining (**Fig. 2.3B & 2.3C**). However, we found that the phosphorylation state of HSP27 did regulate mRNA stability in pre-senescent and senescent cells, independent of AUF1 levels. Cells expressing HSP27-WT, HSP27-TriD, or HSP27-TriA were treated with bleomycin to induce senescence for 24h and then treated with ActD to inhibit transcription either immediately following bleomycin treatment (pre-senescent) or 96h post-bleomycin treatment (senescent). In pre-senescent cells, as expected, transcriptional inhibition resulted in degradation of SASP factor mRNAs in cells expressing HSP27-WT (**Fig. 2.3D**). However, expression of the HSP27-TriD mutant resulted in significantly increased mRNA stability compared to cells expressing HSP27-WT, demonstrating that phosphorylated HSP27 protects SASP factor mRNAs from degradation and is sufficient to create a senescent-like mRNA stabilization state in pre-senescent cells (**Fig. 2.3D**). Conversely, expression of the non-phosphorylatable mutant HSP27-TriA in senescent cells resulted in significantly decreased mRNA stability compared to HSP27-WT. This demonstrated that HSP27 phosphorylation on p38MAPK-MK2 target sites is necessary for senescence-associated mRNA stabilization and preventing this phosphorylation can create a pre-senescent-like mRNA instability state in senescent cells. Because the endogenous and FLAG-tagged HSP27 expression levels were so low in cells expressing shHSP27 + HSP27-TriD, and the phenotype recapitulates that observed in cells only expressing shHSP27, we transduced FLAG-tagged HSP27-TriD without the hairpin

into BJ fibroblasts and repeated the mRNA stability assay in pre-senescent cells to ensure the observed stabilization was due to HSP27-TriD expression rather than loss of endogenous HSP27. We again found that expression of HSP27-TriD significantly increased the stability of IL-6 and IL-8 mRNAs, recapitulating a senescent-like mRNA stability state in pre-senescent cells (**Fig. 2.3E & 2.3F**).

We previously found that AUF1 binding to SASP factor mRNAs decreases from pre-senescence to senescence in a p38MAPK-dependent manner. Thus, we next wanted to determine whether the pre-senescent-like state created by expression of HSP27-TriA in senescent cells recapitulated the pre-senescent AUF1 binding state, *i.e.* increased AUF1 occupancy. We performed a RIP in senescent BJ fibroblasts expressing shHSP27 and either HSP27-WT or HSP27-TriA. When AUF1 was immunoprecipitated from these cells we found that expression of HSP27-TriA significantly increased AUF1 binding from 0.15% to 0.30% of input for IL-6, 0.92% to 1.58% of input for IL-8, and 0.26% to 0.41% of input for GM-CSF mRNAs as compared to HSP27-WT (**Fig. 2.3G**). Previous studies and our data from shHSP27-expressing cells (**Fig. 2.1F & 2.1G**) argue that AUF1 binding to target mRNAs is not the only determinant of ARE-mediated mRNA degradation. However, we did find that AUF1 binding in HSP27-TriA-expressing senescent cells was increased while mRNA stability was decreased, recapitulating what is observed in wild type pre-senescent cells thus confirming that decreased AUF1 binding is a component of SASP mRNA stability regulation in senescent cells.

The p38MAPK-MK2-HSP27 axis promotes stromal-supported tumor cell growth.

Previously we demonstrated that senescent stroma promotes tumor cell growth, and inhibiting p38MAPK signaling in the stroma significantly reduces this growth promotion (10). Because p38MAPK inhibition studies in patients have suggested that cells develop resistance mechanisms to p38MAPK inhibition (31-33) and we find that MK2 is an important player in SASP mRNA stability, we investigated whether targeting the MK2 arm of the p38MAPK pathway would inhibit stromal-supported tumor growth. Along with the p38MAPK inhibitor CDD111 (p38i′), we again utilized CDD450 (MK2i), which prevents p38MAPK from phosphorylating MK2, providing a more selective inhibition of the MK2 pathway while preserving alternate p38MAPK activity. Both p38i′ and MK2i inhibited the pathway as evidenced by reduced HSP27 phosphorylation, inhibition of the upregulation and post-transcriptional stabilization of SASP factors. Both IL-6 and IL-8 upregulation and mRNA stabilization were significantly inhibited by treatment with both p38i′ and MK2i (Fig. 4A-D). To test whether MK2 pathway inhibition could prevent senescent stroma from promoting tumor growth, we cultured BJ skin fibroblasts with preneoplastic HaCaT keratinocytes expressing click beetle red (CBR) luciferase (HaCaT-CBR). BJ fibroblasts were treated with bleomycin and p38i′ or MK2i for 96h to allow the fibroblasts to senesce, and then HaCaT-CBR cells were plated as indicated (**Fig. 2.4E**). As expected, senescent BJ fibroblasts significantly increased the growth of HaCaT-CBR cells compared to non-senescent BJ fibroblasts (**Fig. 2.4E**). Further, as previously reported, p38MAPK inhibition abrogated this growth by an average of 66.1%. Importantly, treatment with MK2i resulted in an average 73.6% reduction in tumor cell growth promotion

(**Fig. 2.4E**) and this reduction in HaCaT-CBR growth was due to inhibition of the p38MAPK-MK2 pathway in the stroma specifically, because neither p38i′ nor MK2i treatment significantly affected the growth of HaCaT-CBR cells cultured independently. These data indicate that MK2 pathway inhibition is a viable therapeutic strategy that can specifically prevent senescent stromal promotion of tumor cell growth.

Discussion

The SASP is regulated by a multitude of signaling pathways at the levels of transcription, mRNA stability, and translation. In cells irradiated to induce senescence, p38MAPK is activated with slow kinetics, with peak phosphorylation of p38MAPK and HSP27 not occurring until 8-10 days post-irradiation (9). Inhibition of p38MAPK with SB203580 or knockdown using an shp38α hairpin prevented the expression of SASP factors at the protein and mRNA levels, suggesting that p38MAPK regulates SASP factor transcription (9, 10). Indeed, NFκB binding activity increases slowly in senescence reflecting p38MAPK activation, and p38MAPK activity is sufficient to induce NFκB binding.

In addition to transcriptional regulation, we previously demonstrated that p38MAPK regulates SASP factor expression through stabilization of target mRNAs in senescent cells, in an AUF1-dependent manner (10). Here, we demonstrate that the presence of HSP27 and its p38MAPK-MK2-dependent phosphorylation state regulate SASP mRNA stability in pre-senescent and senescent cells. In pre-senescent cells, increased levels of non-phosphorylated

HSP27 relative to senescent cells (**Fig. 2.2B & 2.2C**) promotes SASP factor mRNA degradation in a manner independent of AUF1 binding, as depletion of HSP27 increased both mRNA stability and AUF1 binding to SASP mRNAs (**Fig. 2.1G**). Additionally, the stability of SASP factor mRNAs is dependent on the phosphorylation state of MK2 target sites on HSP27. In pre-senescent cells, mRNA degradation correlates with reduced levels of HSP27 phosphorylation, while in senescent cells increased mRNA stability is correlated with increased HSP27 phosphorylation. The importance of HSP27 phosphorylation was underscored by our finding that expression of the phosphomimic HSP27-TriD in pre-senescent cells recapitulated the senescent state (i.e. stabilized mRNA). In contrast, expression of the phospho-dead HSP27-TriA resulted in destabilization of SASP mRNAs and thus created a pre-senescent-like state in senescent cells (**Fig. 2.3D**). These data support the hypothesis that HSP27 phosphorylation is required to stabilize SASP mRNAs. Furthermore, phosphorylation of HSP27 is required for removal of AUF1 from SASP mRNAs in senescent cells, since HSP27-TriA expression increased AUF1 binding in senescent cells while decreasing mRNA stability (**Fig. 2.3G**). This suggests that in senescent cells, AUF1 binding is correlated with stability and binding may be a regulatory mechanism in that state. A previous study in lymphocytes demonstrated that HSP27's phosphorylation state regulates the abundance and stability of AUF1 resulting in mRNA stabilization in that system (20, 22). However, we did not observe consistent changes in AUF1 levels upon HSP27 knockdown or expression of the HSP27 mutants, suggesting that an alternate p38-MK2-HSP27 dependent mechanism of regulating AUF1-mediated mRNA degradation is active in senescent fibroblasts.

AUF1 activity is regulated at several levels in different cellular contexts. In certain systems, AUF1-mediated mRNA degradation is regulated by AUF1 binding to target mRNAs, which can be affected by altering AUF1's binding ability or through modulation of AUF1 levels within the cell. However, AUF1 binding alone is not always predictive of mRNA degradation, since AUF1 binding has also been reported to protect mRNAs from degradation (15, 17, 34). Indeed, all four isoforms of AUF1 can promote mRNA degradation and/or protection depending on cell type and context, and the isoforms have different ARE-binding affinities, suggesting that AUF1 can regulate mRNA stability through context-specific binding of its four isoforms (12, 14, 16, 17, 35). Furthermore, AUF1 activity can be regulated by post-translational modifications. In THP-1 lymphocytes, phosphorylated $p40^{AUF1}$ is associated with TNFα mRNA degradation whereas non-phosphorylated $p40^{AUF1}$ is associated with longer TNFα mRNA half-life and higher levels of translation, suggesting phosphorylated $p40^{AUF1}$ is actively involved in AMD (18, 19). Conversely, phosphorylation of $p40^{AUF1}$ is required for ubiquitin-mediated AUF1 degradation in HeLa cells, resulting in increased mRNA stability (20). Together, these observations illustrate the complexity and context-specificity of the regulatory mechanisms governing AUF1's roles in mRNA stability.

Our data suggest that the phosphorylation state of HSP27 and the binding of AUF1 impact mRNA stability in pre-senescent and senescent cells (**Fig. 2.5**). Indeed, non-phosphorylated HSP27 favors AMD as evidenced by our findings that (i) in pre-senescent cells, which have low p38MAPK activity and reduced levels of phosphorylated HSP27, HSP27 depletion results in mRNA stabilization despite increased AUF1 binding, and (ii) expression of the non-phosphorylatable allele HSP27-TriA results in mRNA degradation in senescent cells.

Thus, our data suggest an important role for non-phosphorylated HSP27 in AMD in pre-senescent cells, because if phosphorylated HSP27 were the only state in which HSP27 regulated mRNA stability, then HSP27 depletion in pre-senescent cells should result in increased mRNA degradation due to the lack of basal phospho-HSP27 in the system. This activity may occur through HSP27-dependent recruitment or activation of other ASTRC members.

Together, these observations suggest that senescence-associated AMD is regulated by HSP27 and AUF1 activity, and that the role of HSP27 may be upstream of AUF1 during pre-senescence. In pre-senescent cells, p38MAPK activity is low, and both AUF1 and HSP27 actively promote AMD, resulting in SASP mRNA degradation (**Fig. 2.5A**). This suggests that non-phospho-HSP27 is its AMD-promoting state. When HSP27 is depleted in pre-senescent cells, the lack of non-phospho, AMD-promoting HSP27 results in mRNA stabilization despite AUF1 binding to target mRNAs (the increase in AUF1 binding observed in shHSP27 cells may be due to the reduction of basal levels of phospho- or AMD-inhibiting HSP27). This indicates that although AUF1 is necessary, AUF1 binding is insufficient to drive AMD without HSP27 in pre-senescent cells. Once the p38MAPK pathway is activated and cells are senescent (**Fig. 2.5B**), AUF1 activity appears to be regulated at the level of binding, since both inhibition of the p38MAPK pathway as well as expression of the non-phosphorylatable HSP27-TriA result in loss of the senescence-associated decrease in AUF1 binding and subsequent destabilization of SASP mRNAs (10).

Like p38MAPK inhibition, inhibition of the MK2 pathway prevents SASP mRNA stabilization, and our data with HSP27-TriA and HSP27-TriD suggest that phosphorylation of

MK2 target sites on HSP27 drives this phenotype. Recently, Herranz *et al.* demonstrated that mTOR modulates MK2 translation in the context of oncogene-induced senescence (OIS), allowing MK2 to phosphorylate and inactivate ZFP36L1, another mRNA destabilizing protein that binds AU rich elements similarly to AUF1. They suggest that this ZFP26L1 phosphorylation then prevents ARE-containing SASP mRNAs from being degraded in senescent cells resulting in SASP factor upregulation. Our previous data demonstrate that AUF1 binds and targets SASP mRNAs for degradation in pre-senescent but not senescent cells and that depletion of AUF1 from pre-senescent cells stabilizes SASP mRNAs (10). Here we demonstrate HSP27's MK2-dependent regulation of AUF1 occupancy on SASP mRNAs in senescent cells. These findings together suggest that MK2 has a multifaceted role in the regulation of SASP factor mRNA stability and upregulation, further supporting MK2 as a promising drug target for inhibition of the p38MAPK pathway.

The p38MAPK pathway regulates the expression of many pro-inflammatory cytokines and other factors responsible for chronic inflammatory diseases such as chronic obstructive pulmonary disease (COPD), rheumatoid arthritis (RA), psoriasis, and Chron's disease (33), and therefore has been an attractive target for treating the inflammation associated with these diseases. Furthermore, we previously demonstrated that p38MAPK inhibition prevents tumor growth driven by a senescent microenvironment (10). However, clinical trials for the inflammatory diseases discussed above have so far been met with disappointing outcomes, due to problems such as low efficacy, adverse side effects, and a rebound effect observed in trials using p38MAPK inhibitors for the treatment of multiple diseases, wherein a transient drop in inflammation as measured by the level of C-reactive protein (CRP) is quickly followed by a

return to baseline (31, 36, 37). This rebound effect may be due to inhibition of downstream anti-inflammatory substrates of p38MAPK (e.g. MSK1/2 or MKP1), and could be circumvented by more selectively targeting the pro-inflammatory p38MAPK substrate MK2. Furthermore, decreased inflammatory responses in MK2 knockout mice have been associated with decreased tumorigenesis in colon and skin models (38, 39). Current cancer treatment modalities largely target tumor cells, neglecting the critical impact of the tumor microenvironment on tumor establishment and growth. Modulation of the tumor microenvironment is sufficient to promote or restrain tumor cell growth, demonstrating that stromal-specific therapies or co-therapies are a promising therapeutic avenue, and targeting the SASP through p38MAPK and MK2 activity is a possible means to do so. Herranz *et al.* demonstrated that the mTOR/MK2/ZFP36L1 pathway mediates the pro-tumorigenic aspects of the SASP. Here, we have demonstrated that MK2 also regulates the SASP through HSP27 and AUF1. Furthermore, we have shown that inhibition of the MK2 pathway is as effective as p38MAPK inhibition at limiting the expression and mRNA stabilization of SASP factors, thereby preventing senescent stroma from promoting the growth of pre-neoplastic HaCaT keratinocytes *in vitro* and demonstrating that targeting the MK2 pathway is a viable means of circumventing the putative shortcomings seen with p38MAPK inhibition in a clinical setting. Further studies in an *in vivo* setting will investigate the viability of inhibiting the MK2 pathway by CDD450 as a stromal-specific cancer therapy.

Acknowledgements

We thank Julie Prior and the ICCE Institute at Washington University School of Medicine for live cell imaging, and Megan Ruhland and Kevin Flanagan for helpful comments.

This work was supported by the Cancer Biology Pathway, Siteman Cancer Center at Barnes Jewish Hospital and Washington University Medical School (HM), NIH grants GM007067 to (EA) and CA130919 (SAS), and American Cancer Society Research Scholar Award (SAS).

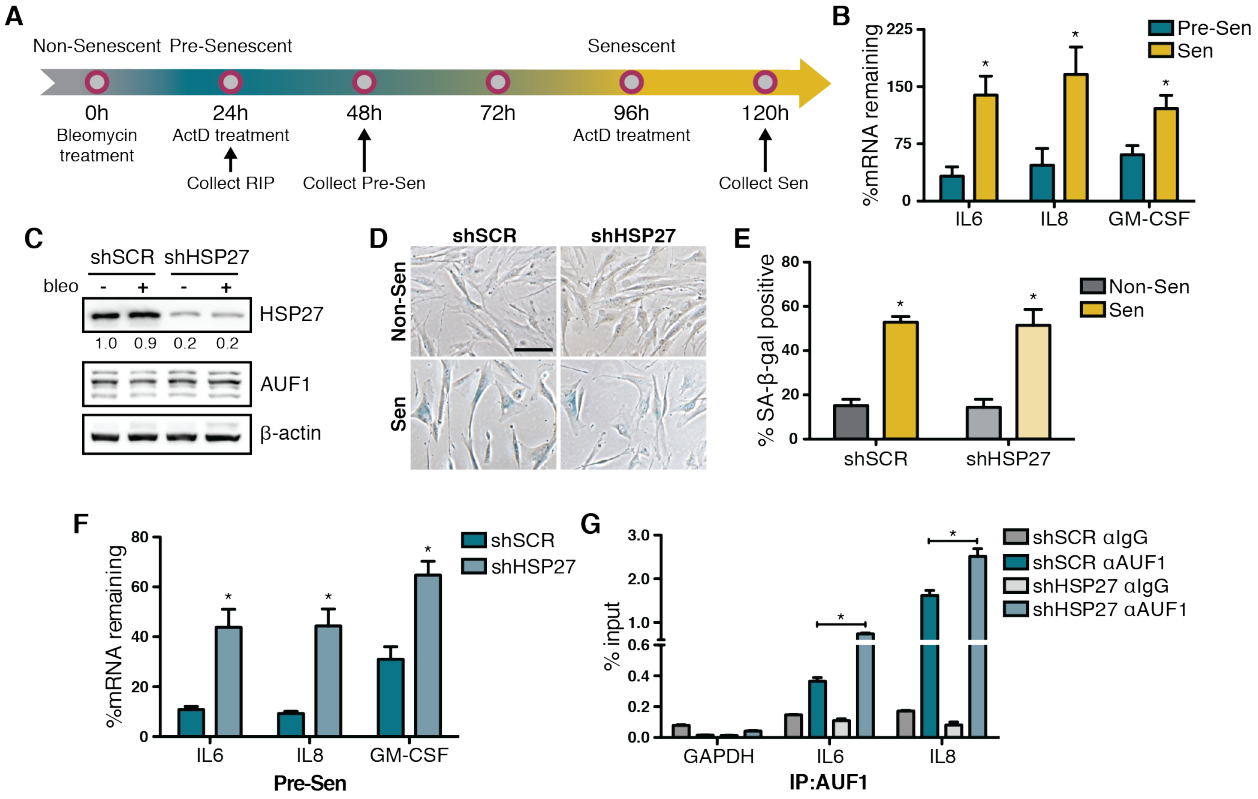

Figure 2.1: HSP27 promotes SASP mRNA degradation in pre-senescent cells.

A. Timeline of bleomycin and actinomycin D (ActD) treatment to induce stress-induced premature senescence and inhibit transcription in BJ fibroblasts. Fibroblasts were treated with bleomycin (0.1 units/mL) for 24h and subsequently treated with 10μg/mL ActD for 24h starting either 24h or 96h after bleomycin treatment. Cells collected at 48h were considered pre-senescent (Pre-Sen) while those collected at 120h were considered senescent (Sen). **B.** Cells were collected after ActD treatment and SASP factor levels were quantified by qRT-PCR. Percent mRNA (%mRNA) remaining was calculated as the ratio of ActD-treated to vehicle-treated levels of target mRNA, normalized to GAPDH, n=6. **C.** Immunoblot of indicated proteins in cells expressing an shSCR or shHSP27 hairpin, treated as indicated. The ratio of knockdown is reported under the HSP27 blot as amount of protein remaining in shHSP27 compared to shSCR cells after normalizing to β-actin. **D, E.** Representative images, *D*, and quantification, *E*, of senescence-associated β-galactosidase (SA-β-Gal) activity in non-senescent and senescent cells expressing either shSCR or shHSP27. Images acquired with a 10x objective, scale bar = 10μm, n=3. **F.** Control or HSP27-depleted cells were treated as in A, ActD treated at the pre-senescent timepoint, and collected 24h later. n=9 for IL-6 and IL-8, and n=3 for GM-CSF. **G.** BJ fibroblasts expressing either shSCR or shHSP27 were induced to senesce and collected 24h post-bleomycin addition (pre-senescent), and AUF1-bound RNA was isolated by RNA immunoprecipitation. Lysates were incubated with 15 μg of either control rabbit IgG (gray bars) or rabbit anti-AUF1 antibody (blue bars). The RNA bound to precipitated protein was isolated and levels were analyzed by qRT-PCR. Representative experiment shown, n=4. * = $p<0.05$, error bars are + S.E.M.

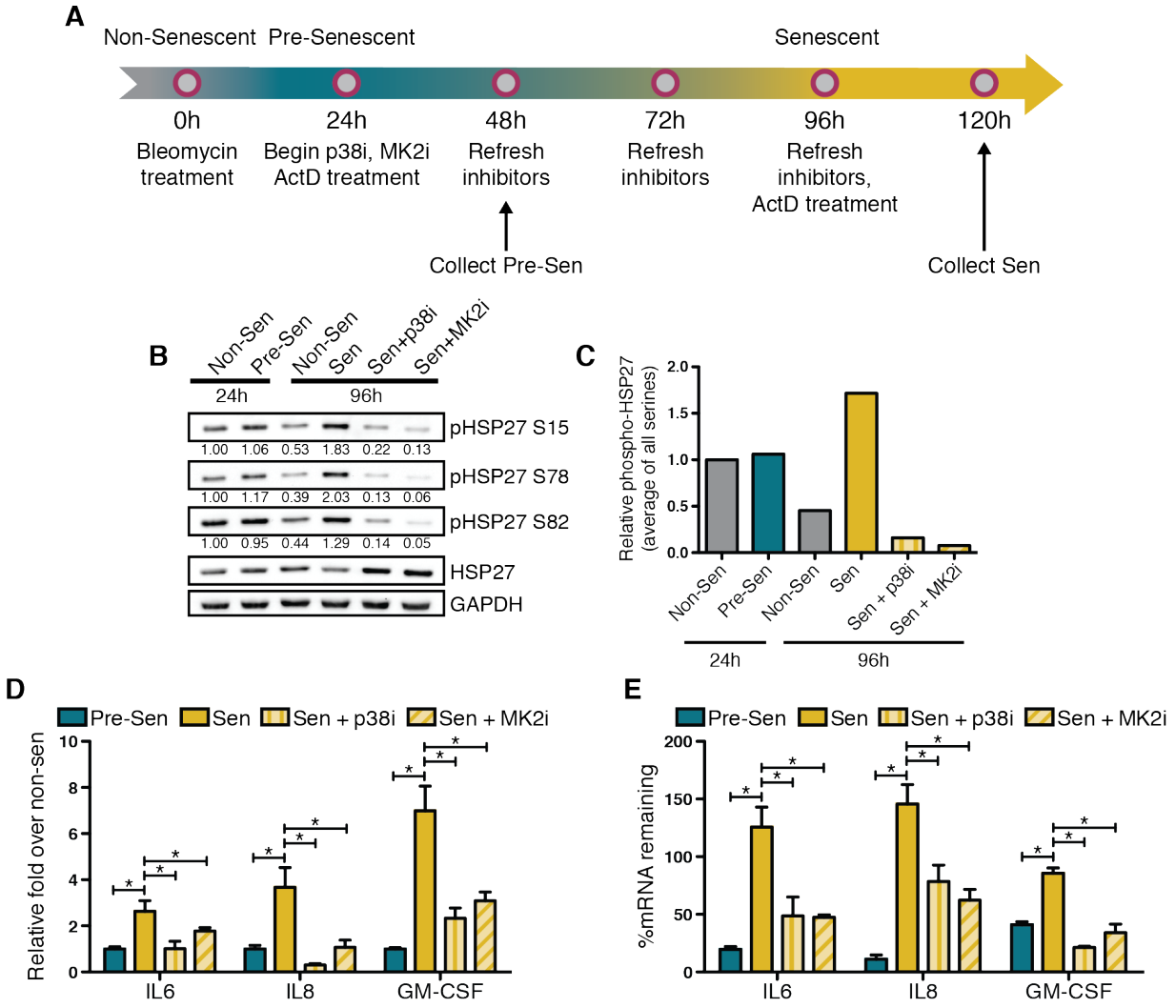

Figure 2.2: p38MAPK and MK2 regulate SASP mRNA stability in senescent cells.

A. Schematic of senescence induction by bleomycin treatment and inhibition of p38MAPK and MK2 pathways by treatment with 10 μM SB203580 or 1 μM CDD450, respectively. **B, C.** Immunoblot and quantification of phospho-HSP27 at Ser15, Ser78 and Ser82, the three MK2 targets, upon p38MAPK or MK2 pathway inhibition 48h (Pre-Sen) and 120h (Sen) post-bleomycin treatment. Phospho-HSP27 was normalized to total HSP27 and the ratio of phosphorylation at each site is found under each blot and the average of all three phosphorylated residues is represented in *C*. **D.** Upregulation of SASP factors in senescent cells treated with p38i or MK2i as in *A* without transcriptional inhibition. mRNA levels were determined by qRT-PCR and are represented as fold increase over non-senescent cells, normalized to GAPDH. **E.** Cells were induced to senesce and treated with p38i and MK2i as shown in *A*, and ActD treated to inhibit transcription for 24h. %mRNA remaining is calculated as the amount of mRNA in ActD-treated cells relative to vehicle-treated cells. D and E are representative experiments, n=5, *=p<0.05, error bars are + S.E.M

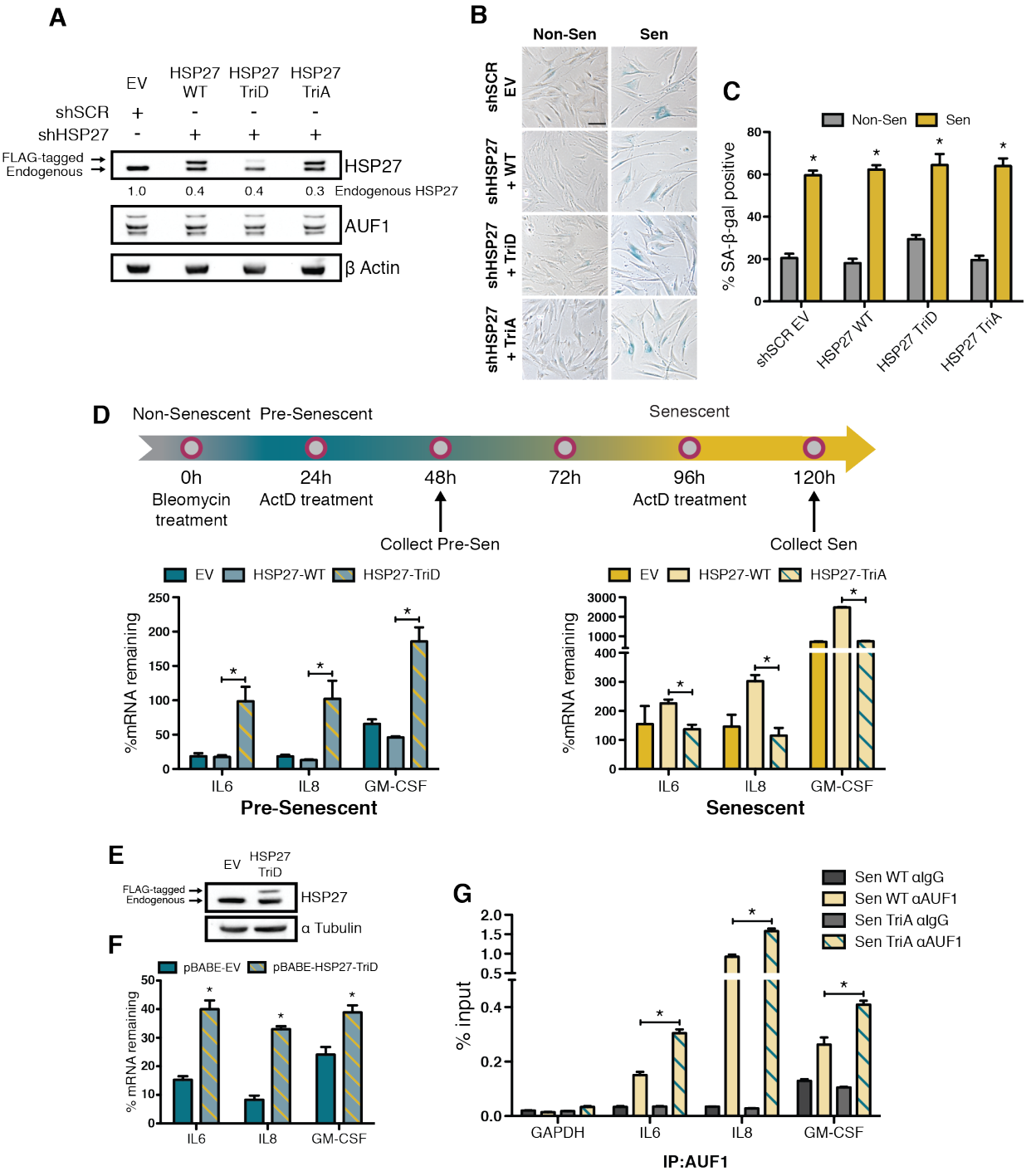

Figure 2.3: p38MAPK-dependent phosphorylation of HSP27 regulates SASP factor mRNA stability in senescent cells.

A. Immunoblot of simultaneous knockdown of endogenous HSP27 (lower band) and ectopic expression of FLAG-tagged HSP27 mutant alleles (upper band) in BJ fibroblasts. Percent of HSP27 knockdown after normalization to β-actin is presented under the HSP27 immunoblot. **B, C.** Representative images, *B*, and quantification, *C*, of SA-β-Gal expression in non-senescent and senescent cells expressing pRESQ-

shSCR-EV or pRESQ-shHSP27-Flag-HSP27 WT, TriD, or TriA. Images acquired with a 10x objective, scale bar = 10μm, n=2. **D.** (Top) Timeline of senescence induction and ActD treatment. BJ fibroblasts expressing the HSP27 constructs were treated with bleomycin for 24h and ActD for 24h either immediately after bleomycin treatment (pre-senescent, left) or 96h post-bleomycin treatment (senescent, right), mRNA levels were analyzed by qRT-PCR. %mRNA remaining was calculated as the mRNA level in ActD-treated cells relative to vehicle-treated cells, normalized to GAPDH. Representative experiment, n=3. **E.** Immunoblot of HSP27 expression in cells transduced with pBABE-EV or pBABE-HSP27-TriD. **F.** Cells expressing either pBABE-EV or HSP27 TriD were treated as in *A* and collected at the pre-senescent timepoint. Representative experiment, n=2, *=$p<0.05$. **G.** BJ fibroblasts expressing a hairpin targeting HSP27 while simultaneously expressing flag-tagged HSP27 WT or TriA were induced to senesce by bleomycin treatment. Cells were collected 96h post-bleomycin (senescent) and anti-AUF1 RIP was performed using nonspecific IgG or an anti-AUF1 specific antibody. Representative experiment, n=3. *=$p<0.05$, error bars are + S.E.M.

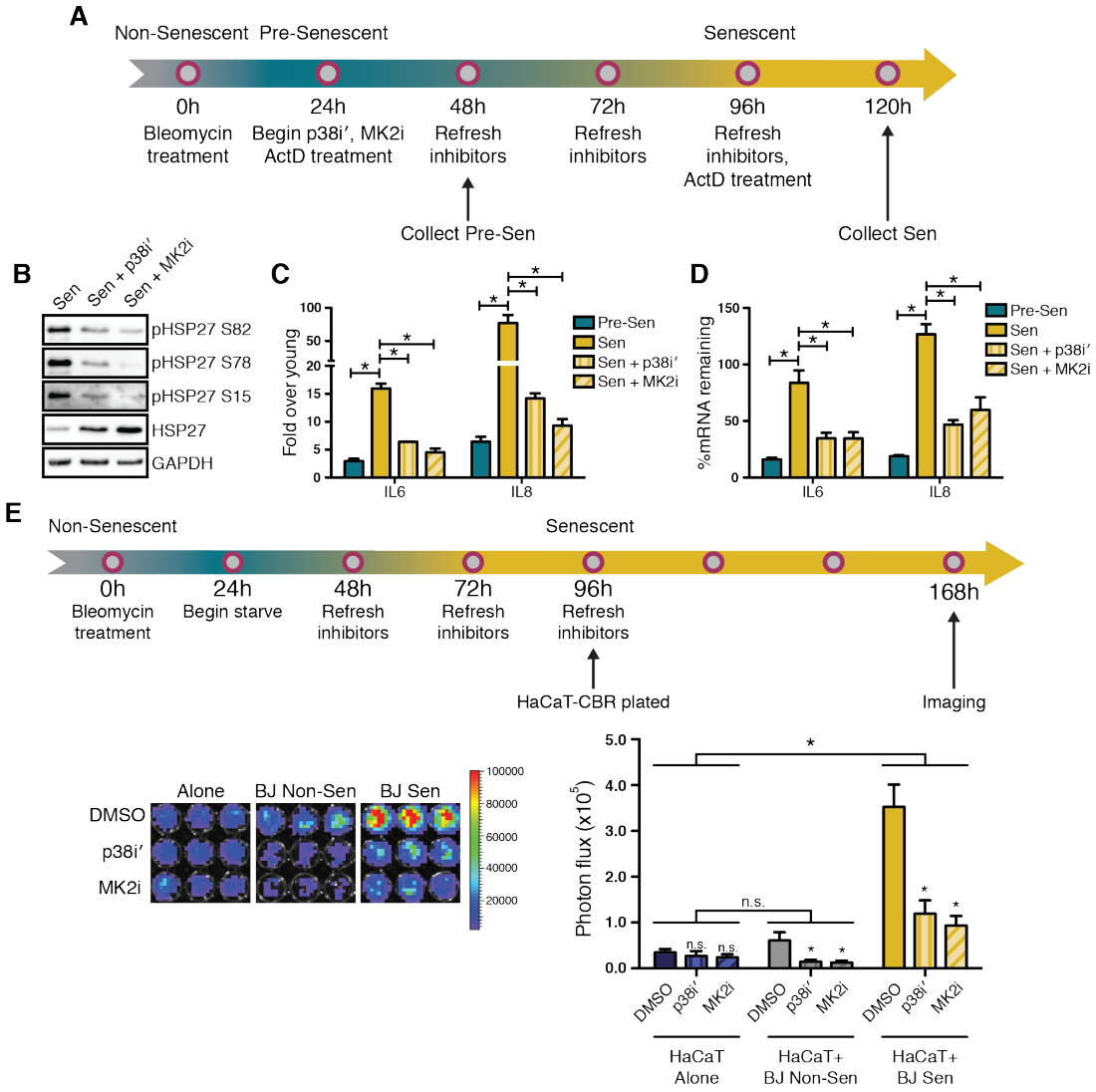

Figure 2.4: Inhibiting the p38-MK2-HSP27 axis prevents promotion of tumor cell growth by senescent stroma.

A. Schematic of senescence induction by bleomycin treatment and inhibition of p38MAPK or MK2 activity by treatment with p38i′ (CDD111, 1μM) or MK2i (CDD450, 1μM), respectively. Inhibitors were refreshed every 24h until collection. **B.** Immunoblot of HSP27 phosphorylation in cells treated with either p38i′ or MK2i as in *A*. **C, D.** Upregulation, *C*, and mRNA stability, *D*, of SASP factors in cells treated as in *A*. SASP mRNA levels were quantified by qRT-PCR. Representative experiments, n=4 for *C* and n=2 for *D*. **E.** BJ fibroblasts were plated in a 96-well plate and induced to senesce by 24h of bleomycin treatment. 24h after removal of bleomycin, cells were treated with DMSO, p38i′ or MK2i for 48h, refreshing the inhibitors after 24h. Once the fibroblasts were senescent 96h post-bleomycin treatment, click beetle red luciferase (CBR)-expressing HaCaT keratinocytes were plated either alone or on the young or senescent fibroblasts, and treated with DMSO, p38i′ or MK2i. To prevent disruption of the epithelial layer, inhibitors were not refreshed after HaCaT-CBR addition. HaCaT-CBR cell growth was measured 3 days after plating by addition of D-luciferin and bioluminescence quantification. Color bar: minimum=2434.5 flux-photons, maximum=10^5 flux-photons. n=3. n.s. = not significant, *=$p<0.05$, error bars are + S.E.M.

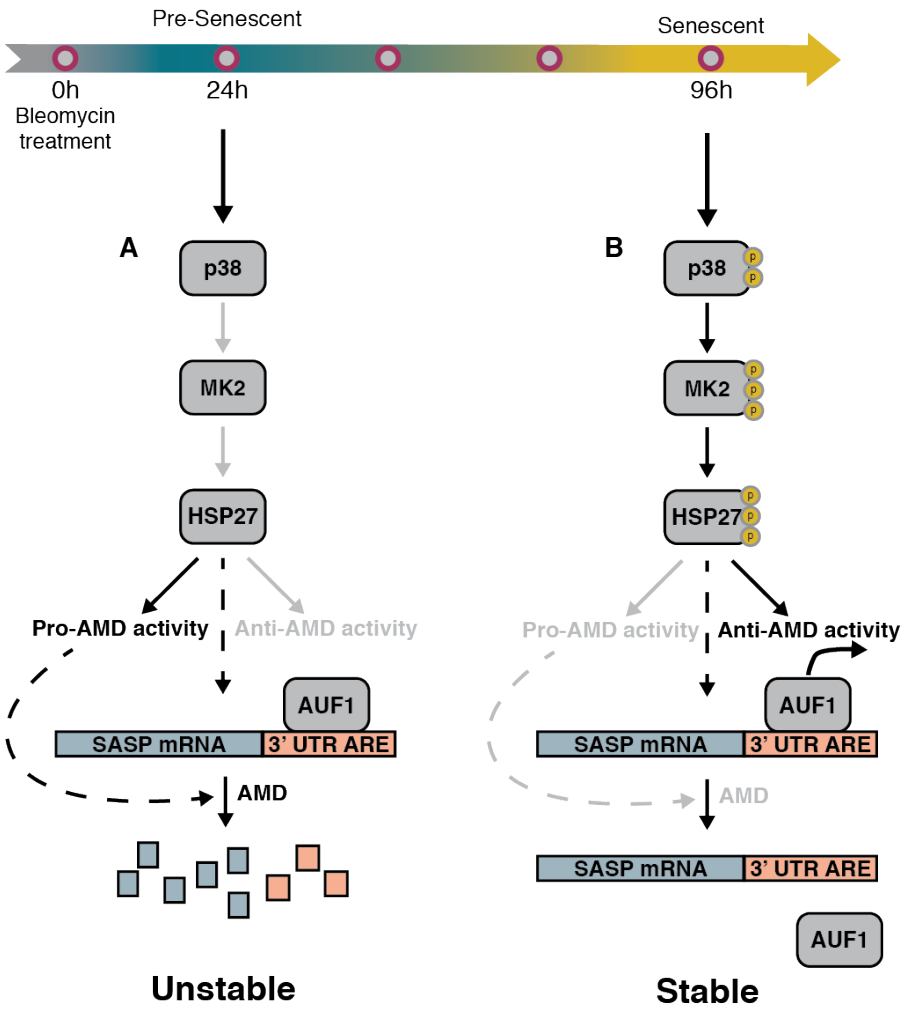

Figure 2.5: Model of p38MAPK-MK2-HSP27-AUF1 axis regulation of SASP factor mRNA stability in pre-senescent and senescent fibroblasts.

A. In pre-senescent cells, p38MAPK is not yet activated to the level observed in senescent cells, so p38MAPK-MK2-dependent phosphorylation of HSP27 is low and AUF1 binds target mRNAs. Non-phosphorylated HSP27 performs a putative pro-AMD activity, and the levels of phospho-HSP27 are insufficient to abrogate this function and thus mRNA degradation is dominant. **B.** In senescent cells, p38MAPK phosphorylation activates the MK2-HSP27 pathway stabilizing SASP mRNAs, potentially through several mechanisms. Reduced levels of non-phosphorylated HSP27 result in decreased HSP27-dependent pro-AMD activity, and phosphorylation of HSP27 on MK2 target sites results in AUF1 removal and stabilization of target SASP mRNAs.

References

1. **Prieur A, Peeper DS.** 2008. Cellular senescence in vivo: a barrier to tumorigenesis. Curr Opin Cell Biol **20:**150-155.

2. **Bavik C, Coleman I, Dean JP, Knudsen B, Plymate S, Nelson PS.** 2006. The gene expression program of prostate fibroblast senescence modulates neoplastic epithelial cell proliferation through paracrine mechanisms. Cancer Res **66:**794-802.

3. **Coppe JP, Patil CK, Rodier F, Sun Y, Munoz DP, Goldstein J, Nelson PS, Desprez PY, Campisi J.** 2008. Senescence-associated secretory phenotypes reveal cell-nonautonomous functions of oncogenic RAS and the p53 tumor suppressor. PLoS Biol **6:**2853-2868.

4. **Kuilman T, Peeper DS.** 2009. Senescence-messaging secretome: SMS-ing cellular stress. Nat Rev Cancer **9:**81-94.

5. **Xue W, Zender L, Miething C, Dickins RA, Hernando E, Krizhanovsky V, Cordon-Cardo C, Lowe SW.** 2007. Senescence and tumour clearance is triggered by p53 restoration in murine liver carcinomas. Nature **445:**656-660.

6. **Pazolli E, Luo X, Brehm S, Carbery K, Chung JJ, Prior JL, Doherty J, Demehri S, Salavaggione L, Piwnica-Worms D, Stewart SA.** 2009. Senescent stromal-derived osteopontin promotes preneoplastic cell growth. Cancer Res **69:**1230-1239.

7. **Krtolica A, Parrinello S, Lockett S, Desprez PY, Campisi J.** 2001. Senescent fibroblasts promote epithelial cell growth and tumorigenesis: a link between cancer and aging. Proc Natl Acad Sci U S A **98:**12072-12077.

8. **Parrinello S, Coppe JP, Krtolica A, Campisi J.** 2005. Stromal-epithelial interactions in aging and cancer: senescent fibroblasts alter epithelial cell differentiation. J Cell Sci **118:**485-496.

9. **Freund A, Patil CK, Campisi J.** 2011. p38MAPK is a novel DNA damage response-independent regulator of the senescence-associated secretory phenotype. EMBO J **30:**1536-1548.

10. **Alspach E, Flanagan KC, Luo X, Ruhland MK, Huang H, Pazolli E, Donlin MJ, Marsh T, Piwnica-Worms D, Monahan J, Novack DV, McAllister SS, Stewart SA.** 2014. p38MAPK plays a crucial role in stromal-mediated tumorigenesis. Cancer Discov **4:**716-729.

11. **Rodier F, Coppe JP, Patil CK, Hoeijmakers WA, Munoz DP, Raza SR, Freund A, Campeau E, Davalos AR, Campisi J.** 2009. Persistent DNA damage signalling triggers senescence-associated inflammatory cytokine secretion. Nat Cell Biol **11:**973-979.

12. **Gratacós FM, Brewer G.** 2010. The role of AUF1 in regulated mRNA decay. Wiley Interdiscip Rev RNA **1:**457-473.

13. **White EJ, Brewer G, Wilson GM.** 2013. Post-transcriptional control of gene expression by AUF1: mechanisms, physiological targets, and regulation. Biochim Biophys Acta **1829:**680-688.

14. **Loflin P, Chen CY, Shyu AB.** 1999. Unraveling a cytoplasmic role for hnRNP D in the in vivo mRNA destabilization directed by the AU-rich element. Genes Dev **13:**1884-1897.

15. **Palanisamy V, Park NJ, Wang J, Wong DT.** 2008. AUF1 and HuR proteins stabilize interleukin-8 mRNA in human saliva. J Dent Res **87:**772-776.

16. **Raineri I, Wegmueller D, Gross B, Certa U, Moroni C.** 2004. Roles of AUF1 isoforms, HuR and BRF1 in ARE-dependent mRNA turnover studied by RNA interference. Nucleic Acids Res **32:**1279-1288.

17. **Xu N, Chen CY, Shyu AB.** 2001. Versatile role for hnRNP D isoforms in the differential regulation of cytoplasmic mRNA turnover. Mol Cell Biol **21:**6960-6971.

18. **Wilson GM, Lu J, Sutphen K, Suarez Y, Sinha S, Brewer B, Villanueva-Feliciano EC, Ysla RM, Charles S, Brewer G.** 2003. Phosphorylation of p40AUF1 regulates binding to A + U-rich mRNA-destabilizing elements and protein-induced changes in ribonucleoprotein structure. J Biol Chem **278:**33039-33048.

19. **Wilson GM, Lu J, Sutphen K, Sun Y, Huynh Y, Brewer G.** 2003. Regulation of A + U-rich element-directed mRNA turnover involving reversible phosphorylation of AUF1. J Biol Chem **278:**33029-33038.

20. **Li ML, Defren J, Brewer G.** 2013. Hsp27 and F-box protein beta-TrCP promote degradation of mRNA decay factor AUF1. Mol Cell Biol **33:**2315-2326.

21. **Herranz N, Gallage S, Mellone M, Wuestefeld T, Klotz S, Hanley CJ, Raguz S, Acosta JC, Innes AJ, Banito A, Georgilis A, Montoya A, Wolter K, Dharmalingam G, Faull P, Carroll T, Martinez-Barbera JP, Cutillas P, Reisinger F, Heikenwalder M, Miller RA, Withers D, Zender L, Thomas GJ, Gil J.** 2015. mTOR regulates MAPKAPK2 translation to control the senescence-associated secretory phenotype. Nat Cell Biol **17:**1205-1217.

22. **Knapinska AM, Gratacos FM, Krause CD, Hernandez K, Jensen AG, Bradley JJ, Wu X, Pestka S, Brewer G.** 2011. Chaperone Hsp27 modulates AUF1 proteolysis and AU-rich element-mediated mRNA degradation. Mol Cell Biol **31:**1419-1431.

23. **Sinsimer KS, Gratacos FM, Knapinska AM, Lu J, Krause CD, Wierzbowski AV, Maher LR, Scrudato S, Rivera YM, Gupta S, Turrin DK, De La Cruz MP, Pestka S,**

Brewer G. 2008. Chaperone Hsp27, a novel subunit of AUF1 protein complexes, functions in AU-rich element-mediated mRNA decay. Mol Cell Biol **28:**5223-5237.

24. **Winzen R, Kracht M, Ritter B, Wilhelm A, Chen CY, Shyu AB, Muller M, Gaestel M, Resch K, Holtmann H.** 1999. The p38 MAP kinase pathway signals for cytokine-induced mRNA stabilization via MAP kinase-activated protein kinase 2 and an AU-rich region-targeted mechanism. EMBO J **18:**4969-4980.

25. **Saharia A, Guittat L, Crocker S, Lim A, Steffen M, Kulkarni S, Stewart SA.** 2008. Flap endonuclease 1 contributes to telomere stability. Curr Biol **18:**496-500.

26. **Dimri GP, Lee X, Basile G, Acosta M, Scott G, Roskelley C, Medrano EE, Linskens M, Rubelj I, Pereira-Smith O, Peacocke M, Campisi J.** 1995. A biomarker that identifies senescent human cells in culture and in aging skin in vivo. Proc Natl Acad Sci U S A **92:**9363-9367.

27. **Larsen JK, Yamboliev IA, Weber LA, Gerthoffer WT.** 1997. Phosphorylation of the 27-kDa heat shock protein via p38 MAP kinase and MAPKAP kinase in smooth muscle. Am J Physiol **273:**L930-940.

28. **Alimbetov D, Davis T, Brook AJ, Cox LS, Faragher RG, Nurgozhin T, Zhumadilov Z, Kipling D.** 2015. Suppression of the senescence-associated secretory phenotype (SASP) in human fibroblasts using small molecule inhibitors of p38 MAP kinase and MK2. Biogerontology doi:10.1007/s10522-015-9610-z.

29. **Cuenda A, Rouse J, Doza YN, Meier R, Cohen P, Gallagher TF, Young PR, Lee JC.** 1995. SB 203580 is a specific inhibitor of a MAP kinase homologue which is stimulated by cellular stresses and interleukin-1. FEBS Lett **364:**229-233.

30. **Wilson KP, McCaffrey PG, Hsiao K, Pazhanisamy S, Galullo V, Bemis GW, Fitzgibbon MJ, Caron PR, Murcko MA, Su MS.** 1997. The structural basis for the specificity of pyridinylimidazole inhibitors of p38 MAP kinase. Chem Biol **4:**423-431.

31. **Genovese MC.** 2009. Inhibition of p38: has the fat lady sung? Arthritis Rheum **60:**317-320.

32. **Goldstein DM, Kuglstatter A, Lou Y, Soth MJ.** 2010. Selective p38alpha inhibitors clinically evaluated for the treatment of chronic inflammatory disorders. J Med Chem **53:**2345-2353.

33. **Saklatvala J.** 2004. The p38 MAP kinase pathway as a therapeutic target in inflammatory disease. Curr Opin Pharmacol **4:**372-377.

34. **Hendrayani SF, Al-Khalaf HH, Aboussekhra A.** 2014. The cytokine IL-6 reactivates breast stromal fibroblasts through transcription factor STAT3-dependent up-regulation of the RNA-binding protein AUF1. J Biol Chem **289:**30962-30976.

35. **Wilson GM, Sun Y, Lu H, Brewer G.** 1999. Assembly of AUF1 oligomers on U-rich RNA targets by sequential dimer association. J Biol Chem **274:**33374-33381.

36. **Genovese MC, Cohen SB, Wofsy D, Weinblatt ME, Firestein GS, Brahn E, Strand V, Baker DG, Tong SE.** 2011. A 24-week, randomized, double-blind, placebo-controlled, parallel group study of the efficacy of oral SCIO-469, a p38 mitogen-activated protein kinase inhibitor, in patients with active rheumatoid arthritis. J Rheumatol **38:**846-854.

37. **Schreiber S, Feagan B, D'Haens G, Colombel JF, Geboes K, Yurcov M, Isakov V, Golovenko O, Bernstein CN, Ludwig D, Winter T, Meier U, Yong C, Steffgen J, Group BS.** 2006. Oral p38 mitogen-activated protein kinase inhibition with BIRB 796 for active Crohn's disease: a randomized, double-blind, placebo-controlled trial. Clin Gastroenterol Hepatol **4:**325-334.

38. **Johansen C, Vestergaard C, Kragballe K, Kollias G, Gaestel M, Iversen L.** 2009. MK2 regulates the early stages of skin tumor promotion. Carcinogenesis **30:**2100-2108.

39. **Ray AL, Castillo EF, Morris KT, Nofchissey RA, Weston LL, Samedi VG, Hanson JA, Gaestel M, Pinchuk IV, Beswick EJ.** 2016. Blockade of MK2 is protective in inflammation-associated colorectal cancer development. Int J Cancer **138:**770-775.

Chapter 3

Conclusions and Future Directions

Senescence

3.1 Summary

Since tumor cells do not exist in isolation and are instead supported and defined by the environment in which they grow, it is vital to understand the contribution of the microenvironment to tumor establishment and progression. Age-dependent changes to the stromal compartment of tissues, such as accumulation of senescent fibroblasts, can suppress anti-tumor immunity, drive structural changes, increase blood flow, and create an environment rich in growth factors primed to promote the growth and progression of benign neoplasias in the epithelial compartment into malignant lesions (1-3). Conversely, young stroma can restrain tumor growth and promote tumor clearance. Implantation of rat liver epithelial tumor cells into the livers of young and aged rats initially resulted in tumor establishment in both groups, but over time as the tumors in the aged livers persisted, the tumors in young livers regressed completely, highlighting the active role of the tumor microenvironment in regulating tumor activity (4). Understanding the mechanisms that govern the transition from tumor-restraining to tumor-promoting stroma is a vital step to being able to modulate this process in the context of cancer therapy.

One change that occurs in aged stroma is the accumulation of senescent fibroblasts and expression of the senescence-associated secretory phenotype, or SASP. As fibroblasts senesce, the usually short-lived mRNAs encoding for inflammatory SASP factors including IL6, IL8, and GM-CSF are stabilized, and expression of these factors is increased. Activated by senescence, p38MAPK phosphorylates MK2, which phosphorylates HSP27 on three key residues. In chapter 2, I have demonstrated that HSP27 phosphorylation regulates the binding and activity of AUF1, an AU-rich element binding protein that governs mRNA stability. Modulation of HSP27

phosphorylation is sufficient to regulate the stability of SASP factor mRNAs, and as a result, upregulation of the SASP as a whole. Furthermore, I have demonstrated that disrupting this pathway through chemical inhibition of p38MAPK or MK2 inhibits the upregulation and stabilization of a variety of SASP factors. Thus, inhibition of either of these kinases prevents senescent fibroblasts from promoting the growth of preneoplastic epithelial cells, demonstrating that this critical pathway is a therapeutic target. Below, I discuss the implications of these findings and future work in the context of both a mechanistic understanding of mRNA regulation in senescent cells, as well as the broader implications of the p38MAPK-MK2 pathway as a microenvironment-targeted cancer therapy.

3.2 The p38MAPK-MK2-HSP27-AUF1 axis regulates post-transcriptional stabilization of SASP factor mRNAs in senescence

p38MAPK plays an important and multifaceted role in the regulation of SASP factor expression in senescent fibroblasts. Even in the absence of DDR signaling, p38MAPK promotes NF-κB-dependent transcription of target SASP factors in pre-senescent cells (5). However, in senescent cells, while p38MAPK activity is critical for the upregulation and expression of SASP factors, it is no longer required for NF-κB-dependent transcription, suggesting that p38MAPK is regulating the levels of these factors through a separate mechanism. Indeed, inhibiting transcription in senescent cells reveals that SASP factor mRNAs have been stabilized relative to pre-senescent cells, and this stabilization is p38MAPK-dependent (6). p38MAPK regulates mRNA stabilization in senescent cells through modulating the binding of the AU-rich element

binding protein AUF1, which binds and targets SASP factor mRNAs for degradation in pre-senescent cells, but displays a p38MAPK-dependent reduction in binding of SASP factor mRNAs in senescent cells. Because p38MAPK does not directly target AUF1, and the downstream target of p38MAPK, HSP27, is known to function with AUF1 in mRNA degradation, we investigated whether the p38MAPK-MK2-HSP27 pathway regulated AUF1 activity and SASP factor mRNA stabilization in senescent fibroblasts (7, 8).

When p38MAPK activity is inhibited either by small molecule inhibitors or by shRNA-mediated depletion, mRNA stability of SASP factors in senescent cells is decreased (chapter 2 and (6)). Specific inhibition of MK2 activation by p38MAPK through the use of a small molecule inhibitor that selectively targets the p38MAPK/MK2 complex similarly abrogates SASP factor upregulation and mRNA stabilization in senescent fibroblasts, indicating that p38MAPK acts through MK2 to stabilize SASP factor mRNAs (**Fig. 2.2**). Pre-senescent cells expressing an HSP27 mutant with serine-to-asparagine mutations at MK2 target sites to mimic phosphorylation have increased SASP factor mRNA stability compared to those expressing wild type HSP27. This finding demonstrates that the MK2-dependent phosphorylation of HSP27 is sufficient to create a senescent-like state with regards to mRNA stability in pre-senescent cells. Conversely, expression of a non-phosphorylatable HSP27 mutant, with serine-to-alanine mutations at the MK2 target sites, prevents stabilization of SASP factor mRNAs in senescent cells, creating a pre-senescent-like mRNA stability state (**Fig 2.3**). Taken together, this demonstrates that p38MAPK-MK2-dependent phosphorylation of HSP27 is sufficient to alter the mRNA stability of SASP factors in both pre-senescent and senescent cells, and suggests that the

p38MAPK-MK2-HSP27 axis regulates the transition from transcriptionally-driven SASP factor upregulation in pre-senescent cells to mRNA stability-driven upregulation in senescent cells.

Several aspects of this regulatory mechanism remain to be investigated. We find that AUF1 binding is reduced in senescent compared to pre-senescent cells, and this is dependent on p38MAPK. Further, MK2-dependent phosphorylation of HSP27 is required for AUF1 removal from SASP factor mRNAs in senescent cells. Together, these findings suggest that SASP mRNA stability is regulated at the level of AUF1 binding in senescent cells. However, in pre-senescent cells, depletion of HSP27 leads to both mRNA stabilization as well as increased AUF1 binding to target mRNAs, suggesting that AUF1 binding ability is not the only determinant in the degradation of SASP factor mRNAs during pre-senescence. Furthermore, unlike in other systems described, HSP27 phosphorylation does not appear to have a consistent affect on AUF1 levels in senescent fibroblasts (7-9). This has several implications. First, it suggests that both phosphorylated and non-phosphorylated HSP27 may have roles in regulating mRNA stability, and the presence of non-phosphorylated HSP27, rather than simply the absence of phosphorylated HSP27, may be required for SASP mRNA degradation in pre-senescent cells. Non-phosphorylated HSP27 may be required for proper assembly or activity of the AUF1-and signal transduction-regulated complex (ASTRC), acting as a structural determinant or possibly to recruit or activate the deadenylation effectors. Furthermore, it suggests that AUF1 may require activation in pre-senescent cells, since it is able to bind but not promote degradation in the absence of HSP27. The presence of phosphorylated $p40^{AUF1}$ in monocytes correlates with ASTRC degradation activity, and glycogen synthase kinase 3-beta (GSK3β) is able to phosphorylate $p40^{AUF1}$ on Ser83 (10, 11). p38MAPK phosphorylates and inhibits GSK3β, so it is

possible that GSK3β phosphorylates and activates $p40^{AUF1}$ in pre-senescent cells (potentially through an HSP27-dependent mechanism wherein non-phosphorylated HSP27 promotes access to $p40^{AUF1}$ Ser83), but senescence-dependent p38MAPK activity results in phosphorylation and inhibition of GSK3β and therefore inactivation of $p40^{AUF1}$. Studies into the means by which HSP27 regulates AUF1 in senescence will provide further mechanistic understanding of the process regulating SASP expression and regulation of mRNA stability as a whole.

3.3 Inhibiting the p38MAPK-MK2-HSP27 pathway abrogates the growth promotion of epithelial cells by senescent fibroblasts

Secretion of SASP factors by senescent stroma is sufficient to drive epithelial cell growth both in *in vitro* co-culture settings as well as in xenograft experiments. Several different SASP factors, such as IL6, IL8, and OPN are sufficient to drive this growth individually (12, 13), but understanding the regulatory mechanisms behind SASP factor expression will allow for therapies targeting specific pathways that regulate groups of SASP factors together, potentially increasing therapeutic efficacy compared to treatments that target specific factors. Indeed, treatment with the p38MAPK inhibitor CDD111 prevented expression of a large number of inflammatory and other SASP factors essential to senescent stromal-mediated growth promotion of preneoplastic cells, dramatically reducing tumor size in a xenograft setting (6). This effect was due exclusively to abrogation of microenvironmental support, because CDD111 treatment had no effect on *in vitro* growth of the epithelial cells. This drug and other p38MAPK inhibitors have been the subject of several different clinical trials studying the potential for p38MAPK inhibition as a

treatment for several different inflammatory diseases such as rheumatoid arthritis. However, a rebound effect, wherein early suppression of inflammation is quickly overcome and markers of inflammation reach levels higher than those observed pre-treatment, has plagued these trials, and support for p38MAPK inhibitors as a treatment strategy is waning (14-18). While CDD111 treatment was highly effective in limiting tumor growth in the context and treatment duration studied by Alspach and colleagues, it is possible that similar rebound from inhibition could result in loss of efficacy or even enhancement of tumor growth in experimental settings closer to those that would be experienced clinically. It has been suggested that compensatory action by MK2 is responsible for this rebound effect, and the potent inhibition of preneoplastic cell growth promotion by senescent fibroblasts upon treatment with the MK2-specific inhibitor CDD450 is a promising finding in regards to alternatives for pan-p38MAPK inhibitors (**Fig. 2.4**).

These findings indicate that further study of CDD450 as an anti-cancer therapy is warranted. *In vivo* experiments utilizing a xenograft system composed of senescent human fibroblasts and preneoplastic human cells such as BPH-1 prostate epithelial cells in mice with systemic MK2 inhibition through CDD450-compounded chow could reveal whether this pathway is required for a senescent human tumor microenvironment to promote preneoplastic cell growth. Furthermore, similar experiments utilizing CDD450-compounded chow could be performed in either a spontaneous tumor model with an inducible senescence phenotype to assess the contribution of MK2-dependent SASP expression in senescent tissues on the initial development of tumors, or in an injectable model, where the effects of pre-treatment with CDD450 and the resulting alterations to the senescent microenvironment on tumor implantation or outgrowth could be studied.

Because DNA damaging chemotherapy itself is capable of inducing senescence and the SASP, current cancer treatments may be promoting the development of future disease or metastasis through the generation of favorable metastatic niches, or chemoprotective areas that protect subsets of tumor cells from efficient drug action (19). Indeed, chemotherapy induces p38MAPK-dependent expression of a pro-inflammatory cytokine profile similar to the SASP and promotes tumorigenesis in pancreatic cancer-associated fibroblasts, which function similarly to senescent fibroblasts (19, 20). It would be intriguing to determine whether these effects could be mitigated through concurrent treatment of current chemotherapies with drugs such as CDD450 that could inhibit development of favorable metastatic or chemoprotective environments. Although current avenues of research tend to focus on the identification and targeting of individual factors responsible for disease promotion and progression in both cell-autonomous and non-autonomous ways, targeting the pathways that drive coordinate expression of numerous pro-tumorigenic factors may be a means of enhancing therapeutic efficacy by inhibiting a broader network of factors that drive disease.

3.4 Conclusions

Although senescence is a mechanism to protect cells that have aged or experienced DNA damage from continuing to proliferate and potentially become tumorigenic, senescence cells also have significant tumor-promoting characteristics including the activation of the senescence-associated secretory phenotype, a gene expression profile rich in pro-tumorigenic factors that act through both direct stimulation of tumor growth and invasion as well as through modifications to tissues that create a favorable tumor microenvironment. The work presented here investigates

post-transcriptional regulatory mechanisms that govern the expression of the SASP, demonstrating that the p38MAPK-MK2 pathway regulates SASP factor mRNA stability through phosphorylation of HSP27, adding to our understanding of physiological changes associated with senescence as well as mechanisms regulating mRNA stability. Furthermore, this work identifies inhibition of MK2 in the tumor microenvironment as a rebound-resistant alternative to p38MAPK inhibition and a novel therapeutic approach to cancer treatment.

References

1. **Alspach E, Fu Y, Stewart SA.** 2013. Senescence and the pro-tumorigenic stroma. Crit Rev Oncog **18:**549-558.

2. **Coppe JP, Desprez PY, Krtolica A, Campisi J.** 2010. The senescence-associated secretory phenotype: the dark side of tumor suppression. Annu Rev Pathol **5:**99-118.

3. **Pazolli E, Stewart SA.** 2008. Senescence: the good the bad and the dysfunctional. Curr Opin Genet Dev **18:**42-47.

4. **McCullough KD, Coleman WB, Smith GJ, Grisham JW.** 1997. Age-dependent induction of hepatic tumor regression by the tissue microenvironment after transplantation of neoplastically transformed rat liver epithelial cells into the liver. Cancer Res **57:**1807-1813.

5. **Freund A, Patil CK, Campisi J.** 2011. p38MAPK is a novel DNA damage response-independent regulator of the senescence-associated secretory phenotype. EMBO J **30:**1536-1548.

6. **Alspach E, Flanagan KC, Luo X, Ruhland MK, Huang H, Pazolli E, Donlin MJ, Marsh T, Piwnica-Worms D, Monahan J, Novack DV, McAllister SS, Stewart SA.** 2014. p38MAPK plays a crucial role in stromal-mediated tumorigenesis. Cancer Discov **4:**716-729.

7. **Knapinska AM, Gratacos FM, Krause CD, Hernandez K, Jensen AG, Bradley JJ, Wu X, Pestka S, Brewer G.** 2011. Chaperone Hsp27 modulates AUF1 proteolysis and AU-rich element-mediated mRNA degradation. Mol Cell Biol **31:**1419-1431.

8. **Sinsimer KS, Gratacos FM, Knapinska AM, Lu J, Krause CD, Wierzbowski AV, Maher LR, Scrudato S, Rivera YM, Gupta S, Turrin DK, De La Cruz MP, Pestka S, Brewer G.** 2008. Chaperone Hsp27, a novel subunit of AUF1 protein complexes, functions in AU-rich element-mediated mRNA decay. Mol Cell Biol **28:**5223-5237.

9. **Li ML, Defren J, Brewer G.** 2013. Hsp27 and F-box protein beta-TrCP promote degradation of mRNA decay factor AUF1. Mol Cell Biol **33:**2315-2326.

10. **Wilson GM, Lu J, Sutphen K, Suarez Y, Sinha S, Brewer B, Villanueva-Feliciano EC, Ysla RM, Charles S, Brewer G.** 2003. Phosphorylation of p40AUF1 regulates binding to A + U-rich mRNA-destabilizing elements and protein-induced changes in ribonucleoprotein structure. J Biol Chem **278:**33039-33048.

11. **Wilson GM, Lu J, Sutphen K, Sun Y, Huynh Y, Brewer G.** 2003. Regulation of A + U-rich element-directed mRNA turnover involving reversible phosphorylation of AUF1. J Biol Chem **278:**33029-33038.

12. **Coppe JP, Patil CK, Rodier F, Sun Y, Munoz DP, Goldstein J, Nelson PS, Desprez PY, Campisi J.** 2008. Senescence-associated secretory phenotypes reveal cell-nonautonomous functions of oncogenic RAS and the p53 tumor suppressor. PLoS Biol **6:**2853-2868.

13. **Pazolli E, Luo X, Brehm S, Carbery K, Chung JJ, Prior JL, Doherty J, Demehri S, Salavaggione L, Piwnica-Worms D, Stewart SA.** 2009. Senescent stromal-derived osteopontin promotes preneoplastic cell growth. Cancer Res **69:**1230-1239.

14. **Genovese MC.** 2009. Inhibition of p38: has the fat lady sung? Arthritis Rheum **60:**317-320.

15. **Genovese MC, Cohen SB, Wofsy D, Weinblatt ME, Firestein GS, Brahn E, Strand V, Baker DG, Tong SE.** 2011. A 24-week, randomized, double-blind, placebo-controlled, parallel group study of the efficacy of oral SCIO-469, a p38 mitogen-activated protein kinase inhibitor, in patients with active rheumatoid arthritis. J Rheumatol **38:**846-854.

16. **Goldstein DM, Kuglstatter A, Lou Y, Soth MJ.** 2010. Selective p38alpha inhibitors clinically evaluated for the treatment of chronic inflammatory disorders. J Med Chem **53:**2345-2353.

17. **Saklatvala J.** 2004. The p38 MAP kinase pathway as a therapeutic target in inflammatory disease. Curr Opin Pharmacol **4:**372-377.

18. **Schreiber S, Feagan B, D'Haens G, Colombel JF, Geboes K, Yurcov M, Isakov V, Golovenko O, Bernstein CN, Ludwig D, Winter T, Meier U, Yong C, Steffgen J, Group BS.** 2006. Oral p38 mitogen-activated protein kinase inhibition with BIRB 796 for active Crohn's disease: a randomized, double-blind, placebo-controlled trial. Clin Gastroenterol Hepatol **4:**325-334.

19. **Gilbert LA, Hemann MT.** 2010. DNA damage-mediated induction of a chemoresistant niche. Cell **143:**355-366.

20. **Toste PA, Nguyen AH, Kadera BE, Duong M, Wu N, Gawlas I, Tran LM, Bikhchandani M, Li L, Patel SG, Dawson DW, Donahue TR.** 2016. Chemotherapy-induced Inflammatory Gene Signature and Pro-tumorigenic Phenotype in Pancreatic CAFs via Stress-associated MAPK. Mol Cancer Res doi:10.1158/1541-7786.MCR-15-0348.

Chapter 4

Background and Significance

DNA metabolism

4.1 Overview and significance

Preserving genomic stability is a crucial component of not only cellular health, but also the health of an organism as a whole. The genome is constantly under threat from potentially harmful external sources such as UV radiation and other environmental DNA damaging agents as well as endogenous threats including oxidative stress, metabolic byproducts such as alkylating agents, and DNA replication itself. Humans are estimated to experience over 10,000 oxidative damage events per cell per day, and a single round of replication can induce between 10 and 50 DNA double strand breaks (DSBs), the most deleterious and mutagenic type of DNA damage (1-3). Uncovering the mechanisms by which the genome safeguards itself against these and other threats is an important step in understanding and potentially treating the wide variety of disorders that arise as a result of defects in these pathways.

4.2 Genomic instability as a driver of disease

Genomic instability is an underlying factor in a variety of different diseases, including cancer, several types of anemia, and certain premature aging disorders. Because of the essential nature of guarding genomic stability, many redundant pathways cooperate to ensure proper execution of processes such as DNA replication, repair, and telomere maintenance. However, these backup pathways are not entirely efficient. Due to the overlapping nature of these processes and the fact that many proteins participate in multiple facets of genomic maintenance, mutations in a single gene or disruption of a single pathway can have wide-reaching consequences on the health of an organism.

4.2.1 DNA replication fidelity

Tens of billions of cells replicate per day in the human body, including generation of 1×10^{11} neutrophils and 2×10^{11} erythrocytes, highlighting the need for cells to efficiently replicate their DNA with minimal introduction of mutations or other DNA damage (4). Eukaryotic DNA polymerases have a mutation rate of approximately one per 10^4-10^5 nucleotides, so between 100,000 and 1,000,000 mutations per round of replication are potentially introduced into human tissues (5, 6). Therefore, multiple mechanisms exist to ensure DNA replication fidelity, primarily through proofreading newly synthesized DNA and mismatch repair (MMR). The leading- and lagging-strand DNA polymerases, ε and δ respectively, have proofreading activities mediated by their intrinsic 3' exonucleases (7-9). Disruption of this proofreading activity is vital to preventing mutational accumulation. Underscoring the critical role this proofreading function plays, introduction of a single base pair substitution to the 3' active site of Pol ε in mice resulted in spontaneous generation of adenomas and adenocarcinomas of the lung and intestine, among other tumors (10). Interestingly, inactivation of the proofreading function of Pol δ in mice resulted in a different distribution of tumor types than Pol ε, with the majority of mice presenting with thymic lymphomas, tail skin carcinomas, or lung adenomas and adenocarcinomas (10-12). Together, these studies highlight the importance of the proofreading capability of Pols ε and δ in preventing mutational accumulation and cancer development. Those replication-generated mutations that are not corrected during proofreading are typically repaired through MMR. Defects in the MMR pathway are associated with colon cancer in humans, with inherited MMR defects responsible for ~1-5% of colorectal cancer cases, and spontaneous mutations to the

MMR pathway genes or their regulatory elements are found in ~15-20% of sporadic colorectal cancers (8, 13).

4.2.2 DNA repair and replication fork progression

In order to preserve the integrity of the genome, it is vital that DNA breaks and other lesions are repaired efficiently while ideally minimizing mutational consequences. The genome faces many threats including oxidative damage that can break or mutate DNA, bulky adducts that prevent replication fork progression, and DNA single- and double-strand breaks that can result in loss of genetic information. A vast network of pathways exist to repair these and other DNA lesions, and while there is a good deal of redundancy in protein function and alternate repair mechanisms, mutations in DNA repair proteins can have a wide variety of negative and pathogenic consequences.

DSBs are considered the most dangerous type of DNA break, because they can lead to loss of genetic information and structural changes to chromosomes. Homologous recombination (HR) is an error-free means of repairing DSBs, and there are diseases characterized by cancer predisposition among other symptoms associated with mutations in proteins involved in almost every step of the pathway. Two such diseases are Ataxia telangiectasia (A-T), and Nijmegen breakage syndrome (NBS). A-T is a neurodegenerative disease caused by mutations to the ATM (Ataxia telangiectasia mutated) kinase, which initiates DDR signaling. It is characterized by motor and movement difficulties, immunodeficiency, and cancer predisposition, among other symptoms (14, 15). NBS is caused by mutations to NBS1, which acts as part of the MRN (Mre11-Rad50-NBS1) complex to bind DSBs and initiate the resection required to create the 3’

single stranded DNA (ssDNA) overhang necessary for HR. NBS is characterized by immunodeficiency, cancer predisposition, and sensitivity to ionizing radiation, similar to the symptoms of A-T, but can also cause microcephaly and intellectual impairments that differ from those found in A-T (14, 16).

Interstrand DNA crosslinks are a barrier to replication fork progression, which can lead to replication fork stalling, collapse, or DSBs. One pathway involved in removal of interstrand crosslinks among other repair activities is the Fanconi anemia (FA) pathway, a family that includes 19 distinct functional complementation groups. FA is characterized by chromosomal instability, which leads to cognitive and physical developmental abnormalities, predisposition to leukemia and solid tumors, and progressive bone marrow failure among other symptoms (17, 18). The FA core complex, comprised of nine FA proteins, activates the FANCD2-FANCI heterodimer, while other recombinational and nucleolytic functions required to repair the lesions are mediated by the other eight proteins (17, 19).

4.2.3 Telomere maintenance

Telomeres are specialized nucleoprotein structures at the ends of chromosomes that act to mitigate the effects of DNA loss caused by multiple rounds of replication, as well as to distinguish chromosome ends from DSBs. Incorrect recognition of linear chromosome ends as DSBs would initiate DNA repair mechanisms such as non-homologous end joining (NHEJ) or HR. This can result in cycles of inappropriate chromosomal ligations and chromosomal instability, characterized by amplification of extensive regions and large terminal deletions (20). The main mechanism by which telomeres are distinguished from chromosome ends is through

formation of the t-loop structure, wherein the 3'ssDNA overhang at the telomere end folds back and invades the more proximal region of the telomere, and through binding of the shelterin complex, a group of proteins that repress DDR signaling at the telomere and protect telomere ends from DNA repair machinery (21, 22).

Genetic disruption of telomere integrity through inherited, monogenic mutations to one of 11 genes identified thus far can result in a spectrum of disorders. These mutations are either in genes encoding for telomerase components or telomere binding and protection proteins (23-25). While the disorders affect a diverse set of tissues with differing outcomes, they are generally characterized by a core set of symptoms including: depletion of bone marrow stem cell reserves resulting in immune function loss, gastrointestinal disorders, pulmonary fibrosis, liver cirrhosis, neuropsychiatric conditions, and predisposition to certain cancers (23, 24, 26).

Telomere dysfunction can also result in aging defects, as seen in Werner syndrome (WS), which caused by mutation of WRN, one of five RecQ-family helicases in humans. WS is a progeroid syndrome, characterized by the premature appearance of diseases typically associated with aging, including type II diabetes, osteoporosis, and cardiovascular disease, in addition to cancer predisposition (27). WRN is involved in a multitude of DNA maintenance activities including DSB repair, and promoting restart of stalled or regressed replication forks, particularly through telomeric regions replicated by lagging strand synthesis (28-30). Loss of WRN function causes telomere shortening and premature senescence, and it has been suggested that this is a disease mechanism leading to the premature aging phenotypes associated with WS.

4.3 Dna2 functions to ensure genomic stability

Dna2 is a highly conserved, essential helicase/nuclease that is important for maintaining many aspects of genomic stability. Initially discovered in a screen for proteins required for DNA replication and identified as an Okazaki fragment processing (OFP) factor, Dna2 has since been shown to participate in DSB repair, replication fork recovery and restart, and telomere maintenance (30-34). Although Dna2 knockout mice die before embryonic day 7.5, Dna2 mutations are associated with a variety of diseases, highlighting the critical role of this enzyme in genomic maintenance (34-36).

Dna2 is a helicase/nuclease capable of performing a variety of biochemical activities. Originally described as a 3' to 5' replicative DNA helicase with a preference for forked substrates, it was later confirmed to translocate in the 5' to 3' direction instead (31, 37). This helicase activity allows Dna2 to load onto the 5' end of flap structures and translocate to its site of activity (38). Dna2 also has essential endonucleolytic activity, specific for ssDNA (39, 40). Human Dna2 (hDna2) has been shown to have both 5' to 3' and 3' to 5' nuclease activities that require free ssDNA ends, wherein the 3' to 5' activity is not stimulated by RPA and leaves approximately 10 nucleotides from the cleavage site to the base of the fork or flap, while the 5' to 3' activity is stimulated by RPA and cleaves flaps or forks only a few nucleotides from the base of the flap (41). RPA therefore acts as a mechanism to enforce 5' to 3' polarity of Dna2 endonuclease activity.

hDna2 was initially reported to localize exclusively to the mitochondria, where it was shown to interact with polymerase γ (Polγ) and promote Polγ-dependent DNA synthesis, process

RNA primer intermediates, and function in long-patch base excision repair (42). However, work by Duxin and colleagues demonstrated that hDna2 also localizes to the nucleus. They demonstrated that depletion of hDna2 resulted in genomic instability characterized by aneuploidy and internuclei chromatin bridges, demonstrating that hDna2 has nuclear functions important to nuclear genome maintenance (43). Furthermore, both the nuclear and mitochondrial functions of hDna2 are vital to cell function, and several diseases have been associated with hDna2 mutations. In the mitochondria, hDna2 mutations in the nuclease, helicase, and ATPase activities have been identified in individuals with progressive mitochondrial myopathy stemming from instability of muscle mitochondrial DNA (36). In regards to nuclear hDna2 function, an hDna2 mutation leading to truncation of one isoform and abnormal splicing in two other isoforms was identified in two related individuals with primordial dwarfism (44). Interestingly, fibroblasts from these individuals displayed an increased frequency of senescent cells as well as higher levels of endogenous DNA damage as evidenced by increased comet tails, and this DNA damage was rescued upon exogenous expression of hDna2. Lastly, cellular levels of Dna2 are tightly regulated, and both over- and under-expression of hDna2 can be deleterious. Mice heterozygous for a Dna2 deletion develop cancers such as lymphoma, lung adenocarcinomas, and heptomas at a higher frequency than littermate controls (34). Conversely, overexpression of hDna2 is also detrimental as it enhances tolerance of replication-associated DSBs, and increased Dna2 expression has been identified in a variety of cancer types. Dna2 expression was positively correlated with metastasis frequency and inversely correlated with patient survival in breast cancer (35). Recently, a small molecule inhibitor of Dna2 was demonstrated to sensitize cells to DNA damaging chemotherapies and PARP inhibition, suggesting co-treatment with Dna2 inhibitors may be a feasible therapeutic strategy (45).

4.3.1 Dna2's function in lagging-strand DNA replication

Yeast Dna2 (yDna2) was initially identified as a replicative DNA helicase. yDna2 physically interacts with RAD27, the yeast flap endonuclease 1 (FEN1) nuclease, and overexpression of yDna2 rescued the temperature-sensitive growth defects associated with *rad27Δ* while overexpression of RAD27 suppressed growth defects associated with expression of the yDna2 mutant *dna2-1* (46). These observations suggested that yDna2 and FEN1 shared functionality in DNA replication, namely OFP. The process of lagging strand replication generates RNA primers at the 5' end of each nascent Okazaki fragment, which need to be removed to form the mature DNA duplex. During OFP, Pol δ displaces the DNA/RNA primer of the downstream Okazaki fragment, generating a 5' flap structure that is typically cleaved by FEN1, creating a ligatable nick that is filled in by DNA ligase I. However, if these flaps are not efficiently processed by FEN1, OFP can shift from a one-step to a two-step model (**Fig 4.1**). Biochemical studies have shown that if these flaps become longer than approximately 27 nucleotides, the single stranded DNA binding protein replication protein A (RPA) coats the flap, inhibiting FEN1 activity and necessitating another nuclease to complete flap removal (47). RPA stimulates yDna2 activity, suggesting that Dna2 could cleave the long flap, leaving behind several nucleotides that are subsequently cleaved by FEN1 to generate the ligatable nick. Expression of hDna2 can also rescue *rad27Δ* in yeast, suggesting that hDna2 may function in a similar manner in higher eukaryotes (48).

4.3.2 Dna2 participates in homologous recombination

Formation of a 3'ssDNA flap is a critical step in DSB repair by HR, and Dna2 has been shown to function in its generation. Certain *dna2* mutants in yeast display increased recombination rates and chromosome loss, as well as increased sensitivity to DNA damaging agents and Dna2 relocalizes throughout the nucleus from telomeres after treatment with DSB induction, suggesting that Dna2 participates in DSB repair (49-51). During HR in yeast, the DNA ends are bound by the MRX (Mre11-Rad50-Xrs2/NBS1, MRN in humans) complex, which initiates resection of the 5' DNA ends to form an initial, short 3'ssDNA overhang through the nuclease activities of Mre11 and Sae2 (CtIP in humans, **Fig. 4.2**) (52, 53). Further resection was shown to rely on the activity of exonuclease 1 (Exo1) and Sgs1, the RecQ-family helicase in yeast (54). However, long distance resection still occurred in Sgs1-competent yeast when Exo1 was deleted, and Dna2 was identified as the nuclease that acts in conjunction with Sgs1 (55). Dna2 and Exo1 have similar efficiency within 3kb of the DSB site, but Dna2 has greater efficiency and is therefore predicted to be the primary nuclease when resection is required beyond that point. In human cells, CtIP and BRCA1 recruit hDna2 to DSB sites, where BLM interacts with hDna2 and stimulates 5' end resection by both hDna2 and hExo1 (56, 57). Although the RecQ family helicases BLM and WRN are not always interchangeable, it was demonstrated that hDna2 could also function in conjunction with WRN to mediate long-range resection (58).

4.3.3 Dna2 protects telomere integrity

Telomeres are made up of short tandem repeats, containing a C-rich 5' strand and a G-rich 3' strand, which forms a 3'ssDNA overhang necessary for telomere protection. The

3'ssDNA overhang is generated through two mechanisms: selective elongation by telomerase and resection of the 5' C-strand (**Fig. 4.3**) (22). In yeast, Dna2 localizes to the telomere during the G1 phase, redistributes to replicating DNA throughout most of S phase (or upon DNA damage), and then relocalizes to the telomeres in late S/G2 (50). Expression of a *dna2* mutant in yeast resulted in shortened telomeres with each successive generation, demonstrating that Dna2 is required to maintain telomere length (59). This is due both to its involvement in generating the G-rich 3'ssDNA overhang through nucleolytic resection of the 5' C-rich strand as well as by facilitating telomere synthesis through promoting telomerase binding to telomeres in a manner independent of telomere length (50, 59).

The repetitive nature of the telomere along with its propensity to form secondary structures like G-quadruplexes (G4) makes it a difficult replication template, prone to replication fork stalling. Mammalian cells deficient in Dna2 display elevated telomere abnormalities, such as fragile telomeres, telomeric sister chromatid exchanges, sister telomere loss, and signal free ends, indicative of potential telomeric replication defects (34). In this study, Lin and colleagues demonstrate that Dna2 cleaves G4s within bubble or flap structures and that pharmacological stabilization of G4s leads to increased telomere fragility in cells heterozygous for Dna2. They therefore suggest that Dna2 protects telomere integrity by processing G4 structures to ensure replication fork progression through telomeric substrates. However, as will be discussed in chapter 6, Dna2 has a broader role in promoting replication fork progression, and further Dna2-dependent activities may therefore be involved in ensuring telomere replication and protecting telomere integrity.

4.4 Summary

Elucidating the mechanisms responsible for efficient replication and repair of the genome is vital for expanding our understanding of the causes and consequences of genomic instability. Due to the interconnected pathways guarding the genome, defects in a single protein involved in DNA processes can have wide-reaching effects on DNA replication, repair, and telomere maintenance and lead to a variety of diseases such as cancer, anemia, and cognitive disabilities. In chapter 5, I will elucidate the role of Dna2 in DNA replication, and in chapter 6 I will discuss the significance of this work and questions it raises as well as further advances in understanding the activities of Dna2.

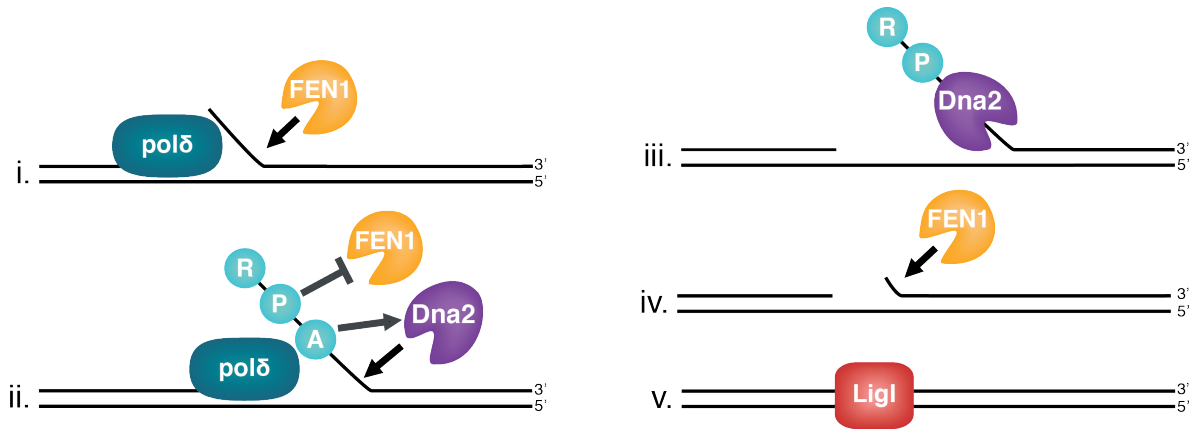

Figure 4.1: Dna2 mediates two-step Okazaki fragment processing.

FEN1 and Dna2 cooperate to process Okazaki fragments in eukaryotes. **i.** DNA polymerase δ, the lagging strand polymerase, synthesizes DNA in the 5' to 3' direction. Once it reaches the 5' end of the previous Okazaki fragment, it or an associated helicase displaces it creating a 5' RNA/DNA flap that is typically cleaved by FEN1 (60, 61). **ii.** In some circumstances, these flaps escape FEN1 cleavage and Polδ or a helicase continues displacing and elongating the ssDNA region. If the flap reaches 27 nucleotides in length it is bound by RPA, which inhibits FEN1 activity but promotes the 5' to 3' endonuclease activity of Dna2 (47, 62-64). **iii.** Dna2 then loads onto the flap and utilizes its helicase activity to track down the flap, where it uses its endonuclease activity to cleave the DNA (38, 64). **iv.** Dna2 cleavage occurs several nucleotides from the ssDNA/dsDNA junction, leaving a small flap that is processed by FEN1. **v.** The remaining nick is filled in by DNA ligase I. In one-step Okazaki fragment processing, there is a single cleavage event, and the process progresses directly from the first to the last step. Adapted from (65).

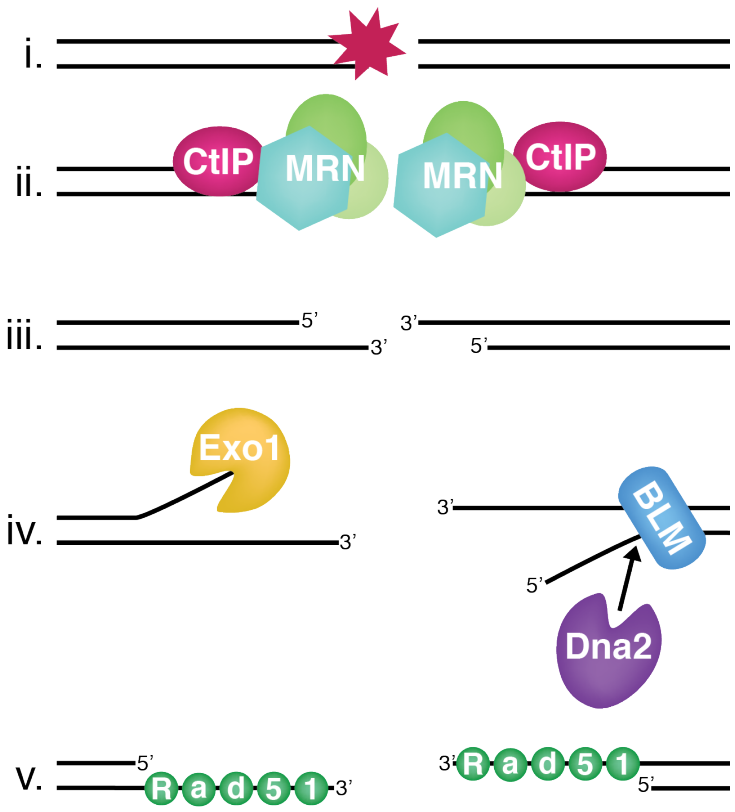

Figure 4.2: Dna2 participates in long-distance end resection in homologous recombination.

Upon experiencing a DNA double strand break (DSB), a cell can repair it through non-homologous end joining or homologous recombination. **i.** A DSB is induced and initial signaling occurs. **ii.** The MRN (Mre11-Rad50-NSB1) complex soon binds the DSB ends, directing repair towards the HR pathway. Both Mre11 and CtIP nucleases begin short-range resection of the 5' DNA end, resulting in short 3'ssDNA overhangs (**iii**) (52, 54, 66). **iv.** Further resection is then carried out through exonucleolytic cleavage by Exo1, or endonucleolytic cleavage by Dna2 in conjunction with the RecQ family helicases BLM or WRN (55, 58, 67, 68). **v.** The 3'ssDNA is bound by Rad51, which directs the homology search and invasion of the ssDNA into the homologous region, where the missing DNA is synthesized and the structure is resolved.

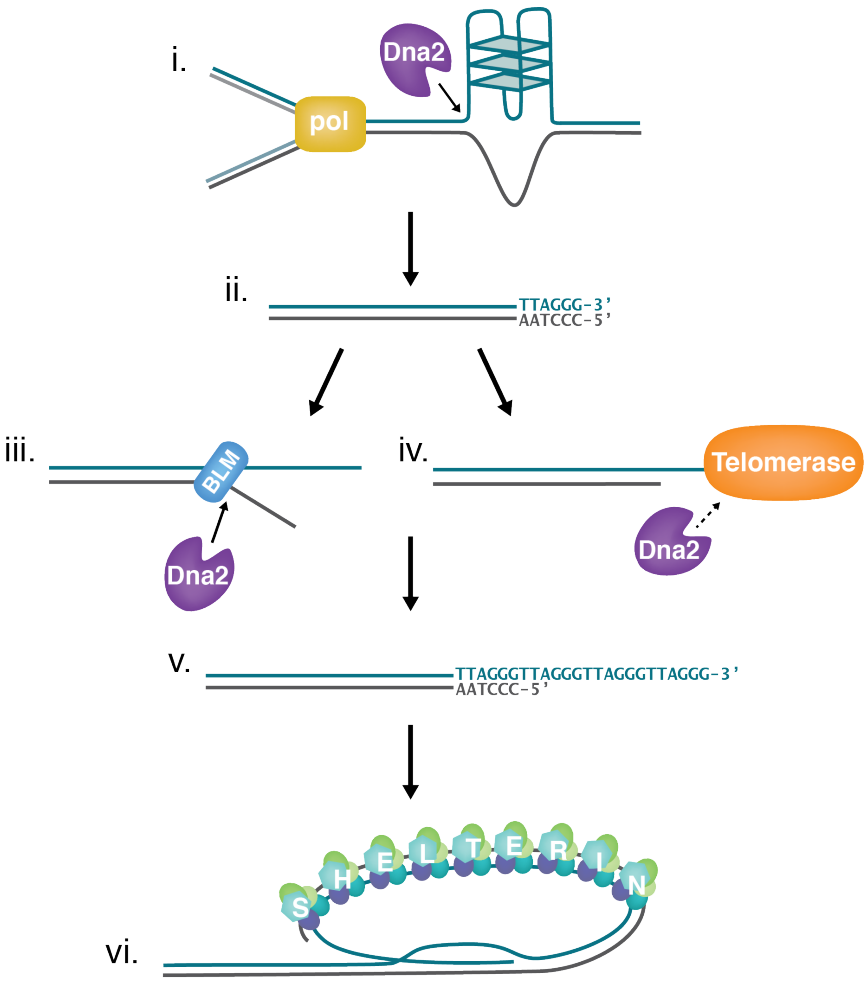

Figure 4.3: Dna2 has a multifaceted role in the synthesis and maintenance of telomeres.

Telomeres are the protective structures at chromosome ends that protect linear chromosomes from being degraded during DNA replication and from being identified and repaired as DNA double strand breaks. **i.** They are a difficult-to-replicate region, due in part to their repetitive sequence and the formation of polymerase-blocking secondary structures such as G quadruplexes. Dna2 is able to cleave these structures and promote the restart of stalled replication forks, allowing replication to progress through the telomere (30, 34, 69). **ii.** Once the telomere is replicated, the 3'ssDNA overhang on the G-rich strand needs to be generated. **iii.** Again working in concert, Dna2 and the RecQ helicase Sgs1 in yeast and possibly BLM in humans promote resection of the 5' telomeric strand, leaving behind the 3'ssDNA (32, 50, 59, 70, 71). **iv.** Dna2 is also able to directly stimulate telomerase activity, leading to elongation of the 3' G-rich strand (32, 50). **v.** After either resection or telomerase-mediated elongation, the 3'ssDNA region is generated. **iv.** The ssDNA then invades and pairs with the C-rich strand forming the T-loop structure, which sequesters the DNA ends. The shelterin complex, comprised of six core telomere binding and stabilizing proteins along with a growing list of accessory factors such FEN1, binds and protects the telomere from aberrant DNA repair activity (22, 70, 72, 73).

References

1. **Helbock HJ, Beckman KB, Shigenaga MK, Walter PB, Woodall AA, Yeo HC, Ames BN.** 1998. DNA oxidation matters: the HPLC-electrochemical detection assay of 8-oxo-deoxyguanosine and 8-oxo-guanine. Proc Natl Acad Sci U S A **95:**288-293.

2. **Vilenchik MM, Knudson AG.** 2003. Endogenous DNA double-strand breaks: production, fidelity of repair, and induction of cancer. Proc Natl Acad Sci U S A **100:**12871-12876.

3. **Haber JE.** 1999. DNA recombination: the replication connection. Trends Biochem Sci **24:**271-275.

4. **Gordon MY, Lewis JL, Marley SB.** 2002. Of mice and men...and elephants. Blood **100:**4679-4680.

5. **Kunkel TA.** 2009. Evolving views of DNA replication (in)fidelity. Cold Spring Harb Symp Quant Biol **74:**91-101.

6. **McCulloch SD, Kunkel TA.** 2008. The fidelity of DNA synthesis by eukaryotic replicative and translesion synthesis polymerases. Cell Res **18:**148-161.

7. **Nick McElhinny SA, Gordenin DA, Stith CM, Burgers PM, Kunkel TA.** 2008. Division of labor at the eukaryotic replication fork. Mol Cell **30:**137-144.

8. **Preston BD, Albertson TM, Herr AJ.** 2010. DNA replication fidelity and cancer. Semin Cancer Biol **20:**281-293.

9. **Pursell ZF, Isoz I, Lundstrom EB, Johansson E, Kunkel TA.** 2007. Yeast DNA polymerase epsilon participates in leading-strand DNA replication. Science **317:**127-130.

10. **Albertson TM, Ogawa M, Bugni JM, Hays LE, Chen Y, Wang Y, Treuting PM, Heddle JA, Goldsby RE, Preston BD.** 2009. DNA polymerase epsilon and delta proofreading suppress discrete mutator and cancer phenotypes in mice. Proc Natl Acad Sci U S A **106:**17101-17104.

11. **Goldsby RE, Hays LE, Chen X, Olmsted EA, Slayton WB, Spangrude GJ, Preston BD.** 2002. High incidence of epithelial cancers in mice deficient for DNA polymerase delta proofreading. Proc Natl Acad Sci U S A **99:**15560-15565.

12. **Goldsby RE, Lawrence NA, Hays LE, Olmsted EA, Chen X, Singh M, Preston BD.** 2001. Defective DNA polymerase-delta proofreading causes cancer susceptibility in mice. Nat Med **7:**638-639.

13. **Poulogiannis G, Frayling IM, Arends MJ.** 2010. DNA mismatch repair deficiency in sporadic colorectal cancer and Lynch syndrome. Histopathology **56:**167-179.

14. **Ribezzo F, Shiloh Y, Schumacher B.** 2016. Systemic DNA damage responses in aging and diseases. Semin Cancer Biol doi:10.1016/j.semcancer.2015.12.005.

15. **Taylor AM, Byrd PJ.** 2005. Molecular pathology of ataxia telangiectasia. J Clin Pathol **58:**1009-1015.

16. **Chrzanowska KH, Gregorek H, Dembowska-Baginska B, Kalina MA, Digweed M.** 2012. Nijmegen breakage syndrome (NBS). Orphanet J Rare Dis **7:**13.

17. **Michl J, Zimmer J, Tarsounas M.** 2016. Interplay between Fanconi anemia and homologous recombination pathways in genome integrity. EMBO J doi:10.15252/embj.201693860.

18. **Walden H, Deans AJ.** 2014. The Fanconi anemia DNA repair pathway: structural and functional insights into a complex disorder. Annu Rev Biophys **43:**257-278.

19. **Zhang J, Walter JC.** 2014. Mechanism and regulation of incisions during DNA interstrand cross-link repair. DNA Repair (Amst) **19:**135-142.

20. **Lo AW, Sabatier L, Fouladi B, Pottier G, Ricoul M, Murnane JP.** 2002. DNA amplification by breakage/fusion/bridge cycles initiated by spontaneous telomere loss in a human cancer cell line. Neoplasia **4:**531-538.

21. **Martinez P, Blasco MA.** 2015. Replicating through telomeres: a means to an end. Trends Biochem Sci **40:**504-515.

22. **Wei C, Price M.** 2003. Protecting the terminus: t-loops and telomere end-binding proteins. Cell Mol Life Sci **60:**2283-2294.

23. **Armanios M, Blackburn EH.** 2012. The telomere syndromes. Nat Rev Genet **13:**693-704.

24. **Blackburn EH, Epel ES, Lin J.** 2015. Human telomere biology: A contributory and interactive factor in aging, disease risks, and protection. Science **350:**1193-1198.

25. **Glousker G, Touzot F, Revy P, Tzfati Y, Savage SA.** 2015. Unraveling the pathogenesis of Hoyeraal-Hreidarsson syndrome, a complex telomere biology disorder. Br J Haematol **170:**457-471.

26. **Bailey SM, Murnane JP.** 2006. Telomeres, chromosome instability and cancer. Nucleic Acids Res **34:**2408-2417.

27. **Oshima J, Sidorova JM, Monnat RJ, Jr.** 2016. Werner syndrome: Clinical features, pathogenesis and potential therapeutic interventions. Ageing Res Rev doi:10.1016/j.arr.2016.03.002.

28. **Chu WK, Hickson ID.** 2009. RecQ helicases: multifunctional genome caretakers. Nat Rev Cancer **9:**644-654.

29. **Crabbe L, Verdun RE, Haggblom CI, Karlseder J.** 2004. Defective telomere lagging strand synthesis in cells lacking WRN helicase activity. Science **306:**1951-1953.

30. **Thangavel S, Berti M, Levikova M, Pinto C, Gomathinayagam S, Vujanovic M, Zellweger R, Moore H, Lee EH, Hendrickson EA, Cejka P, Stewart S, Lopes M, Vindigni A.** 2015. DNA2 drives processing and restart of reversed replication forks in human cells. J Cell Biol **208:**545-562.

31. **Budd ME, Campbell JL.** 1995. A yeast gene required for DNA replication encodes a protein with homology to DNA helicases. Proc Natl Acad Sci U S A **92:**7642-7646.

32. **Budd ME, Campbell JL.** 2013. Dna2 is involved in CA-strand resection and nascent lagging strand completion at native yeast telomeres. J Biol Chem doi:10.1074/jbc.M113.472456.

33. **Kang YH, Lee CH, Seo YS.** 2010. Dna2 on the road to Okazaki fragment processing and genome stability in eukaryotes. Crit Rev Biochem Mol Biol **45:**71-96.

34. **Lin W, Sampathi S, Dai H, Liu C, Zhou M, Hu J, Huang Q, Campbell J, Shin-Ya K, Zheng L, Chai W, Shen B.** 2013. Mammalian DNA2 helicase/nuclease cleaves G-quadruplex DNA and is required for telomere integrity. EMBO J **32:**1425-1439.

35. **Peng G, Dai H, Zhang W, Hsieh HJ, Pan MR, Park YY, Tsai RY, Bedrosian I, Lee JS, Ira G, Lin SY.** 2012. Human Nuclease/Helicase DNA2 Alleviates Replication Stress by Promoting DNA End Resection. Cancer Res **72:**2802-2813.

36. **Ronchi D, Di Fonzo A, Lin W, Bordoni A, Liu C, Fassone E, Pagliarani S, Rizzuti M, Zheng L, Filosto M, Ferro MT, Ranieri M, Magri F, Peverelli L, Li H, Yuan YC, Corti S, Sciacco M, Moggio M, Bresolin N, Shen B, Comi GP.** 2013. Mutations in DNA2 link progressive myopathy to mitochondrial DNA instability. Am J Hum Genet **92:**293-300.

37. **Bae SH, Seo YS.** 2000. Characterization of the enzymatic properties of the yeast dna2 Helicase/endonuclease suggests a new model for Okazaki fragment processing. J Biol Chem **275:**38022-38031.

38. **Kao HI, Campbell JL, Bambara RA.** 2004. Dna2p helicase/nuclease is a tracking protein, like FEN1, for flap cleavage during Okazaki fragment maturation. J Biol Chem **279:**50840-50849.

39. **Bae SH, Choi E, Lee KH, Park JS, Lee SH, Seo YS.** 1998. Dna2 of Saccharomyces cerevisiae possesses a single-stranded DNA-specific endonuclease activity that is able to act on double-stranded DNA in the presence of ATP. J Biol Chem **273:**26880-26890.

40. **Budd ME, Choe W, Campbell JL.** 2000. The nuclease activity of the yeast DNA2 protein, which is related to the RecB-like nucleases, is essential in vivo. J Biol Chem **275:**16518-16529.

41. **Masuda-Sasa T, Imamura O, Campbell JL.** 2006. Biochemical analysis of human Dna2. Nucleic Acids Res **34:**1865-1875.

42. **Zheng L, Zhou M, Guo Z, Lu H, Qian L, Dai H, Qiu J, Yakubovskaya E, Bogenhagen DF, Demple B, Shen B.** 2008. Human DNA2 is a mitochondrial nuclease/helicase for efficient processing of DNA replication and repair intermediates. Mol Cell **32:**325-336.

43. **Duxin JP, Dao B, Martinsson P, Rajala N, Guittat L, Campbell JL, Spelbrink JN, Stewart SA.** 2009. Human Dna2 is a nuclear and mitochondrial DNA maintenance protein. Mol Cell Biol **29:**4274-4282.

44. **Shaheen R, Faqeih E, Ansari S, Abdel-Salam G, Al-Hassnan ZN, Al-Shidi T, Alomar R, Sogaty S, Alkuraya FS.** 2014. Genomic analysis of primordial dwarfism reveals novel disease genes. Genome Res **24:**291-299.

45. **Liu W, Zhou M, Li Z, Li H, Polaczek P, Dai H, Wu Q, Liu C, Karanja K, Popuri V, Shan S, Schlacher K, Zheng L, Campbell J, Shen B.** 2016. A Selective Small Molecule DNA2 Inhibitor for Sensitization of Human Cancer Cells to Chemotherapy. EBioMedicine doi:10.1016/j.ebiom.2016.02.043.

46. **Budd ME, Campbell JL.** 1997. A yeast replicative helicase, Dna2 helicase, interacts with yeast FEN-1 nuclease in carrying out its essential function. Mol Cell Biol **17:**2136-2142.

47. **Bae SH, Bae KH, Kim JA, Seo YS.** 2001. RPA governs endonuclease switching during processing of Okazaki fragments in eukaryotes. Nature **412:**456-461.

48. **Imamura O, Campbell JL.** 2003. The human Bloom syndrome gene suppresses the DNA replication and repair defects of yeast dna2 mutants. Proc Natl Acad Sci U S A **100:**8193-8198.

49. **Budd ME, Campbell JL.** 2000. The pattern of sensitivity of yeast dna2 mutants to DNA damaging agents suggests a role in DSB and postreplication repair pathways. Mutat Res **459:**173-186.

50. **Choe W, Budd M, Imamura O, Hoopes L, Campbell JL.** 2002. Dynamic localization of an Okazaki fragment processing protein suggests a novel role in telomere replication. Mol Cell Biol **22:**4202-4217.

51. **Fiorentino DF, Crabtree GR.** 1997. Characterization of Saccharomyces cerevisiae dna2 mutants suggests a role for the helicase late in S phase. Mol Biol Cell **8:**2519-2537.

52. **Limbo O, Chahwan C, Yamada Y, de Bruin RA, Wittenberg C, Russell P.** 2007. Ctp1 is a cell-cycle-regulated protein that functions with Mre11 complex to control double-strand break repair by homologous recombination. Mol Cell **28:**134-146.

53. **Clerici M, Mantiero D, Lucchini G, Longhese MP.** 2005. The Saccharomyces cerevisiae Sae2 protein promotes resection and bridging of double strand break ends. J Biol Chem **280:**38631-38638.

54. **Mimitou EP, Symington LS.** 2008. Sae2, Exo1 and Sgs1 collaborate in DNA double-strand break processing. Nature **455:**770-774.

55. **Zhu Z, Chung WH, Shim EY, Lee SE, Ira G.** 2008. Sgs1 helicase and two nucleases Dna2 and Exo1 resect DNA double-strand break ends. Cell **134:**981-994.

56. **Hoa NN, Kobayashi J, Omura M, Hirakawa M, Yang SH, Komatsu K, Paull TT, Takeda S, Sasanuma H.** 2015. BRCA1 and CtIP Are Both Required to Recruit Dna2 at Double-Strand Breaks in Homologous Recombination. PLoS One **10:**e0124495.

57. **Nimonkar AV, Genschel J, Kinoshita E, Polaczek P, Campbell JL, Wyman C, Modrich P, Kowalczykowski SC.** 2011. BLM-DNA2-RPA-MRN and EXO1-BLM-RPA-MRN constitute two DNA end resection machineries for human DNA break repair. Genes Dev **25:**350-362.

58. **Sturzenegger A, Burdova K, Kanagaraj R, Levikova M, Pinto C, Cejka P, Janscak P.** 2014. DNA2 cooperates with the WRN and BLM RecQ helicases to mediate long-range DNA end resection in human cells. J Biol Chem **289:**27314-27326.

59. **Tomita K, Kibe T, Kang HY, Seo YS, Uritani M, Ushimaru T, Ueno M.** 2004. Fission yeast Dna2 is required for generation of the telomeric single-strand overhang. Mol Cell Biol **24:**9557-9567.

60. **Budd ME, Reis CC, Smith S, Myung K, Campbell JL.** 2006. Evidence suggesting that Pif1 helicase functions in DNA replication with the Dna2 helicase/nuclease and DNA polymerase delta. Mol Cell Biol **26:**2490-2500.

61. **Budd ME, Tong AH, Polaczek P, Peng X, Boone C, Campbell JL.** 2005. A network of multi-tasking proteins at the DNA replication fork preserves genome stability. PLoS Genet **1:**e61.

62. **Pike JE, Burgers PM, Campbell JL, Bambara RA.** 2009. Pif1 helicase lengthens some Okazaki fragment flaps necessitating Dna2 nuclease/helicase action in the two-nuclease processing pathway. J Biol Chem **284:**25170-25180.

63. **Stewart JA, Campbell JL, Bambara RA.** 2006. Flap endonuclease disengages Dna2 helicase/nuclease from Okazaki fragment flaps. J Biol Chem **281:**38565-38572.

64. **Stewart JA, Miller AS, Campbell JL, Bambara RA.** 2008. Dynamic removal of replication protein A by Dna2 facilitates primer cleavage during Okazaki fragment processing in Saccharomyces cerevisiae. J Biol Chem **283:**31356-31365.

65. **Burgers PM.** 2011. It's all about flaps: Dna2 and checkpoint activation. Cell Cycle **10:**2417-2418.

66. **Paull TT, Gellert M.** 1998. The 3' to 5' exonuclease activity of Mre 11 facilitates repair of DNA double-strand breaks. Mol Cell **1:**969-979.

67. **Gravel S, Chapman JR, Magill C, Jackson SP.** 2008. DNA helicases Sgs1 and BLM promote DNA double-strand break resection. Genes Dev **22:**2767-2772.

68. **Liao S, Toczylowski T, Yan H.** 2008. Identification of the Xenopus DNA2 protein as a major nuclease for the 5'->3' strand-specific processing of DNA ends. Nucleic Acids Res **36:**6091-6100.

69. **Hu J, Sun L, Shen F, Chen Y, Hua Y, Liu Y, Zhang M, Hu Y, Wang Q, Xu W, Sun F, Ji J, Murray JM, Carr AM, Kong D.** 2012. The intra-s phase checkpoint targets dna2 to prevent stalled replication forks from reversing. Cell **149:**1221-1232.

70. **Barefield C, Karlseder J.** 2012. The BLM helicase contributes to telomere maintenance through processing of late-replicating intermediate structures. Nucleic Acids Res **40:**7358-7367.

71. **Bonetti D, Martina M, Clerici M, Lucchini G, Longhese MP.** 2009. Multiple pathways regulate 3' overhang generation at S. cerevisiae telomeres. Mol Cell **35:**70-81.

72. **Saharia A, Guittat L, Crocker S, Lim A, Steffen M, Kulkarni S, Stewart SA.** 2008. Flap endonuclease 1 contributes to telomere stability. Curr Biol **18:**496-500.

73. **Verdun RE, Karlseder J.** 2006. The DNA damage machinery and homologous recombination pathway act consecutively to protect human telomeres. Cell **127:**709-720.

Chapter 5

An Okazaki fragment processing-independent role for human Dna2 during DNA replication

Julien P. Duxin, Hayley R. Moore, Julia Sidorova, Kenneth Karanja, Yuchi Honaker, Benjamin Dao, Helen Piwnica-Worms, Judith L. Campbell, Raymond J. Monnat, Jr., and Sheila A. Stewart

H. Moore was a contributing author to this work

This research was originally published in The Journal of Biological Chemistry.
Duxin, J.P., Moore, H.R., Sidorova, J., Karanja, K., Honaker, Y., Dao, B., Piwnica-Worms, H., Campbell, J.L., Monnat, R.J. Jr, Stewart, S.A.. Okazaki fragment processing-independent role for human Dna2 enzyme during DNA replication. *The Journal of Biological Chemistry*. 2012; 287(26): 21980-21991. © The American Society for Biochemistry and Molecular Biology.

Abstract

Dna2 is an essential helicase/nuclease that is postulated to cleave long DNA flaps that escape FEN1 activity during Okazaki fragment (OF) maturation in yeast. We previously demonstrated that the human Dna2 orthologue (hDna2) localizes to the nucleus and contributes to genomic stability. Here we investigated the role hDna2 plays in DNA replication. We show that Dna2 associates with the replisome protein And-1 in a cell cycle-dependent manner. Depletion of hDna2 resulted in S/G2 phase specific DNA damage as evidenced by increased γ-H2AX, RPA foci, and Chk1 kinase phosphorylation, a readout for activation of the ATR-mediated S phase checkpoint. In addition, we observed reduced origin firing in hDna2-depleted cells consistent with Chk1 activation. We next examined the impact of hDna2 on OF maturation and replication fork progression in human cells. As expected, FEN1 depletion led to a significant reduction in OF maturation. Strikingly, the reduction in OF maturation had no impact on replication fork progression, indicating that fork movement is not tightly coupled to lagging strand maturation. Analysis of hDna2-depleted cells failed to reveal a defect in OF maturation or replication fork progression. Prior work in yeast demonstrated that ectopic expression of FEN1 rescues Dna2 defects. In contrast, we found that FEN1 expression in hDna2-depleted cells failed to rescue genomic instability. These findings suggest that the genomic instability observed in hDna2-depleted cells does not arise from defective OF maturation and that hDna2 plays a role in DNA replication that is distinct from FEN1 and OF maturation.

Introduction

Genomic maintenance requires coordination of several processes including DNA replication, DNA repair, transcription, and cell cycle progression. Given the importance of genomic stability for ongoing cell proliferation, it is not surprising that DNA replication and repair proteins have evolved multiple functions and participate in several replication and repair pathways. Previously, we demonstrated that human Dna2 (hDna2) localizes to the nucleus and mitochondria and participates in DNA maintenance in both compartments (1). Dna2 is a highly conserved helicase/nuclease, originally discovered in *S. cerevisiae* and found in all organisms from yeast to humans (2-6). Dna2 possesses a 5' to 3' ATP-dependent helicase activity and a flap endonuclease activity (7). Genetic and biochemical experiments conducted in yeast support a model in which Dna2 contributes to Okazaki fragment (OF) maturation in lagging strand DNA replication (8-10), though *in vivo* evidence of Dna2 participating in this process is lacking.

During OF processing, flap endonuclease 1 (FEN1) is the major endonuclease that acts in a coordinated manner with DNA polymerase δ (Pol δ) strand displacement activity to remove short RNA/DNA flaps formed on the previous OF (short flap pathway OF processing) (9-12). Flaps that escape FEN1 cleavage and are longer than 27 nucleotides are subsequently coated by replication protein A (RPA), which inhibits FEN1 nuclease activity (long flap pathway OF processing) (9, 12, 13). RPA-bound OF flaps recruit Dna2, which cleaves the RPA-coated DNA and displaces RPA, leaving a short 5-6 nucleotide RNA-free DNA flap that is further processed by FEN1 to produce a ligatable nick (9, 10, 14-18). In support of this long flap model, both PIF1 helicase and Pol δ processivity subunit (Pol 32) promote long flap formation *in vitro*, and their deletion rescues the lethality associated with yeast Dna2 (yDna2) loss, presumably because long

flaps no longer form (12, 19-22). Conversely, mutations that increase Pol δ processivity are synthetically lethal with *dna2* mutations (19).

In addition to its role in OF processing, Dna2 functions in DNA repair and telomere maintenance through its DNA end-resection activity. In yeast, Dna2 undergoes a dynamic localization where it is present at telomeres in G1, relocalizes throughout the genome in S phase, and moves back to the telomeres in late S/G2 phase (23). In addition, upon bleomycin treatment, yDna2 leaves the telomere and localizes to sites of double strand breaks (DSBs) (23). Recent studies have demonstrated that yDna2 nuclease activity participates in the formation of a 3' single strand DNA overhang essential to initiate the homologous recombination process or to maintain telomeric stability (24-30). Furthermore, Nimonkar *et al.* elegantly reconstituted DNA end resection *in vitro* using purified human proteins and demonstrated that hDna2 physically interacts with BLM to resect 5' DNA ends in a process that depends on hDna2's nuclease, but not hDna2 helicase activity (31). Nonetheless, *in vivo* and *in vitro* studies in yeast and humans indicate that Exo1 can compensate for Dna2's nuclease activity in this process (24, 29, 31). This suggests that the essential function of Dna2 is not its resection activity during DSB repair but rather its function in removing long flaps during DNA replication.

Our previous work revealed that hDna2 contributes to genomic stability (1). Here, we provide evidence that hDna2 ensures genomic stability by virtue of a critical role in DNA replication that is independent of FEN1 and OF processing.

Materials and Methods

Cell culture

U-2-OS and HeLa were grown in Dulbecco's modified Eagle's medium (DMEM) (Sigma, St Louis, MO) containing 10% heat-inactivated fetal bovine serum (FBS) and 1% penicillin/streptomycin at 37°C in 5% CO_2.

Virus production and infection

Viral production and infections were carried out as described previously (1, 32). Briefly, 293T cells were transfected using TransIT-LT1 (Mirus, Madison, WI) and virus was collected 48 hours post-transfection. Subsequent infections were carried out overnight in the presence of 10 μg/ml of protamine sulfate, and followed 48 hours post-infection by selection of transduced cells with 2 μg/ml of puromycin. The pLKO.1 shDna2, pResQ shDna2' and pLKO.1 shSCR lentiviruses were produced by co-transfection with pCMV8.2ΔR and pCMV-VSV-G (8:1 ratio). The sequence for the shDna2 short hairpin was 5'-CATAGCCAGTAGTATTCGATG-3', for shDna2' was 5'-GCAGTATCTCCTCTAGCTAGT-3' and for shSCR was 5'-AAGGTTAAGTCGCCC TCGCTC-3' as previously reported (1). The sequences used for the FEN1 short hairpins were previously reported (32). The sequence used for the LigI-specific shLigI was 5'-GCTCAAGCTGAAGAAGGACTA-3'.

The pBabe-hygro-3xFLAG-Dna2 wild-type (wt), D294A (nuc), K671E (hel) and D294A/K671E double mutant (dm) cDNAs were cloned from pFastBACHTc-hDna2-FLAG and confirmed by DNA sequencing (5). Briefly, depletion rescue experiments utilized pBabe-Hygro-3XFLAG-

Dna2 (wt, nuc, hel or dm) or pBabe-hygro-3xFLAG control constructs produced in 293T cells. U-2-OS cells were transduced with different constructs and selected in the presence of 200 μg/ml of hygromycin B (Sigma, St Louis, MO). After selection, hDna2 overexpression was confirmed by western blot, and cells were transduced with pResQ shDna2' which does not target the exogenous hDna2 cDNAs followed by puromycin selection as described above. Five days post-infection, cells were analyzed for DNA content by flow cytometry as previously described (Fig. 5.2A) (1).

For FEN1 ectopic expression experiments, viral production and infections were carried out as described previously (32). U-2-OS cells were infected with pLKO.1 shSCR or pLKO.1 shDna2 lentiviruses for 5 hours. Cells were then counted and re-seeded in the presence of media containing Adeno-FEN1 or Adeno-GFP (33). 48 hrs post-infection, cells were re-plated at $0.8x10^6$ cells/10-cm plate, and then analyzed 24 to 48 hrs later by hypotonic propidium iodide staining and flow cytometry as previously described (1). FEN1 ectopic expression was confirmed by western blot and immunofluorescence (data not shown).

Immunoprecipitation and western blot analysis

For co-immunoprecipitation studies cells were washed in PBS and lysed in TBS-Tx buffer containing 50 mM Tris-HCl pH 7.4, 150 mM NaCl, 1 mM EDTA, 1% Triton-X100 and protease and phosphatase inhibitors. 2 mg of protein extracts were immunoprecipitated with 2.4 μg of anti-hDna2 or IgG control antibodies using protein A beads overnight at 4°C. The following morning, beads were washed 3 times in 1 mL of TBS-Tx buffer before eluting bound proteins in

2X Laemmli buffer by boiling for 5 min at 95°C. Anti-hDna2 antibody was produced as previously described (5) and anti-And-1 was kindly provided by Dr. Anindya Dutta (34).

For the cell cycle experiments, cells were enriched in G0/G1 and G1/S by serum starvation and double thymidine block respectively, as previously described (35). Briefly, for G0/G1 enrichment, exponentially growing cells were cultured in DMEM medium containing 0.6% FBS for 38 hours, then harvested, analyzed by FACS to ensure arrest, and used for immunoprecipitation of hDna2 followed by western blotting for And-1. For G1/S enrichment, exponentially growing cells were cultured in medium supplemented with 3 mM thymidine for 16 hours, washed twice in pre-warmed PBS and fresh media without thymidine was added for 12 hours. Then, fresh medium with 3 mM thymidine was added and cells grown for another 16 hours. Arrest was monitored by flow cytometry analysis and cells were harvested and used for co-immunoprecipitation studies as described above.

For western blot analysis, cells were washed in phosphate buffered saline (PBS), lysed in MCL buffer (50 mM Tris pH 8.0, 5 mM EDTA, 0.5% NP40, 100 mM NaCl, 2 mM DTT, and freshly-added protease and phosphatase inhibitors), sonicated (6 cycles of a 30 s pulse and 30 s cooling interval), and centrifuged for 20 min at 4 °C. Western blot analysis was carried out on whole cell lysates with the following antibodies: anti-hDna2 (ab96488, Abcam, Cambridge, MA); anti-FEN1 (A300-255A, Bethyl Laboratories, Montgomery, TX); anti-DNA Ligase I (ab615, Abcam, Cambridge, MA); anti-FLAG M2 (F3165, Sigma, St. Louis, MO); anti-Chk1 (G-4 #SC-8408, Santa Cruz, Santa Cruz, CA); anti-phospho-Chk1 (Ser 317) (36, Cell Signaling); anti-β-Catenin (#610154, BD Biosciences); anti-γ Actin (NB600-533, Novus Biological, Littleton, CO); and anti-phospho-histone H3 (Ser 10) (#9701, Cell Signaling). For western blot analysis of γ-H2AX,

cells were washed with PBS and lysed in RIPA buffer (150 mM NaCl, 1% Triton X-100, 0.5% sodium deoxycholate, 0.1% SDS, 50 mM Tris [pH 8.0], and freshly added protease and phosphatase inhibitors), then probed with anti-phospho-histone H2A.X (Ser139) (clone JBW301, #05-636, Millipore, Temecula, CA). All protein concentrations were measured using the Bradford assay.

Immunofluorescence

U-2-OS cells were grown for 1-2 days on coverslips, then washed in PBS, fixed in 4% paraformaldehyde, and permeabilized in 0.5% Triton X-100 prior to treatment with blocking buffer (10% FBS, 2% goat serum, and 0.2% Tween 20) at room temperature. Antibodies were diluted in blocking buffer and incubated with cells for 1 hr at room temperature or overnight at 4˚C. Cells were washed in PBS containing 0.02% Tween 20 and mounted in ProLong Gold mounting medium (Invitrogen, Grand Island, NY) containing 4', 6-diamidino-2-phenylindole (DAPI). Immunofluorescence detection was carried out with anti-phospho-histone H2A.X (Ser139) (clone JBW301, #05-636, Millipore, Temecula, CA) or anti-phospho-ATM (Ser1981) (clone 10H11.E12, #4526, Cell Signalling) as primary antibodies. Secondary antibodies were anti-mouse IgG-Alexa-Fluor® 488 or 546 (Invitrogen, Carlsbad, CA).

For RPA immunofluorescence, cells were pre-extracted before fixing as previously described (37). Briefly, U-2-OS cells were grown for 1-2 days on coverslips. Cells were washed in ice-cold cytoskeleton (CSK) buffer (10 mM HEPES/KOH pH 7.4, 300 mM sucrose, 100 mM NaCl, 3 mM $MgCl_2$), and then extracted for 6 min on ice with 0.5% Triton X-100 in CSK buffer supplemented with protease and phosphatase inhibitors. Following extraction, cells were fixed in

3.7% formaldehyde at room temperature for 25 min followed by immunofluorescence staining using anti-Replication Protein A antibody (RPA-70-9, #NA13, Calbiochem, La Jolla, CA).

Inter-nuclei chromatin bridges and micronuclei counts

hDna2-depleted (shDna2 and shDna2') and control (shSCR) U-2-OS cells were seeded in a 12 well plate at $5x10^4$ cells per well four days post-infection. After 36-48 hours, cells were fixed and stained with DAPI and the number of inter-nuclei bridges (ICBs) and micronuclei were counted. At least 1000 nuclei were counted per well, and 6 wells were quantified per experiment. Two independent experiments were quantified for micronuclei counts in Fig. 5.1C and ICB counts in Fig. 5.5D. To inhibit Chk1, cells were treated with either 300 nM Gö 6976 (Calbiochem) (38) or 100 nM AZD7762 (Axon Medchem BV, Netherlands) (39) for 8 hours before fixing and quantification of ICBs. Inhibition of Chk1 was confirmed by flow cytometry and western blot (Fig. 5.5C and data not shown). Images were processed using Photoshop 7.0 gray scale and invert function (Adobe, San Jose, CA).

Flow cytometric analysis

U-2-OS cells were seeded at 0.8 $x10^6$ cells/10 cm plate four days post-infection, and resuspended 36 to 48 hrs later for hypotonic propidium iodide staining (0.1 % sodium citrate tribasic, 0.3% triton X-100, 0.01 % propidium iodide, 50 μg/ml RNase A (Sigma, St Louis, MO)) prior to flow cytometry to determine DNA content as previously described (40).

S phase progression assay

U-2-OS cells were cultured for 30 min in the presence of 20 μM bromo-2-deoxyuridine (BrdU) in the dark as previously described (33). Briefly, cells were washed, cultured in fresh medium and harvested by trypsinization at the indicated times. Cells were washed in PBS and fixed in 4% paraformaldehyde and 0.1% Triton X-100 in PBS for 20 min at room temperature prior to DNase I treatment (30 μg DNase I (Sigma, St. Louis, MO) at 37 °C for 1 hour). BrdU was detected with an Alexa Fluor 488-conjugated anti-BrdU antibody (A21303, Invitrogen, Carlsbad, CA), and cellular DNA content was determined by propidium iodide staining followed by flow cytometric analysis.

Metaphase preparation and chromosome FISH

Subconfluent U-2-OS cells were incubated for 3.5 to 4 hr with 0.1 μg/ml of colcemid in order to isolate mitotic cells by mitotic shake off. After hypotonic swelling in 75 mM KCl for 10 min at 37 °C, cells were fixed in methanol/acetic acid (3:1), dropped onto glass slides, and aged at room temperature for 3 days. FISH was performed as previously described (32). Briefly, slides were rehydrated for 10 min in PBS, fixed with 4% paraformaldehyde in PBS for 2 min then hybridized with 0.3 μg/ml of a telomeric PNA probe (Cy3-$(CCCTAA)_3$) and a centromeric probe (Flu-OO-CTTCGTTGGAAACGGGA) in 70% formamide, 10 mM Tris HCl (pH 7.2) plus blocking reagent (Roche Applied Science, Indianapolis, IN). DNA was denatured for 3 min at 80 °C, and hybridizations were carried out at 37 °C for 4 hrs in a moist chamber. Slides were subsequently washed, dehydrated and mounted using VectaShield (Vector Labs, Burlingame, CA) containing DAPI. Images were taken using a Nikon 90i microscope and analyzed using the ISIS FISH imaging software (Metasystems, Altlussheim, Germany).

BrdU-comet assay

The BrdU-comet assay was performed as previously described (41). Briefly, U-2-OS cells were plated at $5x10^5$ cells/6 cm plate and grown for 36 hrs at 37°C. Cells were then pulsed for 30 min with 100 μM BrdU (Sigma, St. Louis, MO), and chased for 1 to 8 hrs in growth medium lacking BrdU. Cells were then trypsinized and embedded in low-melting-point agarose at 37°C prior to spreading onto comet slides (Trevigen, Gaithersburg, MD). Cells on slides were then lysed, denatured and run through electrophoresis under denaturing conditions (200 mM NaOH, 1 mM EDTA) prior to immunostaining with anti-BrdU antibody (#555627, BD Biosciences) for 1 hr in the dark. The primary antibody was detected using anti-mouse IgG-Alexa-Fluor® 488 (Invitrogen, Carlsbad, CA), and cells were counterstained with DAPI. At least 40 comet tails were quantified per sample time point using CometScore™ (TriTek). A total of 3 independent experiments were conducted.

maRTA assay

Replication fork progression rates were determined using microfluidic-assisted replication track analysis (maRTA) (42). Briefly, hDna2-depleted (shDna2) or control (shSCR) U-2-OS cells were labeled for 30 min each with 50 μM IdU followed by 50 μM CldU (Sigma, St. Louis, MO). For FEN1-depleted cells, U-2 OS-hTert cells were used to avoid potential telomeric defects induced by FEN1 depletion (43). Cells were then collected by trypsinization and used to prepare agarose plugs as previously described (42). High-molecular-weight DNA was isolated from cells embedded in agarose by brief heating to 75°C to melt the agarose, followed by agarose digestion. The resulting high-molecular-weight DNA was then loaded by capillary tension into microchannels to uniformly stretch and capture long, high molecular weight DNA molecules on

glass coverslips for immunostaining and fluorescence microscopy. Origin firing efficiency was determined by counting the fraction of origin firing events among all active replication events. Replication elongation efficiency was determined by measuring the mean length of first-label replication tracks in double-labeled tracks in order to analyze active/ongoing fork rates. Track lengths were measured in digital images of track using the AxioVision software package (Carl Zeiss). Three replicate samples of hDna2-depleted U-2-OS cells or mock-depleted U-2-OS cells (hDna2 experiment), or FEN1 depleted U-2 OS-hTert *vs*. mock-depleted U-2 OS-hTert cells (FEN1 experiment) were analyzed for each determination. A total of 250 to 450 replication tracks were measured in each sample.

Results

hDna2 contributes to genomic stability.

We previously reported that hDna2 depletion in U-2-OS cells leads to genomic instability characterized by the appearance of aneuploid cells, inter-nuclear chromatin bridges (ICBs), and an accumulation of cells in the late S/G2 phase of the cell cycle (1). Here we further report that hDna2 depletion results in an increase in γ-H2AX, a well-characterized marker of DNA damage including double strand breaks (DSBs) and the appearance of micronuclei indicative of aberrant mitosis. U-2-OS cells were transduced with one of two shRNA hairpins that led to a greater than 70% reduction in hDna2 mRNA and protein levels (**Fig. 5.1A & 5.1B**). Analysis of hDna2-depleted cells revealed a two-fold increase in micronuclei compared to cells expressing a control shRNA (**Fig. 5.1C**). Furthermore, hDna2-depleted cells displayed an increase in γ-H2AX foci

that was confirmed by western blot analysis (**Fig. 5.1D & 5.1B**). In addition to the appearance of γ-H2AX foci, we also observed phosphorylated-ATM foci in hDna2-depleted cells (**Fig. 5.1D**), confirming that hDna2 depletion results in the generation of DNA damage with activation of the DNA damage checkpoint.

ICBs arise from unresolved replication intermediates, defective mitosis, and/or telomere fusions that form upon loss of telomeric integrity (44). Because Dna2 plays an important role in telomere stability in yeast, we investigated whether the ICBs observed upon hDna2 depletion were the result of telomeric fusions. To address this possibility, we analyzed metaphases from control or hDna2-depleted cells. No increase in chromosomal end-to-end fusions was observed in cells expressing shRNAs targeting hDna2, suggesting that telomere dysfunction is not responsible for the formation of ICBs in these cells (**Sup. Fig. 5.S1**). Interestingly, analysis of metaphases isolated from hDna2-depleted cells revealed the appearance of abnormal chromosomes (**Fig. 5.1E**). These metaphases are reminiscent of chromosomes isolated from cells entering mitosis with incompletely replicated DNA (45) that could lead to the generation of ICBs, DSBs, and micronuclei similar to what is observed in hDna2-depleted cells. Together these experiments suggest that the genomic instability observed in hDna2-depleted cells arises from incomplete DNA replication.

hDna2's nuclease and helicase activities are essential.

Dna2 is a highly conserved enzyme that possesses nuclease and helicase/ATPase activities that are postulated to contribute to its function *in vivo*. While both activities are essential for viability in *S. cerevisiae* (46), recent *in vitro* biochemical studies have called into

question the significance of the helicase activity in the human protein (5, 6). Therefore, we addressed whether hDna2's nuclease and/or helicase activities contribute to genomic stability in mammalian cells. To assess the roles of these activities, we carried out a series of genetic knockdown-rescue experiments utilizing an shRNA targeting the 3' untranslated region (UTR) of endogenous hDna2 while expressing a FLAG-tagged shRNA-resistant hDna2 cDNA. We expressed either a control vector (ctrl) or wild-type (wt) hDna2, nuclease-deficient D294A (nuc) hDna2, or helicase/ATPase-deficient K671E (hel) hDna2 cDNA (5). To distinguish between the endogenous and exogenous hDna2 mRNAs, we designed specific PCR primers that amplify a region encompassing the last exon (exon 21) and the 3' UTR of the endogenous hDna2 gene that is absent in the cDNA constructs. This allowed us to confirm the knockdown of endogenous hDna2 while verifying ectopic expression of the cDNAs by western blot using a FLAG antibody (**Fig. 5.2A & 5.2B**).

We previously demonstrated that depletion of endogenous hDna2 results in a reduced G1 population, a late S/G2 cell cycle arrest, and the appearance of aneuploid cells (1). To assess the role of the helicase and nuclease activity of hDna2, we utilized flow cytometry to measure DNA content and determine the cell cycle profile of cells expressing wild-type or mutant hDna2. Expression of the wild-type allele rescued significantly the cell cycle defects observed upon depletion of hDna2 (**Fig. 5.2C**). In contrast, expression of the nuclease-deficient or helicase-deficient alleles did not rescue the cell cycle defects, indicating that both activities are essential to maintain genomic stability (**Fig. 5.2C**). Furthermore, cells expressing the nuclease-deficient hDna2 protein, at even lower levels than the wild-type or helicase-deficient mutants, displayed cell cycle defects that were more severe than those observed in cells depleted of endogenous

hDna2 alone (**Fig. 5.2B & 5.2C**; compare G1/(S+G2) ratio, and cells with >4N DNA content). Interestingly, cells expressing high levels of the nuclease deficient allele were selected against over the course of the experiment as evidenced by a significant reduction in protein level, suggesting that the nuclease-deficient mutant is either toxic or functions as a dominant negative (**Fig. 5.2A, 5.2B & 5.2C**).

To address whether hDna2 helicase activity contributed to the deleterious properties of the nuclease-deficient Dna2 allele, we expressed a double mutant (dm) allele lacking both the hDna2 nuclease and helicase activities. As seen in Sup. Fig. 5.S2B, expression of the double mutant was maintained at levels similar to the helicase-deficient protein in contrast to the nuclease-deficient mutant whose expression was rapidly lost (**Sup. Fig. 5.S2A & 5.S2B**). These results suggest that the toxic effect of nuclease-deficient hDna2 depends on its helicase activity and that both activities are coupled *in vivo*. Together, these results demonstrate that the nuclease and helicase activities of hDna2 are essential to maintain genomic stability.

hDna2 interacts with the replisome protein And-1 in a replication dependent manner.

Above, we demonstrate that hDna2 depletion leads to DNA damage and the appearance of metaphases reminiscent of cells entering mitosis with incomplete DNA replication. In *Xenopus laevis* extract, Dna2 is recruited to DNA shortly after replication licensing where it interacts with the replisome protein And-1 (47). To determine whether Dna2 associates with the replisome in human cells, we investigated interactions between hDna2 and And-1. We found that endogenous And-1 co-immunoprecipitated with hDna2 from asynchronous cells, suggesting that

hDna2 associates with the replisome (**Fig. 5.3A** and data not shown). Furthermore, comparisons of the And-1/hDna2 interaction in cells arrested in G0/G1 by serum starvation and cells blocked at the G1/S border by a double thymidine treatment revealed a significant increase in And-1/hDna2 interaction in cells arrested at the G1/S transition (**Fig. 5.3B**). These observations demonstrate that hDna2 specifically interacts with And-1 in replicating cells and are similar to observations made in *Xenopus* extract (47). Together they suggest that hDna2 interacts with And-1 shortly after licensing of the pre-RC as part of the replisome.

hDna2 depletion leads to replication checkpoint activation.

Dna2 plays an essential role in DNA replication in yeast. Our results indicate a corresponding, important role in human DNA replication. Therefore, we next tested whether hDna2's depletion altered S phase progression. Control or hDna2-depleted U-2-OS cells were pulsed with BrdU for 30 minutes and chased for 12 hours. While hDna2-depleted cells incorporated BrdU at the same rate as control cells, they displayed a marked delay in completing the S/G2 phase and consequently took longer to appear in the next G1 phase following mitosis (**Fig. 5.4A & 5.4B**) (compare 8, 10 and 12 hour time points). These observations support the original cell cycle profiling data and suggest that hDna2 depletion alters late S/G2 replication rather than bulk DNA replication rates during S phase. Furthermore, western blot analysis revealed a reduction in the phosphorylation of the mitotic marker histone H3 at serine 10 in depleted versus control cells confirming that the block occurs prior to mitosis (**Fig. 5.5A** bottom panel).

Complete replication of the genome relies on efficient replication initiation, progression and maturation. When replication is inhibited at any of these steps, cells respond by activating the S-phase checkpoint. Therefore, given the characteristic damage and cell cycle arrest observed following hDna2 depletion we next investigated the activation status of Chk1. Western blot analysis of hDna2-depleted cells revealed a significant increase in phosphorylation of Chk1 at serine 317 compared to control cells, indicative of DNA replication stress (**Fig. 5.5A** top panel). In agreement with this finding, we observed an accumulation of single stranded DNA, a trigger of the S-phase checkpoint, as evidenced by a significant increase in the number of RPA foci per cell in hDna2-depleted cells compared to control cells (**Fig. 5.5B**).

Chk1 activation prevents cells that have not completed DNA replication from moving into mitosis (48). When Chk1 is inhibited in cells undergoing replication stress, they can move into mitosis with incompletely replicated DNA that if unrepaired will lead to unresolved replication intermediates. To address whether checkpoint activation blocked hDna2-depleted cells from entering mitosis with under-replicated chromosomes and/or unresolved damage, we treated cells with one of two Chk1 inhibitors, Gö 6976 or AZD7762 (38, 39). Cells depleted of hDna2 were grown for 8 hours in the presence of the Chk1 inhibitor. Flow cytometric analysis revealed a drastic alteration in the cell cycle profile of hDna2-depleted cells treated with a Chk1 inhibitor compared to untreated cells (**Fig. 5.5C**). hDna2-depleted cells treated with the Chk1 inhibitor and released from the G2 arrest entered mitosis, but displayed an increase in ICBs compared to untreated hDna2-depleted cells, indicating that cells released from the G2 block underwent aberrant mitosis (**Fig. 5.5D**). Together these experiments establish that cells depleted of hDna2 display replication defects and arrest in late S/G2 due to checkpoint activation. Upon

checkpoint override, cells resume cell cycle progression despite incomplete replication and/or unresolved damage and undergo aberrant mitoses.

Above we demonstrate that hDna2 depletion leads to Chk1 activation and a late S/G2 cell cycle arrest. Chk1 activation following replicative stress occurs to stabilize ongoing replication forks and to inhibit firing of additional forks (48). Therefore, to examine the impact of Chk1 activation on origin firing we used microfluidic-assisted replication track analysis (maRTA), wherein DNA is sequentially labeled *in vivo* with short pulses of the base analogues IdU and CldU (42). Following labeling, DNA is isolated and stretched on coverslips for detection by IdU and CIdU immunostaining (**Fig. 5.6A**). Using maRTA we quantified the fraction of DNA origin firing events present among all tracks labeled with CldU and IdU. We found that hDna2-depleted cells displayed a 20-25% reduction in origin firing events compared to control cells (**Fig. 5.6B**). Together, these experiments establish that hDna2 depletion activates the replication checkpoint, which in turn inhibits the firing of replication forks.

Defects in Okazaki fragment processing do not alter replication fork progression.

Given the type of DNA damage we observed following hDna2 depletion and the model established in yeast suggesting Dna2 participates in OF maturation (9, 10), we next examined the role of hDna2 in DNA replication and fork progression using maRTA. By measuring the lengths of first label segments within replication tracks containing both labels, we determined the rate of DNA replication elongation. Using this method, we found that hDna2 depletion did not alter replication fork rate. Indeed, we found that DNA track lengths were similar in control and

hDna2-depleted cells (**Fig. 5.7A**). This finding suggests that the damage that arises from unprocessed DNA fragments accumulating behind the replication fork does not impede continued replication fork progression and is consistent with our result showing no defects in S phase progression in hDna2-depleted cells (**Fig. 5.4A & 5.4B**).

To further address the possibility that unprocessed OFs do not impact replication kinetics, we also depleted cells of FEN1 (**Sup. Fig. 5.S3**) (10). Because FEN1 is the major OF processing nuclease in the cell, we expected to find that FEN1 depletion would alter replication fork progression. Strikingly, we found that FEN1 depletion also failed to slow replication fork progression. In fact, we found that DNA track lengths were slightly longer in FEN1-depleted cells compared to control cells (**Fig. 5.7B** and **Sup. Fig. 5.S3**). Together these observations strongly suggest that the presence of unprocessed OFs and the associated damage they generate behind the replication fork is not sufficient to slow replication fork progression *in vivo*.

hDna2 depletion does not lead to detectable defects in maturation of newly synthesized DNA.

Long flaps requiring Dna2 for processing are predicted to arise in only a small percentage of OFs, and in specific regions of the genome (4, 12, 20). Therefore, the need for Dna2 should be dispensable for processing the vast majority of OFs, in contrast to the short flaps that are cleaved by FEN1. To determine whether hDna2 participates in OF processing, we measured the maturation kinetics of newly replicated DNA using a BrdU-comet assay. We reasoned that if hDna2 were necessary to process only a minority of the flaps, it would be difficult to observe maturation differences in cells depleted of hDna2 alone. Therefore, we also depleted FEN1 in addition to hDna2 in an effort to increase the accumulation of long flaps that would require Dna2

activity. In parallel we also depleted cells of DNA ligase I (LigI) as a positive control: LigI is required to ligate OF, which is required to complete OF processing (41). Western blot analysis demonstrated that we successfully depleted FEN1, LigI or hDna2 alone, and co-depleted FEN1 and hDna2 (**Fig. 5.8A**).

To assess the maturation of newly replicated DNA, control cells and cells depleted of hDna2, FEN1, or LigI alone, or co-depleted of both hDna2 and FEN1 were pulsed with BrdU and analyzed by an alkaline comet assay. Immunofluorescence against BrdU was used to assess the integrity of newly replicated DNA by measuring its migration from the tail (unligated DNA fragments, i.e., unprocessed OFs) to the head (ligated DNA, i.e., processed OFs) of the comet (**Fig. 5.8B** compare 1 hour to 8 hour images). As expected, LigI depletion slowed the maturation of newly replicated DNA from comet tails to heads (**Fig. 5.8C**) (41). In contrast, we failed to observe a significant difference in OF maturation in hDna2-depleted compared to control cells (**Fig. 5.8C**). Furthermore, FEN1-depleted cells displayed a reduction similar to that of LigI-depleted cells, indicating that FEN1 is the major flap endonuclease responsible for processing OFs during lagging strand replication. Finally, OF maturation did not differ in FEN1-hDna2 co-depleted cells compared with cells depleted of FEN1 alone (**Fig. 5.8C**), suggesting that hDna2 does not compensate for FEN1 loss in OF processing. These results indicate that the DNA damage that arises upon hDna2 depletion (**Fig. 5.9C** compare shDna2 to shFEN1 γ-H2AX levels) is unlikely to arise from a global OF maturation defect. However, it does not rule out a role for hDna2 in the maturation of a small fraction of OFs.

To further assess whether hDna2's primary function in DNA replication involves OF processing, we ectopically expressed FEN1 in hDna2-depleted cells ((33) & data not shown). In yeast, FEN1 overexpression compensates for phenotypes caused by hypomorphic mutations of Dna2 (8). However, ectopic expression of FEN1 in human cells did not improve the cell cycle defects observed in hDna2-depleted cells (**Fig. 5.9A & 5.9B**). These results further reinforce the contention that the key role of hDna2 in DNA replication is independent of FEN1 or OF processing.

Discussion

In this study, we provide evidence that hDna2 is essential to ensure faithful replication of the genome like its yeast homologue, and that unlike in yeast this essential role is independent of a requirement for hDna2 in global OF processing. We further demonstrate that both the nuclease and helicase activities of hDna2 contribute to genomic stability in human cells as they do in yeast. Finally, we report the unexpected finding that defective OF processing has no detectable impact on replication fork progression. This surprising result indicates that fork movement is decoupled from damage that arises behind the replication fork.

In *S. cerevisiae,* temperature sensitive *dna2* mutant alleles arrest cells in G2 with a 2C DNA content when shifted to the restrictive temperature (49). In *S. pombe,* temperature sensitive mutants also arrest in late S phase while displaying no defects in bulk DNA synthesis (4). When combined with a checkpoint inhibitor, these cells bypass the arrest and undergo aberrant mitosis. Similarly, here we demonstrate that hDna2-depleted cells harbor DNA damage and arrest in late

S/G2 phase. Upon Chk1 inhibition, cells bypass the replication checkpoint and progress through mitosis, displaying aberrant mitotic structures (increase in ICBs **Fig. 5.5D**). These phenotypes recapitulate observations in yeast and strongly suggest a conserved role for Dna2 in DNA replication in humans. Supporting our conclusions, ectopic expression of hDna2 suppresses the growth defects of the replication mutant *dna2-1* in *S. cerevisiae* (50).

The requirement for Dna2's helicase activity for yeast viability in *S. cerevisiae* indicates that this function is required *in vivo* (46). Indeed, different studies have demonstrated that Dna2's helicase activity is essential for efficient cleavage of long DNA flaps that may form secondary structures (7, 51). However, several studies demonstrated that the helicase activity of hDna2 is weak or undetectable, and might not serve a corresponding role in human cells (5, 6). Our observation that neither nuclease nor helicase-deficient hDna2 mutants rescue hDna2 depletion demonstrates that both activities are essential to ensure the integrity of the genome. Furthermore, we provide evidence that as in yeast, hDna2 nuclease-deficient expression is toxic to the cell (46, 51). This toxicity depends on its helicase activity, suggesting that both activities need to be coupled within a single Dna2 molecule to act on its substrates *in vivo*. This is in contrast to Dna2's function in 5' end resection during DSB repair where only the nuclease activity of Dna2 participates in this process (24, 29, 52, 53).

OF processing is an essential process that ensures a continuous lagging DNA strand and avoids single and double strand break formation. Several prior studies have suggested that defects in OF processing do not impact the rate of DNA synthesis. Indeed, we previously demonstrated that FEN1 depletion did not slow S-phase progression nor SV40 LargeT antigen-

dependent DNA replication *in vitro* (33). Similarly, LigI mutant cells (46BR.1G1) that exhibit low LigI activity do not activate the intra-S phase checkpoint (41). While protein extracts from these cells are deficient in OF ligation during SV40 DNA replication *in vitro*, they support incorporation of [α-^{32}P] dATP into plasmid DNA with similar kinetics as extracts from control fibroblasts. In addition, yeast deficient in LigI completely replicate their genomes despite being unable to ligate OF (54, 55). Together these studies suggest that replication fork progression is unperturbed in the absence of LigI (56). Here, using the sensitive maRTA technique, we demonstrate that depletion of an essential OF maturation protein, FEN1, does not alter replication fork progression *in vivo*. These observations strongly suggest that flaps that persist behind the replication fork do not affect the synthesis rate of DNA during replication.

FEN1 is postulated to be the primary endonuclease that processes flaps produced during lagging strand synthesis. However, both genetic and biochemical data indicate the presence of an additional long-flap processing pathway. Long DNA flap formation is promoted by PIF1 *in vitro,* and they require Dna2 activity to create shorter flaps that are cleaved by FEN1 to generate a ligatable nick (9, 10, 14). To address the role of hDna2 in long-flap processing in human cells, we depleted FEN1 and hDna2 independently or together, and then measured the maturation of nascent DNA. We found that maturation occurs with slower kinetics in FEN1-depleted cells, thus confirming FEN1 as the primary endonuclease responsible for processing OFs in human cells. In contrast, we did not observe a defect in maturation in hDna2-depleted cells. This indicates that if hDna2 processes long flaps, they do not represent a significant fraction of OFs in accordance with the model. However, our finding that FEN1-hDna2 co-depletion did not result in a significant difference in OF maturation rate compared to cells depleted of FEN1 alone was

surprising, since in yeast *dna2* and *rad27* mutations are synergistic (8). These results suggest either long flaps do not form readily in the absence of FEN1 in human cells, or that another nuclease can process flaps to render them ligatable. In yeast, other nucleases such as RNaseH2 or Exo1 can compensate for FEN1 loss by processing short flaps (20, 57-59). It remains to be seen whether their functions are conserved in humans. Despite the apparent functional dominance of FEN1, we were surprised to find that hDna2-depleted cells display more DNA damage than FEN1-depleted cells as assessed by γ-H2AX levels and abnormal cell cycle profile (**Fig. 5.9B** and data not shown). One explanation for this is that even infrequent unprocessed long flaps are a source of DNA damage and genetic instability in the absence of hDna2. However, we find this to be unlikely because ectopic FEN1 expression had no impact on the defects observed in hDna2-depleted cells. Thus a more likely and interesting possibility is that hDna2 has an important, as yet to be elucidated, role in replication or DNA repair beyond its postulated role in OF processing. This possibility is strengthened by our observation that hDna2 interacts with And-1 specifically in replicating but not resting human cells. This interaction is in accordance with yeast and *Xenopus* observations (47, 60-62) and suggests that hDna2 is a component of the replication fork. The late S/G2 phase arrest and appearance of aberrant post-mitotic structures could suggest a role for hDna2 in completing DNA replication by aiding in the resolution of replication intermediates. Interestingly, the BLM RecQ helicase can resolve late replication intermediates and its ectopic expression rescues Dna2 mutants in yeast (50). Alternatively, *Xenopus* Dna2 has been proposed to play a role in the early steps of DNA replication (3, 47). It remains to be addressed whether hDna2 actively participates in any of these processes.

Acknowledgements

We thank Dr. Soza and Dr. Montecucco for the BrdU/comet assay protocol and technical assistance with the procedure; Dr. Junran Zhang and Dr. Wei Shi for the RPA immunofluorescence protocol and aliquots of the antibody; Megan Ruhland for participating in this project during her rotation in the laboratory; Avi Silver for participating in DNA preparations and data analysis; and members of the Stewart, Campbell and Monnat laboratories for useful comments. We also thank Ermira Pazolli and Daniel Teasley for critical reading of the manuscript. This work was supported by the Cancer Biology Pathway, Siteman Cancer Center at Barnes-Jewish Hospital and Washington University School of Medicine in St Louis (JD, HM).

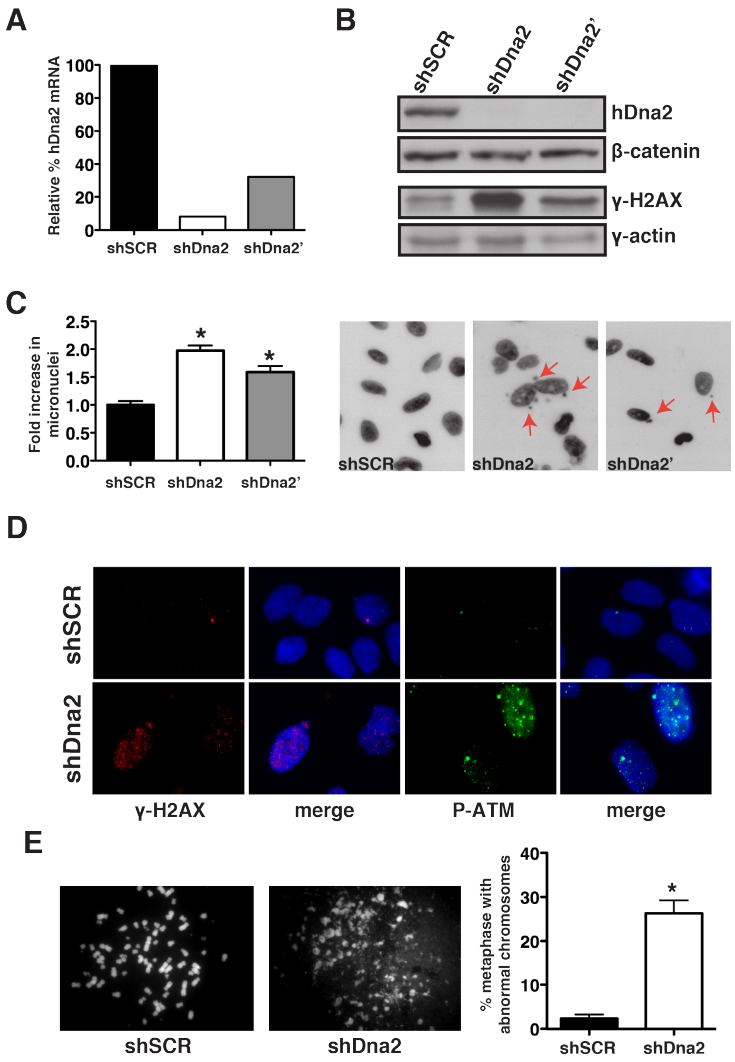

Figure 5.1: hDna2 contributes to genomic maintenance.

A. Knockdown of hDna2 in U-2-OS cells determined by qRT-PCR. Results for two independent hairpins targeting hDna2 (shDna2 & shDna2') are normalized to the shSCR control cell line expression levels. Note: shDna2 induces a better knock down of hDna2 mRNA than shDna2'. **B.** hDna2 knockdown determined by western blot analysis. Lysates were also probed for γ-H2AX to assess DNA damage and DSBs. **C.** Relative micronuclei counts and representative images depicting micronuclei (red arrows) following hDna2 depletion in cells. Results were normalized to shSCR control cells. **D.** Immunofluorescence staining of γ-H2AX (red) and phosphorylated-ATM (P-ATM) (green) in U-2-OS cells depleted of hDna2 (shDna2, bottom panels) or a control hairpin (shSCR, top panels). Nuclei were stained with DAPI (blue). **E.** (Left) Metaphase spread of control cells and hDna2-depleted cells with abnormal chromosomes. (Right) Quantification of 200 metaphases in 2 independent experiments is shown. All error bars represent SEM and * denotes $p<0.01$ compared to shSCR.

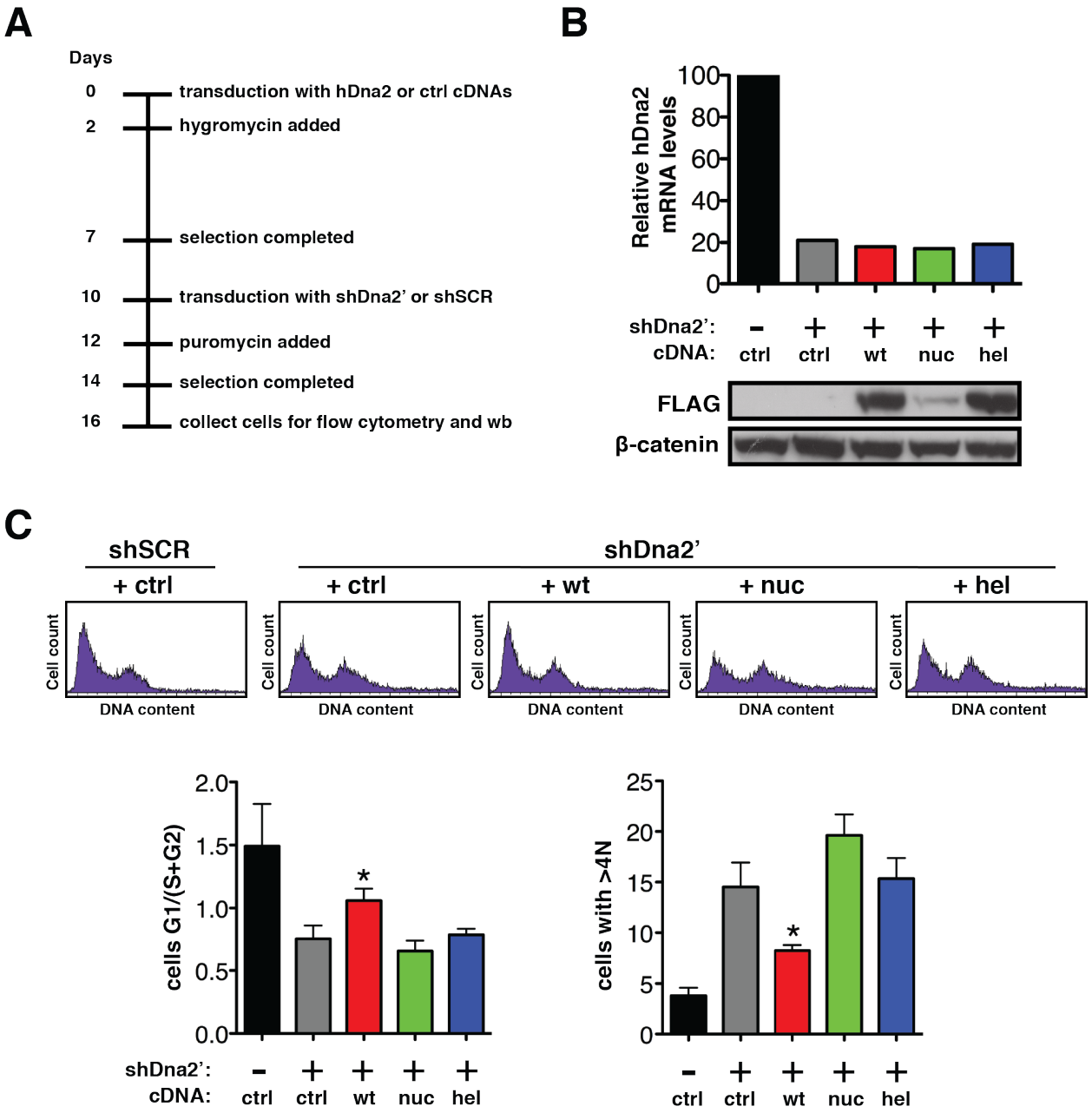

Figure 5.2: hDna2's nuclease and helicase activities contribute to genomic stability.

A. Timeline of experimental procedure given in days; wb denotes western blot. **B.** Relative knockdown of hDna2 in U-2-OS cells determined by qRT-PCR (top panel). Results are normalized to cells co-expressing the control vector (ctrl) + shSCR (-). PCR primers used detect only endogenous hDna2 mRNA. cDNA construct expression was confirmed by anti-FLAG western blot. **C.** Flow cytometric analysis depicting the cell cycle and DNA content of the U-2-OS cells analyzed in B. Bar graphs represent 4 independent experiments. (Left) The ratio of the percent of cells in G1 versus the percent of cells in S+G2. (Right) The percent of aneuploid cells containing abnormally high DNA content (>4N). Error bars represent SEM for 4 independent experiments and * denotes $p<0.05$ compared to cells co-expressing the ctrl vector + shDna2'.

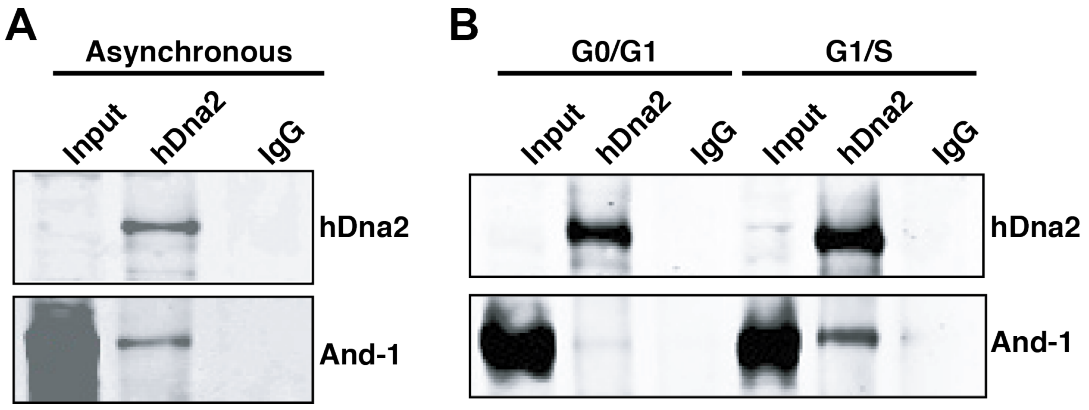

Figure 5.3: hDna2 interacts with And-1 in a replication dependent manner.

A. Interaction between hDna2 and And-1 in asynchronous cells. hDna2 was immunoprecipitated from asynchronous HeLa cells followed by western blot analysis with antibodies against And-1 or hDna2 as indicated. **B.** Interaction between hDna2 and And-1 occurs during G1/S transition. HeLa cells were arrested in G0/G1 by serum starvation or during G1/S by a double thymidine block. hDna2 was immunoprecipitated from the arrested cells and western blot analysis was performed with antibodies against And-1 or hDna2 as indicated.

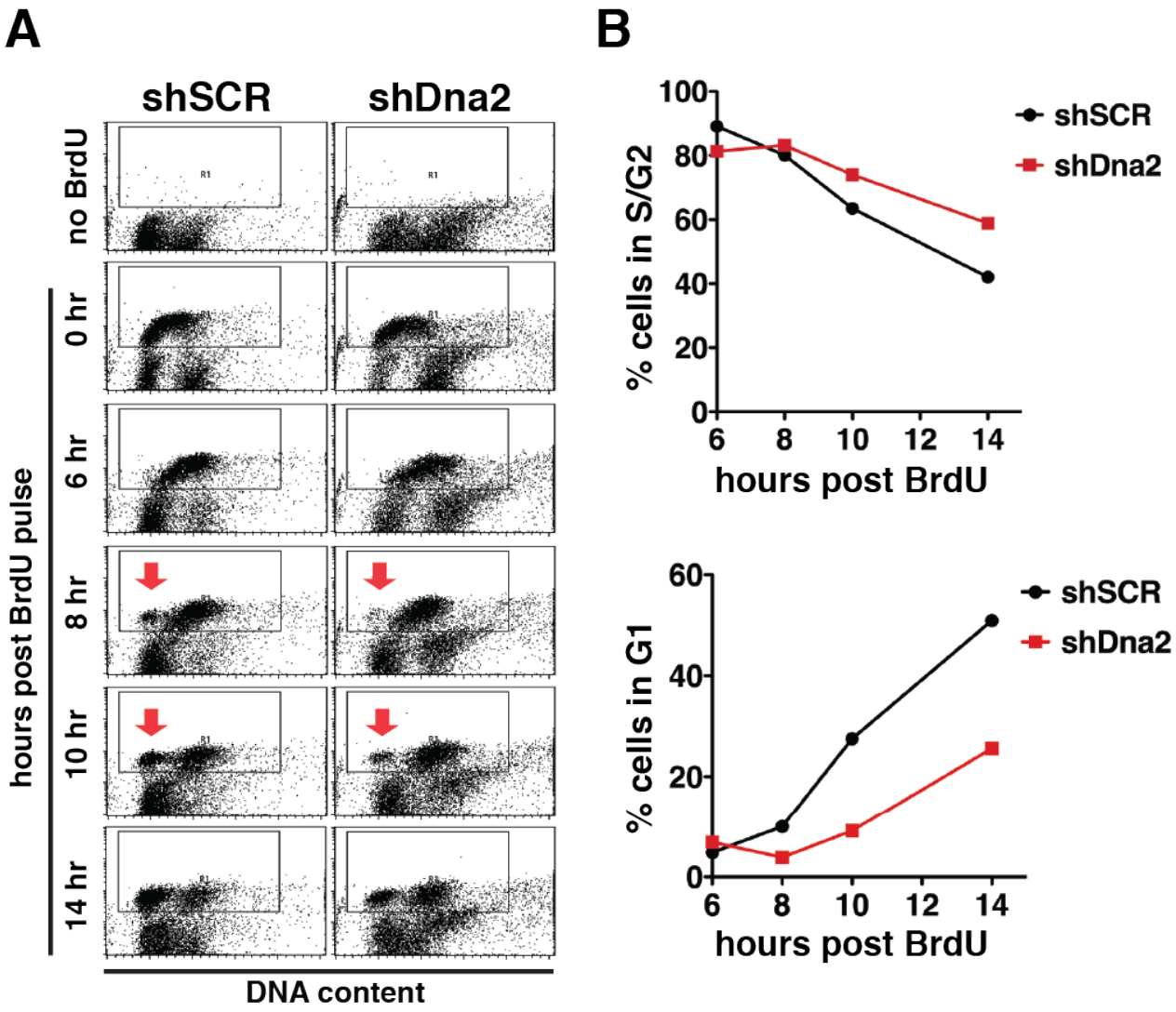

Figure 5.4: hDna2 depletion impedes cell cycle progression in late S/G2.

A. Cell cycle progression. U-2-OS cells expressing shSCR or shDna2 were pulsed with BrdU for 30 minutes and analyzed at the indicated times by flow cytometry using an anti-BrdU antibody (FITC-conjugated) (*y*-axis) and propidium iodide to quantify DNA content (*x*-axis). The inset box represents BrdU-positive cells that are analyzed in B. Red arrows indicate the cells appearing back in G1 8 and 10 hours post-BrdU pulse. **B.** Quantification of BrdU-positive cells in S/G2 phase (top graph) or BrdU-positive cells appearing in G1 (bottom graph). A representative experiment is shown.

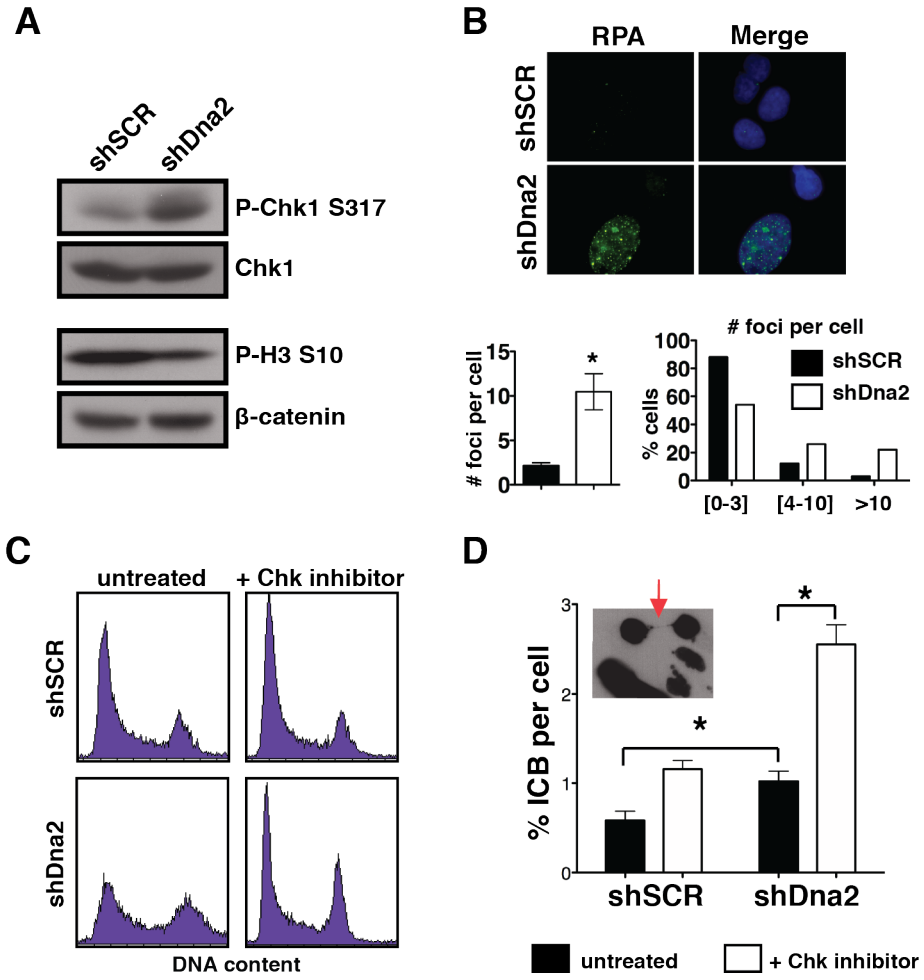

Figure 5.5: hDna2 depletion activates the replication checkpoint.

A. Western blot analysis of control (shSCR) and hDna2-depleted (shDna2) U-2-OS cells. Whole cell lysates were probed for total versus phosphorylated-Chk1 (P-Chk1 S317) (top panels). Samples were also probed for phosphorylated-histone H3 (P-H3 S10). **B.** Immunofluorescence staining of RPA-70 in shSCR and shDna2 U-2-OS cells. Cells were pre-extracted before fixing and staining to eliminate cytoplasmic RPA-70 (37). Quantification of RPA foci: average number (left) and total number (right) of foci per cell. * denotes $p<0.01$. **C.** Cell cycle distribution of shSCR and shDna2 +/- treatment with Chk1 inhibitor (Gö6976) for 8 hours. Similar results were obtained when AZD7762 was used to inhibit Chk1 (data not shown). **D.** Inter-nuclei chromatin bridges (ICBs) (1) were quantified in control (shSCR) and hDna2-depleted (shDna2) U-2-OS cells +/- Chk1 inhibitor. A representative image is shown with an ICB indicated by an arrow. * denotes $p<0.01$.

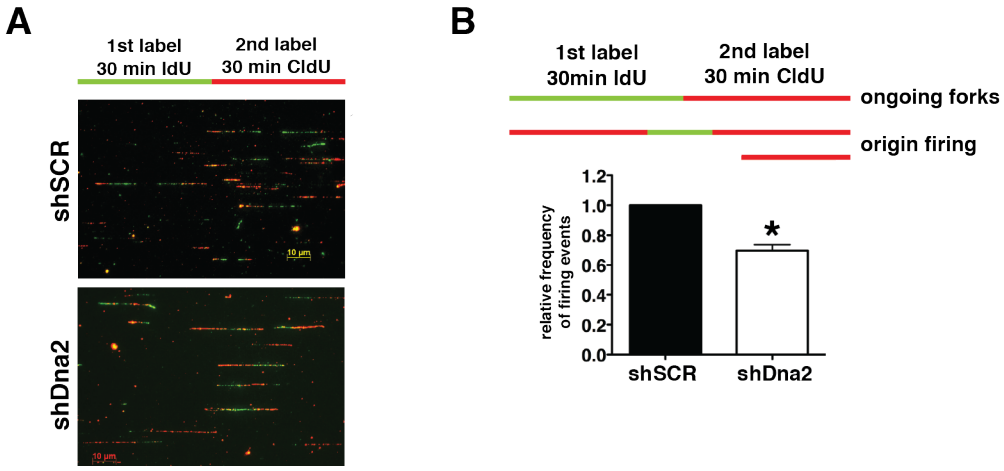

Figure 5.6: hDna2 depletion reduces origin firing.

A. shSCR or shDna2 U-2-OS cells labeled consecutively with IdU (green) and CldU (red) for 30 min each prior to isolating and stretching DNA for immunostaining. **B**. Origin firing events among all tracks labeled were identified as CldU-only (red only) or CldU-IdU-CldU (red-green-red) triple-segment tracks. The mean percentages of new origin firing events defined by these two track types among all labeled tracks are shown for three independent experiments in which 200 to 450 tracks/experiment were analyzed for control shSCR or shDna2. Error bars show SEM between three independent experiments. * denotes $p<0.05$.

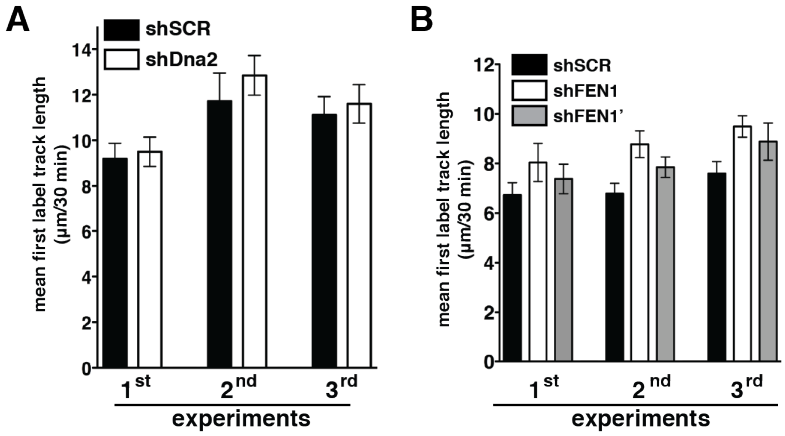

Figure 5.7: Replication fork progression is unperturbed in hDna2 or FEN1-depleted cells.

A. Quantification of three independent maRTA experiments is shown on the right. The bar graph summarizes mean lengths of first-label segments labeled for 30 min in two-segment tracks (i.e. tracks labeled consecutively with IdU and CIdU) to ensure that fork rate measurements were made from active replication forks. Error bars show 95% confidence intervals for sample means. No statistical difference in mean track lengths was observed between shSCR and shDna2 cells using a two-sample Kolmogorov-Smirnov test. **B.** Quantification of three independent experiments summarizing mean track length of the first label in cells depleted of FEN1 (shFEN1, shFEN1') or control cells (shSCR).

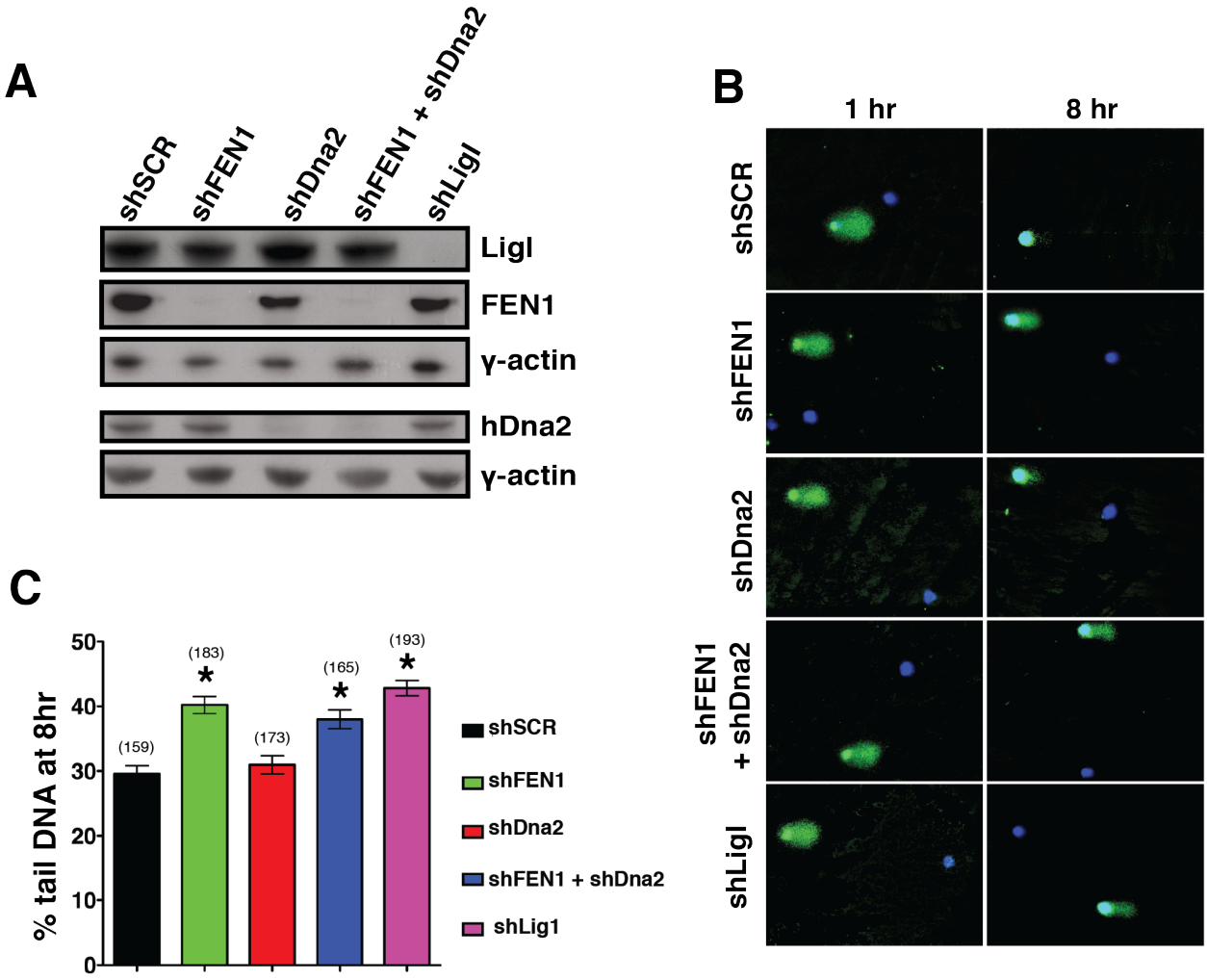

Figure 5.8: **hDna2 depletion does not impact Okazaki fragment maturation.**

A. BrdU-comet analysis of U-2-OS cells depleted of FEN1 (shFEN1), hDna2 (shDna2), LigI (shLigI) or co-depleted of FEN1 and hDna2 (shFEN1 + shDna2). Cells were pulsed for 15 min with BrdU and chased for 1 or 8 hours prior to comet processing**.** A. Western blot analysis of the different cell lines probed for LigI, FEN1, and hDna2. **B.** Representative images of the different samples at 1 and 8 hours post-BrdU pulse. Cells were immunostained for BrdU (green) and DNA was stained with DAPI (blue). **C.** Quantification of the percent BrdU-positive DNA in the tail versus the comet head at the 8-hour time point. Results are based on the analysis of 40 to 65 comets per experiment. A total of three independent experiments were performed and the errors bars correspond to the SEM. The total number of cells analyzed per sample is shown in parenthesis. * denotes $p<0.05$ comparing shFEN1, shFEN1+shDna2 or shLigI to shSCR.

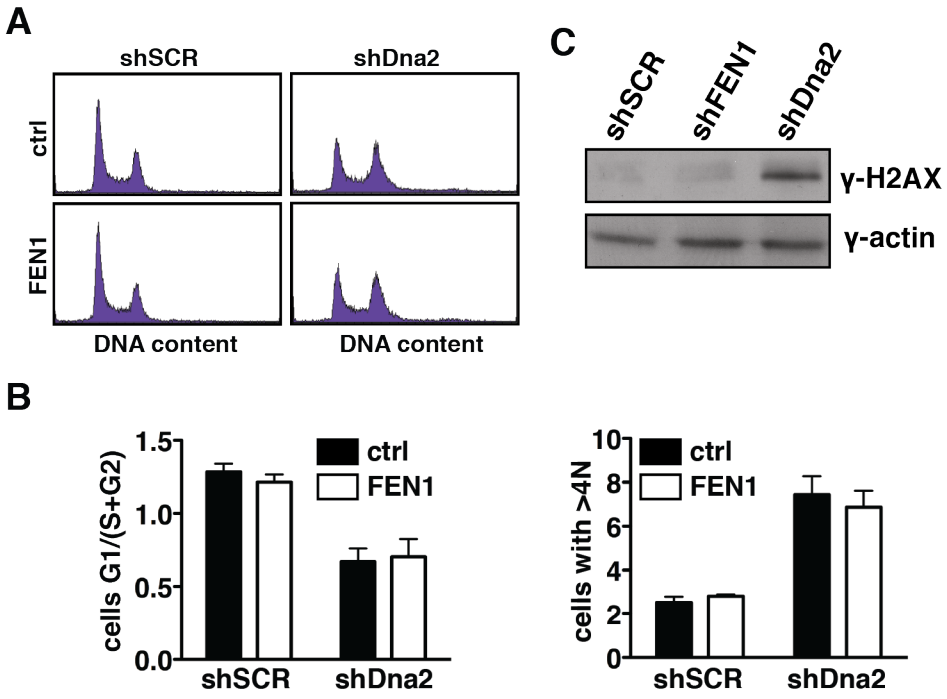

Figure 5.9: FEN1 overexpression does not compensate for hDna2-depletion.

A. hDna2-depleted (shDna2) or control U-2-OS cells (shSCR) were transduced with either GFP (ctrl) or FLAG-FEN1 (FEN1). Immunofluorescence images against FLAG demonstrated >70% of transduction of FEN1 expressing cells (data not shown). Flow cytometry histograms of the cell cycle distribution of the respective cell lines is depicted with the cell count represented on the *y*-axis and DNA content on the *x*-axis. **B.** Quantification of two independent experiments. (Left) graph representing the ratio of the percent of cells in G1 versus the percent of cells in S+G2. (Right) graph representing the percent of cells containing abnormally high DNA content (>4N). Error bars represent SEM. C. γ-H2AX levels determined by western blot analysis in FEN1 or hDna2-depleted cells.

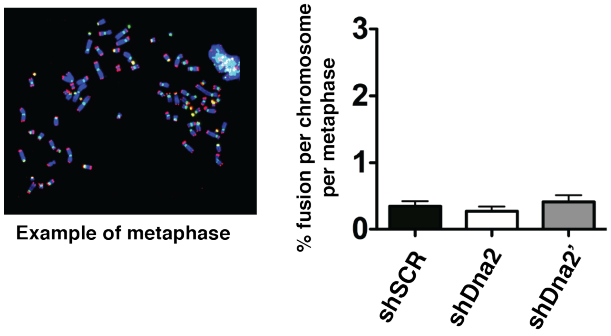

Supplementary Figure 5.S1: hDna2 depletion does not result in telomeric fusions.

Metaphases were prepared from control (shSCR) or hDna2-depleted (shDna2 and shDna2') U-2-OS cells and spreads were analyzed with a telomere-specific (red) and centromere-specific (green) probe. An example metaphase from an shDna2-depleted cell is shown on the left. On the right telomeric fusions were quantified for the different cell types.

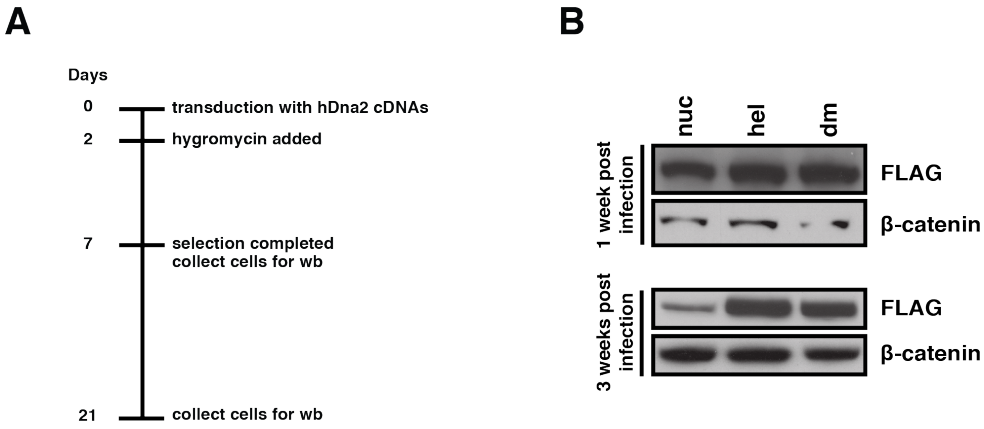

Supplementary Figure 5.S2: hDna2 helicase activity contributes to the deleterious properties of the nuclease-deficient Dna2 mutant.

A. Timeline of experimental procedure given in days. **B.** Western blot analysis of U-2-OS cells expressing a nuclease deficient allele (nuc), a helicase deficient allele (hel), and a nuclease and helicase-deficient double mutant allele (dm). Western blots were performed 1 and 3 weeks post-transduction.

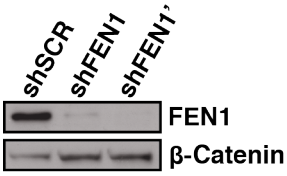

Supplementary Figure 5.S3: shRNA-mediated knockdown of FEN1.
Western blot analysis of FEN1 levels in U-2-OS cells depleted of FEN1 using two independent short hairpins (shFEN1, shFEN1') compared to a control cell line (shSCR). β-Catenin was used as a loading control.

References

1. **Duxin JP, Dao B, Martinsson P, Rajala N, Guittat L, Campbell JL, Spelbrink JN, Stewart SA.** 2009. Human Dna2 is a nuclear and mitochondrial DNA maintenance protein. Mol Cell Biol **29:**4274-4282.

2. **Budd ME, Campbell JL.** 1995. A yeast gene required for DNA replication encodes a protein with homology to DNA helicases. Proc Natl Acad Sci U S A **92:**7642-7646.

3. **Liu Q, Choe W, Campbell JL.** 2000. Identification of the Xenopus laevis homolog of Saccharomyces cerevisiae DNA2 and its role in DNA replication. J Biol Chem **275:**1615-1624.

4. **Kang HY, Choi E, Bae SH, Lee KH, Gim BS, Kim HD, Park C, MacNeill SA, Seo YS.** 2000. Genetic analyses of Schizosaccharomyces pombe dna2(+) reveal that dna2 plays an essential role in Okazaki fragment metabolism. Genetics **155:**1055-1067.

5. **Masuda-Sasa T, Imamura O, Campbell JL.** 2006. Biochemical analysis of human Dna2. Nucleic Acids Res **34:**1865-1875.

6. **Kim JH, Kim HD, Ryu GH, Kim DH, Hurwitz J, Seo YS.** 2006. Isolation of human Dna2 endonuclease and characterization of its enzymatic properties. Nucleic Acids Res **34:**1854-1864.

7. **Kang YH, Lee CH, Seo YS.** 2010. Dna2 on the road to Okazaki fragment processing and genome stability in eukaryotes. Crit Rev Biochem Mol Biol **45:**71-96.

8. **Budd ME, Campbell JL.** 1997. A yeast replicative helicase, Dna2 helicase, interacts with yeast FEN-1 nuclease in carrying out its essential function. Mol Cell Biol **17:**2136-2142.

9. **Bae SH, Bae KH, Kim JA, Seo YS.** 2001. RPA governs endonuclease switching during processing of Okazaki fragments in eukaryotes. Nature **412:**456-461.

10. **Ayyagari R, Gomes XV, Gordenin DA, Burgers PM.** 2003. Okazaki fragment maturation in yeast. I. Distribution of functions between FEN1 AND DNA2. J Biol Chem **278:**1618-1625.

11. **Rossi ML, Purohit V, Brandt PD, Bambara RA.** 2006. Lagging strand replication proteins in genome stability and DNA repair. Chem Rev **106:**453-473.

12. **Rossi ML, Pike JE, Wang W, Burgers PM, Campbell JL, Bambara RA.** 2008. Pif1 helicase directs eukaryotic Okazaki fragments toward the two-nuclease cleavage pathway for primer removal. J Biol Chem **283:**27483-27493.

13. **Kao HI, Veeraraghavan J, Polaczek P, Campbell JL, Bambara RA.** 2004. On the roles of Saccharomyces cerevisiae Dna2p and Flap endonuclease 1 in Okazaki fragment processing. J Biol Chem **279:**15014-15024.

14. **Bae SH, Seo YS.** 2000. Characterization of the enzymatic properties of the yeast dna2 Helicase/endonuclease suggests a new model for Okazaki fragment processing. J Biol Chem **275:**38022-38031.

15. **Stewart JA, Campbell JL, Bambara RA.** 2006. Flap endonuclease disengages Dna2 helicase/nuclease from Okazaki fragment flaps. J Biol Chem **281:**38565-38572.

16. **Stewart JA, Miller AS, Campbell JL, Bambara RA.** 2008. Dynamic removal of replication protein A by Dna2 facilitates primer cleavage during Okazaki fragment processing in Saccharomyces cerevisiae. J Biol Chem **283:**31356-31365.

17. **Stewart JA, Campbell JL, Bambara RA.** 2009. Significance of the dissociation of Dna2 by flap endonuclease 1 to Okazaki fragment processing in Saccharomyces cerevisiae. J Biol Chem **284:**8283-8291.

18. **Stewart JA, Campbell JL, Bambara RA.** 2009. Dna2 is a structure-specific nuclease, with affinity for 5'-flap intermediates. Nucleic Acids Res **38:**920-930.

19. **Budd ME, Reis CC, Smith S, Myung K, Campbell JL.** 2006. Evidence suggesting that Pif1 helicase functions in DNA replication with the Dna2 helicase/nuclease and DNA polymerase delta. Mol Cell Biol **26:**2490-2500.

20. **Stith CM, Sterling J, Resnick MA, Gordenin DA, Burgers PM.** 2008. Flexibility of eukaryotic Okazaki fragment maturation through regulated strand displacement synthesis. J Biol Chem **283:**34129-34140.

21. **Pike JE, Burgers PM, Campbell JL, Bambara RA.** 2009. Pif1 helicase lengthens some Okazaki fragment flaps necessitating Dna2 nuclease/helicase action in the two-nuclease processing pathway. J Biol Chem **284:**25170-25180.

22. **Pike JE, Henry RA, Burgers PM, Campbell JL, Bambara RA.** 2010. An alternative pathway for Okazaki fragment processing: resolution of fold-back flaps by Pif1 helicase. J Biol Chem **285:**41712-41723.

23. **Choe W, Budd M, Imamura O, Hoopes L, Campbell JL.** 2002. Dynamic localization of an Okazaki fragment processing protein suggests a novel role in telomere replication. Mol Cell Biol **22:**4202-4217.

24. **Zhu Z, Chung WH, Shim EY, Lee SE, Ira G.** 2008. Sgs1 helicase and two nucleases Dna2 and Exo1 resect DNA double-strand break ends. Cell **134:**981-994.

25. **Liao S, Toczylowski T, Yan H.** 2008. Identification of the Xenopus DNA2 protein as a major nuclease for the 5'->3' strand-specific processing of DNA ends. Nucleic Acids Res **36:**6091-6100.

26. **Tomita K, Kibe T, Kang HY, Seo YS, Uritani M, Ushimaru T, Ueno M.** 2004. Fission yeast Dna2 is required for generation of the telomeric single-strand overhang. Mol Cell Biol **24:**9557-9567.

27. **Bonetti D, Martina M, Clerici M, Lucchini G, Longhese MP.** 2009. Multiple pathways regulate 3' overhang generation at S. cerevisiae telomeres. Mol Cell **35:**70-81.

28. **Niu H, Chung WH, Zhu Z, Kwon Y, Zhao W, Chi P, Prakash R, Seong C, Liu D, Lu L, Ira G, Sung P.** 2010. Mechanism of the ATP-dependent DNA end-resection machinery from Saccharomyces cerevisiae.

29. **Cejka P, Cannavo E, Polaczek P, Masuda-Sasa T, Pokharel S, Campbell JL, Kowalczykowski SC.** 2010. DNA end resection by Dna2-Sgs1-RPA and its stimulation by Top3-Rmi1 and Mre11-Rad50-Xrs2. Nature **467:**112-116.

30. **Chen X, Niu H, Chung WH, Zhu Z, Papusha A, Shim EY, Lee SE, Sung P, Ira G.** 2011. Cell cycle regulation of DNA double-strand break end resection by Cdk1-dependent Dna2 phosphorylation. Nat Struct Mol Biol **18:**1015-1019.

31. **Nimonkar AV, Genschel J, Kinoshita E, Polaczek P, Campbell JL, Wyman C, Modrich P, Kowalczykowski SC.** 2011. BLM-DNA2-RPA-MRN and EXO1-BLM-RPA-MRN constitute two DNA end resection machineries for human DNA break repair. Genes Dev **25:**350-362.

32. **Saharia A, Guittat L, Crocker S, Lim A, Steffen M, Kulkarni S, Stewart SA.** 2008. Flap endonuclease 1 contributes to telomere stability. Curr Biol **18:**496-500.

33. **Saharia A, Teasley DC, Duxin JP, Dao B, Chiappinelli KB, Stewart SA.** 2010. FEN1 ensures telomere stability by facilitating replication fork re-initiation. J Biol Chem **285:**27057-27066.

34. **Zhu W, Ukomadu C, Jha S, Senga T, Dhar SK, Wohlschlegel JA, Nutt LK, Kornbluth S, Dutta A.** 2007. Mcm10 and And-1/CTF4 recruit DNA polymerase alpha to chromatin for initiation of DNA replication. Genes Dev **21:**2288-2299.

35. **Jackman J, O'Connor PM.** 2001. Methods for synchronizing cells at specific stages of the cell cycle. Curr Protoc Cell Biol **Chapter 8:**Unit 8 3.

36. **Diede SJ, Gottschling DE.** 1999. Telomerase-mediated telomere addition in vivo requires DNA primase and DNA polymerases alpha and delta. Cell **99:**723-733.

37. **Shi W, Feng Z, Zhang J, Gonzalez-Suarez I, Vanderwaal RP, Wu X, Powell SN, Roti Roti JL, Gonzalo S, Zhang J.** 2010. The role of RPA2 phosphorylation in

homologous recombination in response to replication arrest. Carcinogenesis **31:**994-1002.

38. **Kohn EA, Yoo CJ, Eastman A.** 2003. The protein kinase C inhibitor Go6976 is a potent inhibitor of DNA damage-induced S and G2 cell cycle checkpoints. Cancer Res **63:**31-35.

39. **Zabludoff SD, Deng C, Grondine MR, Sheehy AM, Ashwell S, Caleb BL, Green S, Haye HR, Horn CL, Janetka JW, Liu D, Mouchet E, Ready S, Rosenthal JL, Queva C, Schwartz GK, Taylor KJ, Tse AN, Walker GE, White AM.** 2008. AZD7762, a novel checkpoint kinase inhibitor, drives checkpoint abrogation and potentiates DNA-targeted therapies. Mol Cancer Ther **7:**2955-2966.

40. **Stewart SA, Poon B, Jowett JB, Chen IS.** 1997. Human immunodeficiency virus type 1 Vpr induces apoptosis following cell cycle arrest. J Virol **71:**5579-5592.

41. **Soza S, Leva V, Vago R, Ferrari G, Mazzini G, Biamonti G, Montecucco A.** 2009. DNA ligase I deficiency leads to replication-dependent DNA damage and impacts cell morphology without blocking cell cycle progression. Mol Cell Biol **29:**2032-2041.

42. **Sidorova JM, Li N, Schwartz DC, Folch A, Monnat RJ, Jr.** 2009. Microfluidic-assisted analysis of replicating DNA molecules. Nat Protoc **4:**849-861.

43. **Saharia A, Stewart SA.** 2009. FEN1 contributes to telomere stability in ALT-positive tumor cells. Oncogene **28:**1162-1167.

44. **Mandahl N, Mertens F, Willen H, Rydholm A, Kreicbergs A, Mitelman F.** 1998. Nonrandom pattern of telomeric associations in atypical lipomatous tumors with ring and giant marker chromosomes. Cancer Genet Cytogenet **103:**25-34.

45. **Nghiem P, Park PK, Kim Y, Vaziri C, Schreiber SL.** 2001. ATR inhibition selectively sensitizes G1 checkpoint-deficient cells to lethal premature chromatin condensation. Proc Natl Acad Sci U S A **98:**9092-9097.

46. **Budd ME, Choe W, Campbell JL.** 2000. The nuclease activity of the yeast DNA2 protein, which is related to the RecB-like nucleases, is essential in vivo. J Biol Chem **275:**16518-16529.

47. **Wawrousek KE, Fortini BK, Polaczek P, Chen L, Liu Q, Dunphy WG, Campbell JL.** 2010. Xenopus DNA2 is a helicase/nuclease that is found in complexes with replication proteins And-1/Ctf4 and Mcm10 and DSB response proteins Nbs1 and ATM. Cell Cycle **9:**1156-1166.

48. **Cimprich KA, Cortez D.** 2008. ATR: an essential regulator of genome integrity. Nat Rev Mol Cell Biol **9:**616-627.

49. **Fiorentino DF, Crabtree GR.** 1997. Characterization of Saccharomyces cerevisiae dna2 mutants suggests a role for the helicase late in S phase. Mol Biol Cell **8:**2519-2537.

50. **Imamura O, Campbell JL.** 2003. The human Bloom syndrome gene suppresses the DNA replication and repair defects of yeast dna2 mutants. Proc Natl Acad Sci U S A **100:**8193-8198.

51. **Bae SH, Kim DW, Kim J, Kim JH, Kim DH, Kim HD, Kang HY, Seo YS.** 2002. Coupling of DNA helicase and endonuclease activities of yeast Dna2 facilitates Okazaki fragment processing. J Biol Chem **277:**26632-26641.

52. **Niu H, Chung WH, Zhu Z, Kwon Y, Zhao W, Chi P, Prakash R, Seong C, Liu D, Lu L, Ira G, Sung P.** 2010. Mechanism of the ATP-dependent DNA end-resection machinery from Saccharomyces cerevisiae. Nature **467:**108-111.

53. **Peng G, Dai H, Zhang W, Hsieh HJ, Pan MR, Park YY, Tsai RY, Bedrosian I, Lee JS, Ira G, Lin SY.** 2012. Human Nuclease/helicase DNA2 Alleviates Replication Stress by Promoting DNA End Resection. Cancer Res doi:10.1158/0008-5472.CAN-11-3152.

54. **Das-Bradoo S, Nguyen HD, Bielinsky AK.** 2010. Damage-specific modification of PCNA. Cell Cycle **9:**3674-3679.

55. **Das-Bradoo S, Nguyen HD, Wood JL, Ricke RM, Haworth JC, Bielinsky AK.** 2010. Defects in DNA ligase I trigger PCNA ubiquitylation at Lys 107. Nat Cell Biol **12:**74-79; sup pp 71-20.

56. **Mackenney VJ, Barnes DE, Lindahl T.** 1997. Specific function of DNA ligase I in simian virus 40 DNA replication by human cell-free extracts is mediated by the amino-terminal non-catalytic domain. J Biol Chem **272:**11550-11556.

57. **Tishkoff DX, Boerger AL, Bertrand P, Filosi N, Gaida GM, Kane MF, Kolodner RD.** 1997. Identification and characterization of Saccharomyces cerevisiae EXO1, a gene encoding an exonuclease that interacts with MSH2. Proc Natl Acad Sci U S A **94:**7487-7492.

58. **Murante RS, Henricksen LA, Bambara RA.** 1998. Junction ribonuclease: an activity in Okazaki fragment processing. Proc Natl Acad Sci U S A **95:**2244-2249.

59. **Lee BI, Wilson DM, 3rd.** 1999. The RAD2 domain of human exonuclease 1 exhibits 5' to 3' exonuclease and flap structure-specific endonuclease activities. J Biol Chem **274:**37763-37769.

60. **Formosa T, Nittis T.** 1999. Dna2 mutants reveal interactions with Dna polymerase alpha and Ctf4, a Pol alpha accessory factor, and show that full Dna2 helicase activity is not essential for growth. Genetics **151:**1459-1470.

61. **Budd ME, Tong AH, Polaczek P, Peng X, Boone C, Campbell JL.** 2005. A network of multi-tasking proteins at the DNA replication fork preserves genome stability. PLoS Genet **1:**e61.

62. **Araki Y, Kawasaki Y, Sasanuma H, Tye BK, Sugino A.** 2003. Budding yeast mcm10/dna43 mutant requires a novel repair pathway for viability. Genes Cells **8:**465-480.

Chapter 6

Conclusions and Future Directions

DNA metabolism

6.1 Summary

Cells are constantly being exposed to a variety of intrinsic and extrinsic insults that can threaten genomic integrity, from the tens of thousands of oxidative lesions experienced per cell per day to the multitude of mismatched bases and double strand breaks induced within each round of DNA replication (1-3). Therefore, cells have evolved complex and interconnected mechanisms to ensure these lesions are repaired in order to prevent mutational accumulation or cellular dysfunction that can lead to pathologies such as cancer and immunological deficiencies. Elucidating the mechanisms protecting genome stability is an important step in understanding and potentially treating the multitude of diseases that occur as a result of deficiencies in these processes. In chapter 5, we demonstrate that human Dna2, a highly conserved and essential helicase/nuclease, participates in DNA replication in a manner independent of its canonical Okazaki fragment processing (OFP) function. Furthermore, disruption of this activity through shRNA-mediated Dna2 knockdown results in replication-driven genomic instability characterized by activation of the replication checkpoint and DNA double strand breaks, the accumulation of micronuclei, and gross chromosomal abnormalities during mitosis. Below, I will discuss the implications of this work, as well as more recent findings in regards to alternative functions of Dna2 in DNA replication.

6.2 Dna2 has non-Okazaki fragment processing roles in DNA replication

Dna2 has traditionally been thought to participate in two-step Okazaki fragment maturation, wherein 5'ss DNA flaps displaced by continued DNA polymerase δ-driven synthesis

are typically cleaved by flap endonuclease 1 (FEN1) to produce a nick that is ligated by DNA ligase I. However, some flaps escape FEN1 cleavage, and if they reach 27 nucleotides in length, become coated with replication protein A (RPA). This inhibits FEN1 activity and drives the 5' to 3' endonuclease activity of Dna2, which cleaves the RPA-coated DNA leaving several nucleotides at the base of the flap that are cleaved by FEN1 to leave a ligatable nick. In human cells, Dna2 is required for efficient DNA replication, because Dna2 depletion to leads Chk1-dependent activation of the replication checkpoint and late S/G2 cell cycle arrest, as well as other phenotypes indicative of replication stress such as internuclei chromatin bridges (**Fig 5.4 & Fig. 5.5**). If this were due to defects in OFP, then depletion of hDna2 should result in an accumulation of unligated, newly-synthesized DNA fragments including unligated Okazaki fragments. While depletion of Lig1 and FEN1 resulted in a significant accumulation of these fragments, depletion of Dna2 alone did not affect the percentage of unligated DNA. Furthermore, co-depletion of Dna2 and FEN1 did not have an additive affect on the inhibition of nascent DNA ligation, and unlike in yeast, overexpression of FEN1 to prevent the accumulation of long flaps did not alleviate the cell cycle arrest observed in Dna2-depleted human cells (**Fig 5.8 & 5.9**). Defects in LigI, which should affect processing of every Okazaki fragment, result in the accumulation of DNA breaks and replication intermediates and inefficient ligation of nascent DNA, but does not impact cell cycle progression (4). Together, these suggest that processing of long Okazaki fragments is not the primary replication function of Dna2 in human cells, and the replication defects associated with Dna2 depletion are not due to an accumulation of unprocessed Okazaki fragments and raise the question of what function of Dna2 is required to prevent the replication abnormalities observed in Dna2-deficient cells.

6.3 Dna2 is required for replication fork restart

Since performing the work in chapter 5, several reports have been published describing a role for Dna2 in the processing and restart of stalled replication forks (5-7). Replication forks stall when they are unable to continue synthesizing DNA, either due to a blockage on the template such as a bulky adduct, interstrand crosslink, or transcription machinery, as well as due to deficiencies in nucleotide pools. Fork stalling results in S phase checkpoint activation to stabilize the forks, since prolonged stalling can result in replication fork reversal, wherein the nascent strands anneal forming a "chicken foot" structure, which resembles a Holliday junction and is therefore subject to cleavage and recombination, or the fork can collapse, which can also result in DNA breaks (8-12). Several pathways have evolved to stabilize stalled forks by preventing regression or collapse, and to therefore promote replication fork restart.

In *Saccharomyces cerevisiae,* Cdk1-mediated phosphorylation of Dna2 was found to regulate Dna2's resection activity at DSB ends in a cell cycle-dependent manner (13). Chen and colleagues found that recruitment to and long-range resection of a DNA DSB by Dna2 required Cdk1 activity, and that Cdk1 and Mec1 (the functional homolog of the replication stress kinase ATR) phosphorylate Dna2 in response to DNA damage. This indicates that Dna2 activity at DSBs is regulated in a cell cycle-dependent manner, and suggests that Dna2 is primarily active in S phase (13). Shortly thereafter, Dna2 depletion was found to sensitize human cells to camptothecin and etoposide, both of which are topoisomerase inhibitors that induce replication-associated DSBs, and Dna2's nuclease activity was required for efficient HR-mediated repair of these breaks (6). Furthermore, Dna2 was required to restart replication forks that had been stalled by treatment with the DNA polymerase inhibitor aphidicolin and released. Although the authors

suggested that Dna2 functioned to enhance tolerance of replication-associated DSBs through HR-mediated repair mechanisms, their observation that Dna2 was required for restart of replication forks stalled by aphidicolin suggests that Dna2 has a broader function in promoting replication fork restart. Indeed, HR-mediated pathways, such as template switching to repair stalled forks and break-induced replication at collapsed forks, are major mechanisms of fork restart and essential in higher eukaryotes (14-17).

Mechanistically, Dna2 in *Schizosaccharomyces pombe* was shown to prevent the reversal of stalled replication forks. As a replication fork regresses, the complementary nascent DNA strands can anneal to form a chicken foot structure with potentially deleterious consequences. Hu and colleagues demonstrated that the intra-S phase checkpoint phosphorylates Dna2 promoted association of Dna2 with stalled replication forks. There, Dna2 was able to cleave both 5' and 3' DNA flaps to prevent replication fork regression. The helicase activity of Dna2 was not required for this activity, suggesting a scenario in which nascent DNA strands do not simultaneously unpair from their parent strands to anneal to each other, which would necessitate helicase activity to create Dna2 substrates, but rather that a single strand unpairs from the template and is cleaved by Dna2 to prevent further reversal (5). Similarly, Dna2 in humans was shown to resect nascent DNA at replication forks stalled by treatment with hydroxyurea to deplete nucleotide pools or camptothecin to inhibit topoisomerase activity. Furthermore, this Dna2-dependent processing was required to efficient restart forks after release from drug treatment (7). In this setting, Dna2 may act on chicken foot structures that had already formed, since Dna2 and the WRN were epistatic in processing DNA ends and promoting fork restart, suggesting they worked together to unwind and cleave structures at stalled forks. The extent of resection at stalled replication forks

by Dna2 is controlled at by several mechanisms to prevent 'over-resection', which can impair replication fork restart. The RecQ family helicase RecQ1 restrains Dna2 activity at stalled replication forks, as depletion of RecQ1 resulted in shorter tracts of nascent DNA at stalled replication forks than in control cells, and this degradation was Dna2 dependent because co-depletion of Dna2 and RecQ1 rescued this over-resection phenotype (7). While Thangavel and colleagues did not observe Mre11 nuclease activity in this setting, a second, Mre11-dependent mechanism of replication fork regression has been described (7, 18). In this pathway, the Fanconi anemia pathway proteins FANCD2, BRCA1, and BRCA2 bind and protect stalled replication forks from nucleolytic degradation by Mre11 (18). Interestingly, this pathway also regulates Dna2 resection activity (19). FANCD2-deficient cells have increased sensitivity to interstrand crosslinking agents, partially due to over-resection of DNA at the sites of interstrand crosslinks. Depletion of Dna2 in FANCD2-deficient cells rescues this sensitivity, suggesting that in addition to RecQ1, FANCD2 also modulates Dna2 activity at stalled replication forks to ensure proper processing and fork restart (19).

6.4 Dna2 knockout induces a stringent cell cycle arrest and abnormal metaphase chromosomes

Investigating the replication-dependent effects of Dna2 depletion can be difficult in an shRNA-mediated system, since multiple rounds of cell division occur as Dna2 levels drop, potentially leading to accumulation of DNA damage, chromosomal abnormalities, or other phenotypes related to loss of Dna2 function. Utilizing siRNA technology to knock down Dna2 mitigates this problem, as only 24-48h is required before experimentation, but residual Dna2 can

confound results. Therefore, we turned to a tamoxifen-inducible Dna2 knockout system in order to study the short-term effects of Dna2 loss. In HCT116 human colon cancer cell lines, a small duplication of chromosome 10 resulted in the introduction of a third *DNA2* allele. Therefore, two alleles were knocked out and the third was made conditional by introduction of loxP sites flanking a portion of exon 2 and a tamoxifen-inducible CreERT2, allowing us to investigate the differences between wild type HCT116 CreERT2 (wild type) and $Dna2^{Flox/-/-}$ CreERT2 with treated with vehicle or tamoxifen ($Dna2^{F/-/-}$ and $Dna2^{-/-/-}$, respectively).

Depletion of Dna2 by shRNA results in a late S/G2/M cell cycle arrest. This arrest is due to activation of the replication stress checkpoint, as Chk1 phosphorylation is increased in Dna2-depleted cells and treatment with a Chk1 inhibitor rescues cell cycle progression (**Fig. 5.5**). While $Dna2^{F/-/-}$ and wild type cells had similar cell cycle profiles, a strong late S/G2 arrest was observed in $Dna2^{-/-/-}$ cells (**Fig 6.1**). However, unlike what was observed in shDna2-expressing cells, inhibition of the replication stress checkpoint by treatment with AZD7762 to inhibit Chk1 did not rescue cell cycle progression in $Dna2^{-/-/-}$ cells. Furthermore, inhibition of ATM by treatment with Ku55933 or both ATM and ATR with caffeine treatment also failed to rescue cell cycle progression in $Dna2^{-/-/-}$ cells. This suggests that although these checkpoints are likely active in $Dna2^{-/-/-}$ cells, they are not the only mechanism by which the cell cycle is restrained. Preliminary data from cells synchronized at the G1/S transition by double thymidine block indicates that Dna2 knockout cells were able to progress through S phase with similar kinetics to wildtype cells, but that loss of Dna2 prevented cells from progressing through the first M phase after release (**Fig 6.2**). In agreement with an inability to enter M phase, whether due to cell cycle arrest or another factor, treatment with colcemid to isolate mitotic cells produced very few

metaphase spreads in Dna2$^{-/-/-}$ cells. Similar to the "pulverized chromosomes" observed in metaphase spreads from shDna2-expressing cells, preliminary investigation suggests a large majority of Dna2$^{-/-/-}$ spreads were grossly abnormal and fragmented. In contrast to the largely circular chromosome fragments observed in Dna2-depleted cells, the chromosomes in Dna2$^{-/-/-}$ metaphase spreads largely kept their shape. However, they were characterized by chromosome fusions, acentromeric and polycentromeric chromosomes (without overall alteration to centromere number) fragmentation of telomeric regions, and frequent loss of cohesion between sister centromeres and chromatids (**Fig. 6.3**).

These findings raise an interesting possibility. Dna2 interacts with And-1/Ctf4, which is required for sister chromatid cohesion (20-22). Deletion of *CTF4* in *S. cerevisiae* leads to G2/M spindle assembly checkpoint activation, and mutation of *ctf4* in results in a non-*RAD9*-dependent cell cycle delay, indicating the DNA damage checkpoint is not responsible for the delay observed (22, 23). The breakages observed in these metaphase spreads may be indicative of a chromosome condensation defect. Given the cell cycle-dependent Dna2/And-1 interaction, the inability to rescue Dna2$^{-/-/-}$ cell cycle progression with ATM and ATR inhibitors, and the potential sister chromatid cohesion defect observed in Dna2$^{-/-/-}$ metaphase spreads, investigation into a role for Dna2 in sister chromosome cohesion, condensation, or other late S/G2 processes could reveal a novel activity for Dna2 in genomic maintenance.

6.5 Conclusions

Preserving genomic stability is a vital aspect of protecting cellular and organismal health, and therefore many mechanisms have evolved to ensure efficient and efficacious replication and

repair of DNA. The proteins associated with these activities often have a diverse set of functions, allowing them to protect genomic stability through multiple mechanisms. The helicase/nuclease Dna2 is an important component of DNA repair, replication and telomere maintenance. The work presented here adds to the understanding of the diverse activities of Dna2, indicating that human Dna2 has a critical function in DNA replication outside of its canonical Okazaki fragment processing role identified in yeast. Fully characterizing the activities of Dna2 and other essential and multifunctional DNA metabolism proteins is an important aspect of understanding and eventually treating the diseases associated with dysfunctional genome maintenance.

Materials and methods

Cell culture conditions and drug treatments

The relevant HCT116 cell lines, a gift from the Eric Hendrickson lab, were grown in McCoy's 5A modified medium (Gibco) supplemented with 2mM glutamine, 10% FBS, and 1% penicillin/streptomycin at 37˚C in 5% CO_2 and atmospheric O_2 conditions. Cells were frozen in 40% complete medium, 10% DMSO, and 50% FBS. Cells were treated with 10nM 4-hydroxytamoxifen (Sigma, product number H7904) in ethanol at the indicated times. For checkpoint inhibition, cells were treated 48h post-4-OHT addition for 3h with 300nM AZD7762 (Axon Medchem BV), 10μM Ku55933 (Calbiochem) and 4mM caffeine.

Cell cycle synchronization and flow cytometric cell cycle analysis

Cells were synchronized using a double thymidine block. Cells were plated in 10 cm dishes, and the next day, were incubated with 2mM thymidine for two 14h treatments with a 10h recovery in

between. Cells were washed 2x in PBS and released into fresh medium, both of which were at 37˚C and stored in 5% CO_2 incubators to minimize temperature and pH changes to the cells. Samples were collected and the indicated times, and DNA content was analyzed by hypotonic propidium iodide staining and flow cytometry as described (24).

Metaphase analysis

HCT116 cells were treated with tamoxifen or control for 24h and then arrested in metaphase by treatment with 0.1μg/mL colcemid for 3h. Mitotic cells were collected by mitotic shake-off and hypotonic swelling, and fluorescence *in situ* hybridization was used to visualize centromeres and telomeres as described (25).

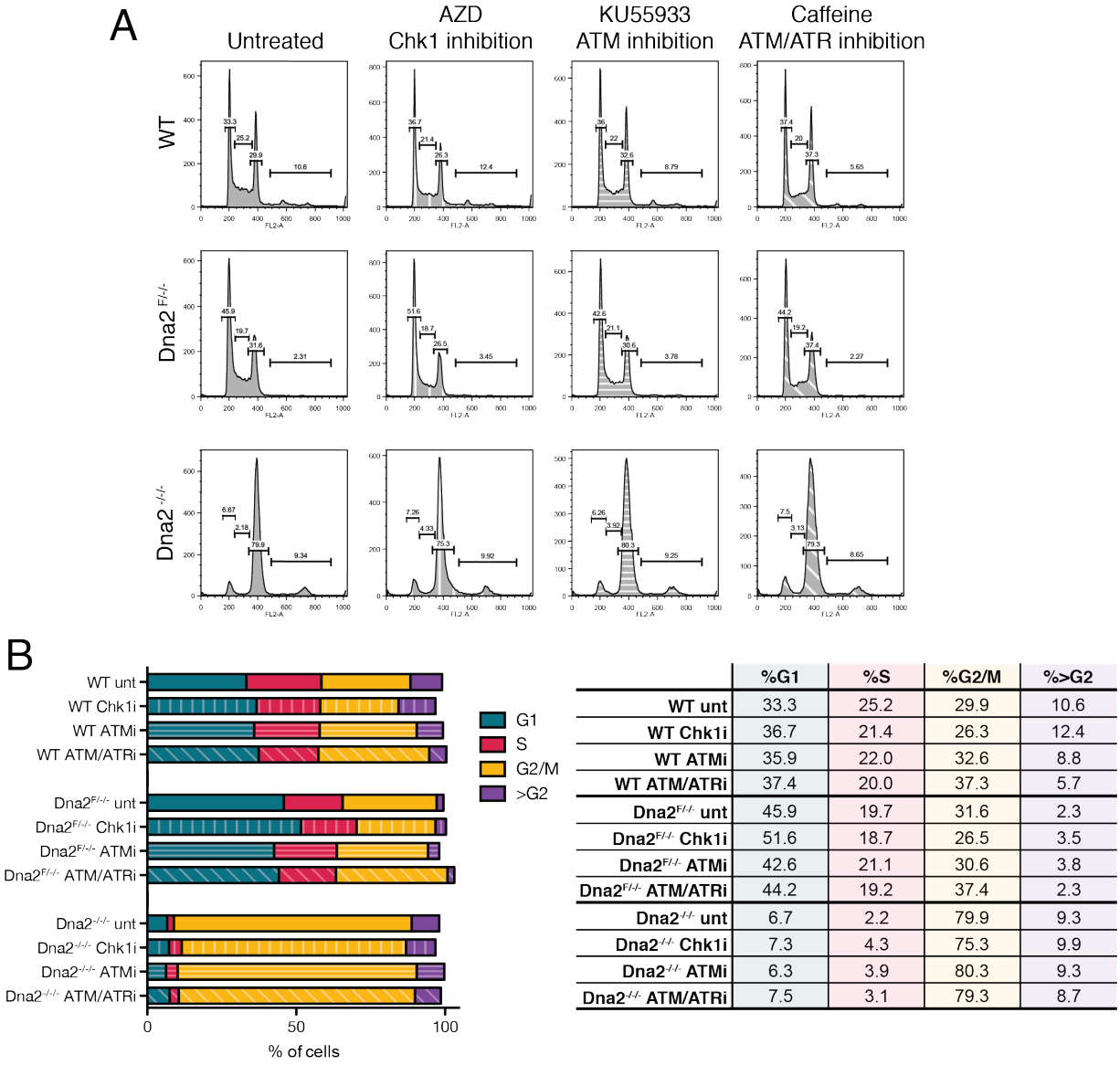

	%G1	%S	%G2/M	%>G2
WT unt	33.3	25.2	29.9	10.6
WT Chk1i	36.7	21.4	26.3	12.4
WT ATMi	35.9	22.0	32.6	8.8
WT ATM/ATRi	37.4	20.0	37.3	5.7
Dna2$^{F/-/-}$ unt	45.9	19.7	31.6	2.3
Dna2$^{F/-/-}$ Chk1i	51.6	18.7	26.5	3.5
Dna2$^{F/-/-}$ ATMi	42.6	21.1	30.6	3.8
Dna2$^{F/-/-}$ ATM/ATRi	44.2	19.2	37.4	2.3
Dna2$^{-/-/-}$ unt	6.7	2.2	79.9	9.3
Dna2$^{-/-/-}$ Chk1i	7.3	4.3	75.3	9.9
Dna2$^{-/-/-}$ ATMi	6.3	3.9	80.3	9.3
Dna2$^{-/-/-}$ ATM/ATRi	7.5	3.1	79.3	8.7

Figure 6.1 Dna2 knockout induces cell cycle arrest resistant to DNA damage checkpoint inhibitors

Cell cycle analysis of HCT116 wild type (WT), Dna2$^{F/-/-}$ and Dna2$^{-/-/-}$ cells treated 4-OHT (WT and Dna2$^{-/-/-}$) or ethanol (Dna2$^{F/-/-}$) and with the indicated inhibitors for 3h before collection. **A.** Flow cytometric analysis of the DNA content as measured by hypo-PI staining. **B.** Cell cycle distributions and quantification of the samples measured in *A*. Representative experiment, AZD7762, n=5; caffeine, n=3; Ku55933, n=2.

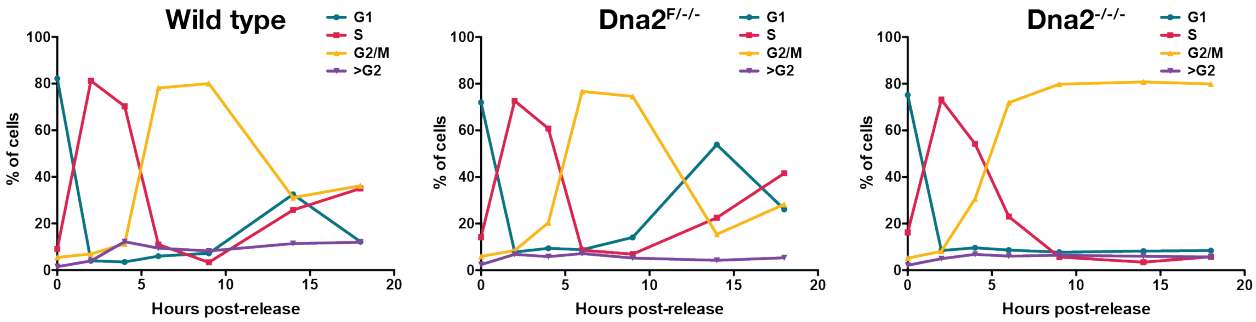

Figure 6.2 Progression through the cell cycle is impaired in Dna2$^{-/-/-}$ cells after release from G1/S block.

HCT116 wild type and Dna2$^{F/-/-}$ cells were synchronized using double thymidine block. 4h prior to the second release, wild type and a subset of Dna2$^{F/-/-}$ cells were treated with 4-OHT to generate Dna2$^{-/-/-}$ and control populations. Cells were then released and collected at the indicated times, stained with hypotonic-PI, and the cell cycle distribution was calculated based on DNA content as measured by flow cytometry. 4-OHT treatment to generate Dna2$^{-/-/-}$ cells at different times before and after release produced similar results. Representative experiment.

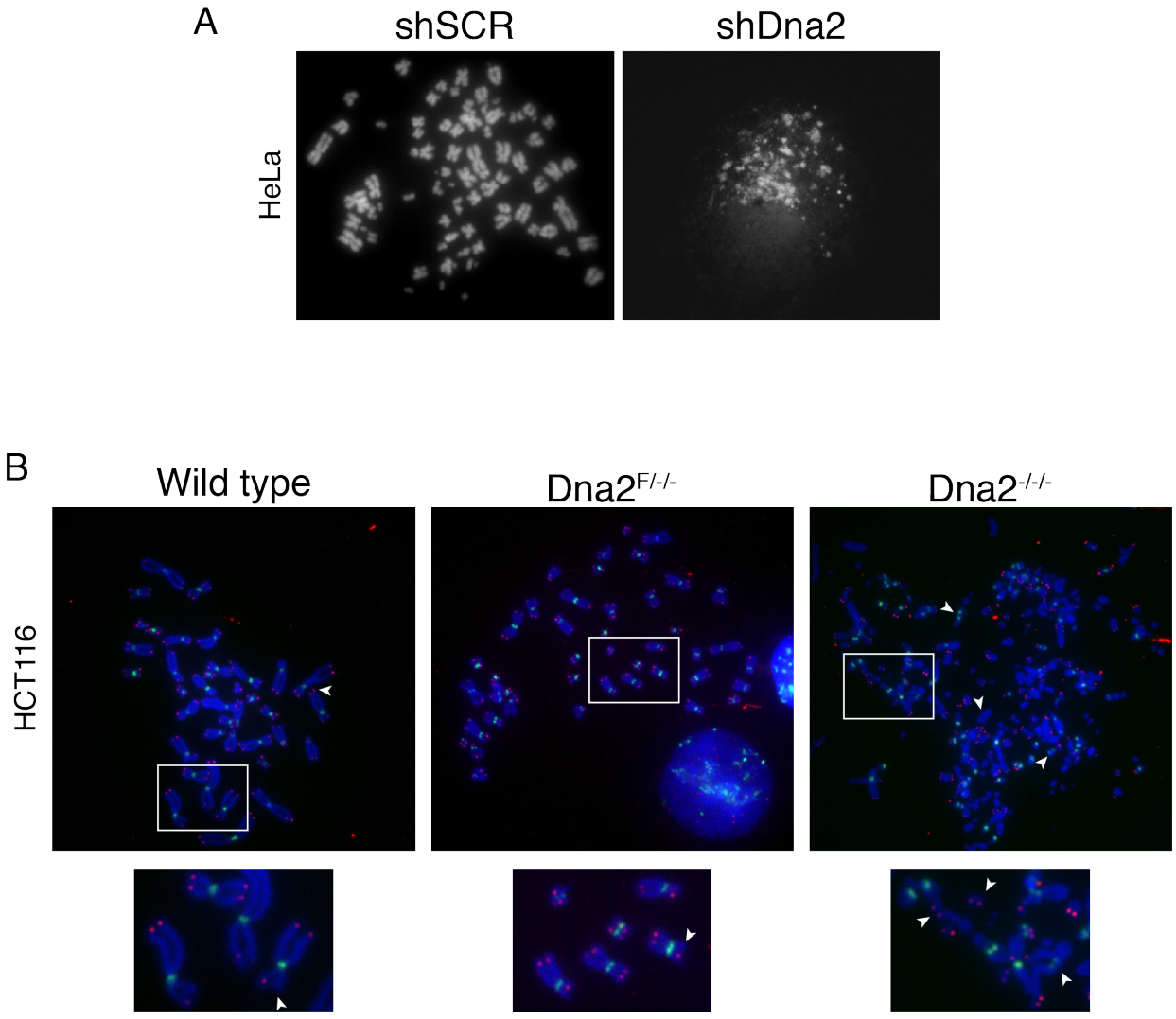

Figure 6.3 Metaphase chromosome spreads from Dna2 knockdown and knockout cells display morphological abnormalities.

A. Representative metaphase chromosome spreads from HeLa cells expressing either a scrambled control (shSCR) or Dna2-targeted (shDna2) hairpin. DNA was visualized by DAPI staining. 'Pulverized chromosomes' in shDna2-expressing cells have a different characteristic appearance than the chromosomes in $Dna2^{-/-/-}$ cells. **B.** Centromeres (green) and telomeres (red) were visualized in HCT116 cells with the indicated genotypes by FISH utilizing fluorescently labeled PNA probes. Arrowheads point to telomeric abnormalities including fragile or missing telomeres, or chromosomal abnormalities including acentromeric chromosomes and chromosomal fusions. Representative images.

References

1. **Haber JE.** 1999. DNA recombination: the replication connection. Trends Biochem Sci **24:**271-275.

2. **Helbock HJ, Beckman KB, Shigenaga MK, Walter PB, Woodall AA, Yeo HC, Ames BN.** 1998. DNA oxidation matters: the HPLC-electrochemical detection assay of 8-oxo-deoxyguanosine and 8-oxo-guanine. Proc Natl Acad Sci U S A **95:**288-293.

3. **Vilenchik MM, Knudson AG.** 2003. Endogenous DNA double-strand breaks: production, fidelity of repair, and induction of cancer. Proc Natl Acad Sci U S A **100:**12871-12876.

4. **Soza S, Leva V, Vago R, Ferrari G, Mazzini G, Biamonti G, Montecucco A.** 2009. DNA ligase I deficiency leads to replication-dependent DNA damage and impacts cell morphology without blocking cell cycle progression. Mol Cell Biol **29:**2032-2041.

5. **Hu J, Sun L, Shen F, Chen Y, Hua Y, Liu Y, Zhang M, Hu Y, Wang Q, Xu W, Sun F, Ji J, Murray JM, Carr AM, Kong D.** 2012. The intra-s phase checkpoint targets dna2 to prevent stalled replication forks from reversing. Cell **149:**1221-1232.

6. **Peng G, Dai H, Zhang W, Hsieh HJ, Pan MR, Park YY, Tsai RY, Bedrosian I, Lee JS, Ira G, Lin SY.** 2012. Human Nuclease/Helicase DNA2 Alleviates Replication Stress by Promoting DNA End Resection. Cancer Res **72:**2802-2813.

7. **Thangavel S, Berti M, Levikova M, Pinto C, Gomathinayagam S, Vujanovic M, Zellweger R, Moore H, Lee EH, Hendrickson EA, Cejka P, Stewart S, Lopes M, Vindigni A.** 2015. DNA2 drives processing and restart of reversed replication forks in human cells. J Cell Biol **208:**545-562.

8. **Osborn AJ, Elledge SJ, Zou L.** 2002. Checking on the fork: the DNA-replication stress-response pathway. Trends Cell Biol **12:**509-516.

9. **Myung K, Datta A, Kolodner RD.** 2001. Suppression of spontaneous chromosomal rearrangements by S phase checkpoint functions in Saccharomyces cerevisiae. Cell **104:**397-408.

10. **Lopes M, Cotta-Ramusino C, Pellicioli A, Liberi G, Plevani P, Muzi-Falconi M, Newlon CS, Foiani M.** 2001. The DNA replication checkpoint response stabilizes stalled replication forks. Nature **412:**557-561.

11. **Lambert S, Watson A, Sheedy DM, Martin B, Carr AM.** 2005. Gross chromosomal rearrangements and elevated recombination at an inducible site-specific replication fork barrier. Cell **121:**689-702.

12. **Sogo JM, Lopes M, Foiani M.** 2002. Fork reversal and ssDNA accumulation at stalled replication forks owing to checkpoint defects. Science **297:**599-602.

13. **Chen X, Niu H, Chung WH, Zhu Z, Papusha A, Shim EY, Lee SE, Sung P, Ira G.** 2011. Cell cycle regulation of DNA double-strand break end resection by Cdk1-dependent Dna2 phosphorylation. Nat Struct Mol Biol **18:**1015-1019.

14. **Allen C, Ashley AK, Hromas R, Nickoloff JA.** 2011. More forks on the road to replication stress recovery. J Mol Cell Biol **3:**4-12.

15. **Llorente B, Smith CE, Symington LS.** 2008. Break-induced replication: what is it and what is it for? Cell Cycle **7:**859-864.

16. **Budzowska M, Kanaar R.** 2009. Mechanisms of dealing with DNA damage-induced replication problems. Cell Biochem Biophys **53:**17-31.

17. **Sonoda E, Sasaki MS, Buerstedde JM, Bezzubova O, Shinohara A, Ogawa H, Takata M, Yamaguchi-Iwai Y, Takeda S.** 1998. Rad51-deficient vertebrate cells accumulate chromosomal breaks prior to cell death. EMBO J **17:**598-608.

18. **Schlacher K, Wu H, Jasin M.** 2012. A Distinct Replication Fork Protection Pathway Connects Fanconi Anemia Tumor Suppressors to RAD51-BRCA1/2. Cancer Cell **22:**106-116.

19. **Karanja KK, Lee EH, Hendrickson EA, Campbell JL.** 2014. Preventing over-resection by DNA2 helicase/nuclease suppresses repair defects in Fanconi anemia cells. Cell Cycle **13:**1540-1550.

20. **Petronczki M, Chwalla B, Siomos MF, Yokobayashi S, Helmhart W, Deutschbauer AM, Davis RW, Watanabe Y, Nasmyth K.** 2004. Sister-chromatid cohesion mediated by the alternative RF-CCtf18/Dcc1/Ctf8, the helicase Chl1 and the polymerase-alpha-associated protein Ctf4 is essential for chromatid disjunction during meiosis II. J Cell Sci **117:**3547-3559.

21. **Mayer ML, Pot I, Chang M, Xu H, Aneliunas V, Kwok T, Newitt R, Aebersold R, Boone C, Brown GW, Hieter P.** 2004. Identification of protein complexes required for efficient sister chromatid cohesion. Mol Biol Cell **15:**1736-1745.

22. **Hanna JS, Kroll ES, Lundblad V, Spencer FA.** 2001. Saccharomyces cerevisiae CTF18 and CTF4 are required for sister chromatid cohesion. Mol Cell Biol **21:**3144-3158.

23. **Miles J, Formosa T.** 1992. Evidence that POB1, a Saccharomyces cerevisiae protein that binds to DNA polymerase alpha, acts in DNA metabolism in vivo. Mol Cell Biol **12:**5724-5735.

24. **Duxin JP, Moore HR, Sidorova J, Karanja K, Honaker Y, Dao B, Piwnica-Worms H, Campbell JL, Monnat RJ, Jr., Stewart SA.** 2012. Okazaki Fragment Processing-independent Role for Human Dna2 Enzyme during DNA Replication. J Biol Chem **287:**21980-21991.

25. **Saharia A, Guittat L, Crocker S, Lim A, Steffen M, Kulkarni S, Stewart SA.** 2008. Flap endonuclease 1 contributes to telomere stability. Curr Biol **18:**496-500.